Seasonal and storm snow distributions in the Bridger Range, Montana
by Michael Jon Pipp

A thesis submitted in partial fulfillment of the requirements for the degree of Master of Science in Earth Sciences
Montana State University

Abstract:
Computer modeling of seasonal snowpack distribution and storm snowfall is a common tool for hydrologist and avalanche forecasters. Spatial scales for models range from global to local with temporal scales ranging from hours to months. The measurement stations available to constrain the models are widely spaced so that meso-scale resolution is difficult. Local-scale seasonal and storm snow distributions were measured to assess the variability and factors that control snow distributions between stations. A network of eleven measurement sites was established in the Ross Pass area in the central Bridger Range, MT. Sites were measured for elevation, aspect, slope, radial distance from Ross Pass, distance from the range crest, and distance north-south of the Pass. Atmospheric data was collected from National Weather Service Rawinsondes at Great Falls, MT. Surface meteorological data was collected locally. The Natural Resources Conservation Service (NRCS) - Snow Survey measures snowpack at four locations in the Bridger Range, two north and south of the Ross Pass Study Area (RPSA). Seasonal snowpack was measured on April 1,1995 at all fifteen sites using Federal snow samplers. Storm snowfall was measured from storm boards at the RPSA sites with modified bulk samplers and spring scales. Results show that the NRCS estimated April 1, 1995 snowpack to have a snow-elevation gradient of 937 mm km-1. Snow accumulation was average when compared with the previous four years. The RPSA April 1,1995 snowpack was significantly different than that predicted from simple elevation based gradient estimates from NRCS data. RPSA had drier high elevation sites and wetter low elevation sites and an overall smaller snow-elevation gradient of 468 mm km-1. Nominal clustering of storm snow distributions identified four classes and two sub-classes prevalent during the season. Correlation analysis showed that distance east of the ridge was significant in 81% of storms, while elevation was significant in only 50%. Due to strong covariance between variables, partitioning the signals is not possible and either variable is considered reasonable as a linear predictor of storm snow distribution. Snow distributions in the RPSA strongly resemble observed spatial patterns using small-scale snow fence and shrub barrier models.

SEASONAL AND STORM SNOW DISTRIBUTIONS IN THE BRIDGER RANGE, MONTANA

by
Michael Jon Pipp

A thesis submitted in partial fulfillment
of the requirements for the degree

of

Master of Science

in

Earth Sciences

MONTANA STATE UNIVERSITY
Bozeman, Montana

August 1997

APPROVAL

of a thesis submitted by

Michael Jon Pipp

This thesis has been read by each member of the thesis committee and has been found to be satisfactory regarding content, English usage, format, citations, bibliographic style, and consistency, and is ready for submission to the College of Graduate Studies.

May 14, 1997
Date

William W Jochim
Chairperson, Graduate Committee

Approval for the Major Department

May 16, 1997
Date

W. A. Marcus KR
Head, Major Department

Approval for the College of Graduate Studies

6/12/97
Date

R L Brown
Graduate Dean

STATEMENT OF PERMISSION TO USE

In presenting this thesis in partial fulfillment of the requirements for a master's degree at Montana State University, I agree that the Library shall make it available to borrowers under rules of the Library.

If I have indicated my intention to copyright this thesis by including a copyright notice page, copying is allowable only for scholarly purposes, consistent with "fair use" as prescribed in the U.S. Copyright Law. Requests for permission for extended quotation from or reproduction of this thesis in whole or in parts may be granted only by the copyright holder.

Signature Michael J Pigg

Date May 10, 1997

ACKNOWLEDGMENTS

This project was partially funded by grants from the Jim Edie Foundation and the John Montagne Family Fund. Their financial support is gratefully acknowledged. The Natural Resources Conservation Service - Snow Survey, Bozeman office, supplied logistical and technical assistance during the length of the project. Hardcopy Rawinsonde data was received from the National Weather Service - Great Falls, MT from November through March. I would like to thank my advisor, Dr. William Locke, for his patience and direction over the duration of this project. Also, appreciation and thanks are extended to the people who assisted me in the field; Phillip Farnes and Dr. William Locke with site selection during the summer of 1994; Dr. Steve Custer and his Snow Dynamics class with April 1 snow cores; and most importantly Brian Guldberg, my most reliable and dependant field assistant (and pub tender) who's contribution to data collection was invaluable. Finally, many thanks go to my family, Ralph and Faith Pipp for their encouragement and support and especially to Andrea, wife and field assistant, for her understanding, support, and many sacrifices.

TABLE OF CONTENTS

TABLE OF CONTENTS -- Continued

TABLE OF CONTENTS -- Continued

LIST OF TABLES

LIST OF TABLES -- Continued

LIST OF FIGURES

LIST OF FIGURES -- Continued

LIST OF FIGURES -- Continued

ABSTRACT

Computer modeling of seasonal snowpack distribution and storm snowfall is a common tool for hydrologist and avalanche forecasters. Spatial scales for models range from global to local with temporal scales ranging from hours to months. The measurement stations available to constrain the models are widely spaced so that meso-scale resolution is difficult. Local-scale seasonal and storm snow distributions were measured to assess the variability and factors that control snow distributions between stations. A network of eleven measurement sites was established in the Ross Pass area in the central Bridger Range, MT. Sites were measured for elevation, aspect, slope, radial distance from Ross Pass, distance from the range crest, and distance north-south of the Pass. Atmospheric data was collected from National Weather Service Rawinsondes at Great Falls, MT. Surface meteorological data was collected locally. The Natural Resources Conservation Service (NRCS) - Snow Survey measures snowpack at four locations in the Bridger Range, two north and south of the Ross Pass Study Area (RPSA). Seasonal snowpack was measured on April 1,1995 at all fifteen sites using Federal snow samplers. Storm snowfall was measured from storm boards at the RPSA sites with modified bulk samplers and spring scales. Results show that the NRCS estimated April 1, 1995 snowpack to have a snow-elevation gradient of 937 mm km^{-1}. Snow accumulation was average when compared with the previous four years. The RPSA April 1, 1995 snowpack was significantly different than that predicted from simple elevation based gradient estimates from NRCS data. RPSA had drier high elevation sites and wetter low elevation sites and an overall smaller snow-elevation gradient of 468 mm km^{-1}. Nominal clustering of storm snow distributions identified four classes and two sub-classes prevalent during the season. Correlation analysis showed that distance east of the ridge was significant in 81% of storms, while elevation was significant in only 50%. Due to strong covariance between variables, partitioning the signals is not possible and either variable is considered reasonable as a linear predictor of storm snow distribution. Snow distributions in the RPSA strongly resemble observed spatial patterns using small-scale snow fence and shrub barrier models.

CHAPTER 1

INTRODUCTION

Background

Water is one of the most important resources in the western United States and the winter snowpack contributes an estimated 80 percent of the annual runoff and water supplies for the region (SCS 1972). Human uses of snow-generated water include agricultural, municipal, recreational, and industrial. Economic and recreation activities are strongly influenced by the distribution of snow and computer modeling of its distribution is now an important management tool for forecasters. However, the variability in seasonal and storm snow distribution is poorly understood at the local-scale of individual basins. Better understanding of meso-scale factors may help improve the models of snow distribution used for water supply and avalanche hazard forecasts at this scale.

Numerical models of snow distribution rely upon data collected from a network of automated and manual snow survey sites. This network is managed by the United States Department of Agriculture - Natural Resource Conservation Service (NRCS) Snow Survey, formally the Soil Conservation Service (SCS) Snow Survey. The network contains automated snow telemetry (SNOTEL) stations with a daily and sub-daily sampling interval and manual snow courses with monthly and bimonthly sampling intervals.

SNOTEL stations (Figure 1) are supplemented with 2,530 snow courses (SCS 1994). This measurement network is placed in the mountains at elevations above 1,525 m (5,000 ft) (Beard 1994) and is higher than those typical for National Weather Service (NWS) climate stations. The distribution of these stations allows synoptic-scale forecasting. Only a few snow survey sites are

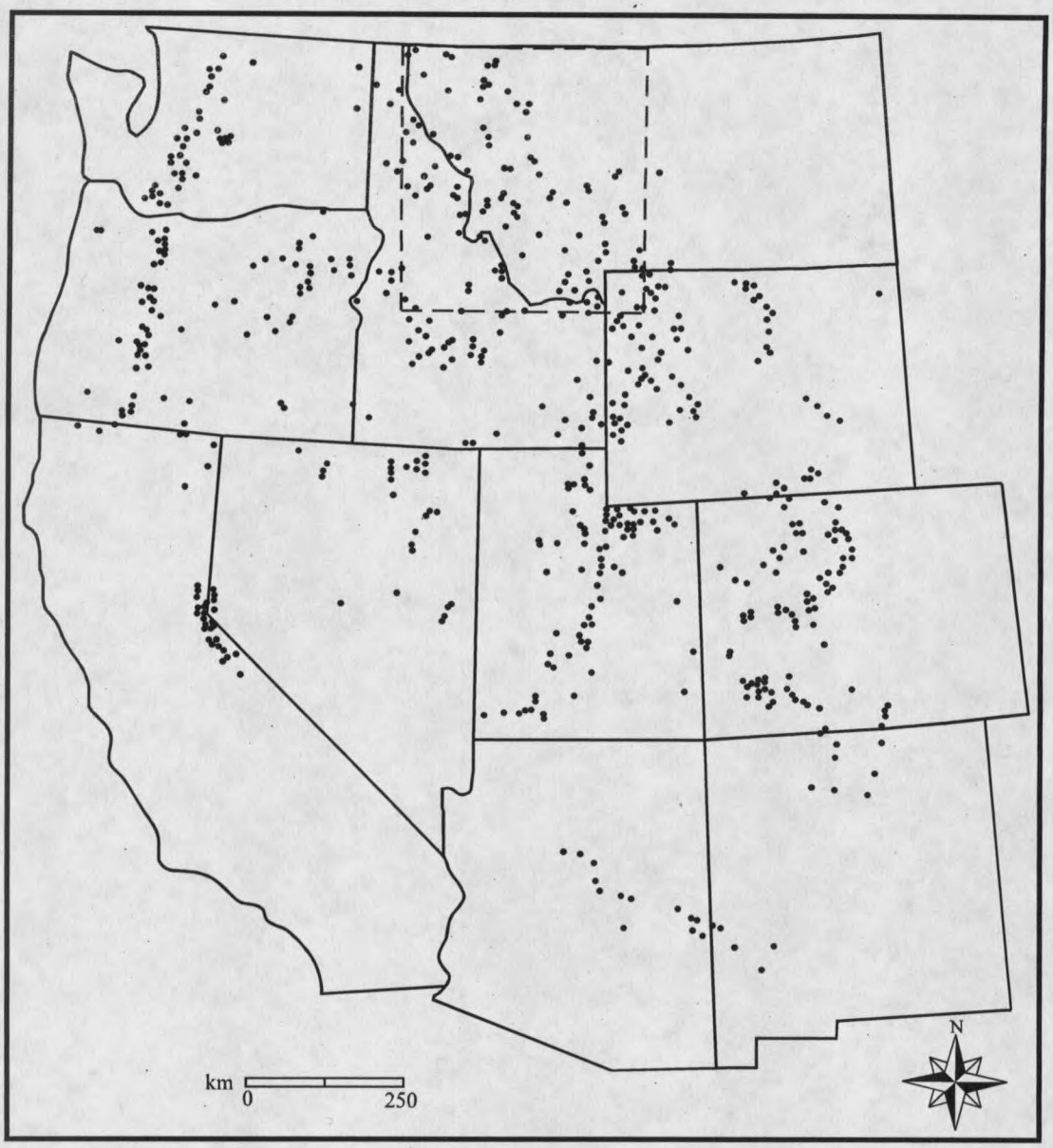

Figure 1. NRCS SNOTEL network as of 1988 representing the synoptic-scale. The dashed square represents the regional-scale depicted in Figure 2.

placed in individual ranges and these are stratified by elevation. Snow-elevation gradients are determined by the difference in snowpack accumulation between high-low elevation pairs. This gradient is then generally applied across the entire range to calculate snowpack accumulation and distribution (Custer et al. 1996).

Two types of sites are measured by the NRCS. SNOTEL sites (Whaley 1983) collect data by measuring the weight of the overlying **snowpack** (seasonal accumulation of snow measured as a depth in inches or centimeters) on a snow pillow (Goodison et al. 1981). Snow courses are transects of five to ten points where the snowpack is measured manually for depth and density (Goodison et al. 1981). Both SNOTEL and snow course data are reported as **snow water equivalent (SWE)**, which is a measure of water content stored in the snowpack and is reported in inches or millimeters of water.

Avalanche hazard forecasts rely on the SNOTEL network for snow accumulation data in the subalpine region. New snow accumulation is used to determine the amount and rate of stress recently added to the existing snowpack. Accumulation rates at SNOTEL sites reported during storm events are extrapolated to alpine starting zones for hazard evaluation, thus making local- and meso-scale snowfall estimates important for recreationists.

The National Weather Service (NWS) also collects snow accumulation data with its surface-monitoring system (Dingman 1994). Hourly measurements are taken at 84 primary climate stations in eleven Western states and daily measurements are collected from a secondary network of cooperative weather stations. NWS snow accumulation data are reported as **snowfall**: snow accumulation during a specified period, measured as a depth of snow in inches or centimeters. The NWS network, however, is biased toward lower elevations, valley bottoms, and populated areas (Farnes 1971; Dingman 1994). This network arrangement is not well suited for determining precipitation in complex terrain (Vuglinski 1972; Custer et al. 1996).

Problem Statement

Water supply managers and avalanche forecasters use computer models as a tool to facilitate their assessment of snowpack and snowfall distribution. Computer models link

measurements with atmospheric and boundary-layer processes operating over a hierarchy of spatial scales (Table 1). Water supply models usually operate at meso- to regional spatial scales and monthly to seasonal temporal scales. Models for avalanche hazard estimation operate at meso- to local spatial scales and daily or sub-daily temporal scales. An understanding of the variability in snow distribution at the meso-scale is important for the calibration and validation of physically-based models to improve resolution of water supply forecasting and avalanche hazard estimation models.

Table 1. Hierarchy and definition of spatial scales.

Scale	Domain	Horizontal Extent	Variables
Global	Planetary	10,000 km	ocean currents, pressure cells/winds, insolation
Synoptic	Continental	1,000 km	physiography, pressure cells, jet streams
Regional	Regional	100 km	regional topography, frontal systems, jet streams
Meso	Neighborhood	10 km	wind fields, air mass characteristics, large-scale topography
Local	Basin	1 km	wind fields, air mass characteristics, local-scale topography
Micro	Site	0.1 km	ground cover, forest structure, .aspect, slope

(adapted from Linacre 1992)

The existing NRCS snow survey network provides adequate coverage for synoptic scale (Figure 1), regional scale (Figure 2), and in some cases meso-scale (Figure 3) topographies. However, at sub-network scales, i.e., local- and even meso-scale, snow distribution variability is not easily predicted from the snow survey network. An understanding of the error produced at meso and smaller scales is important for "hierarchal nested" model tests. In regions of complex terrain, hierarchal nesting of meso- and local-scale models embedded within synoptic and regional scale models may provide a better representation of meso- and local-scale precipitation distribution

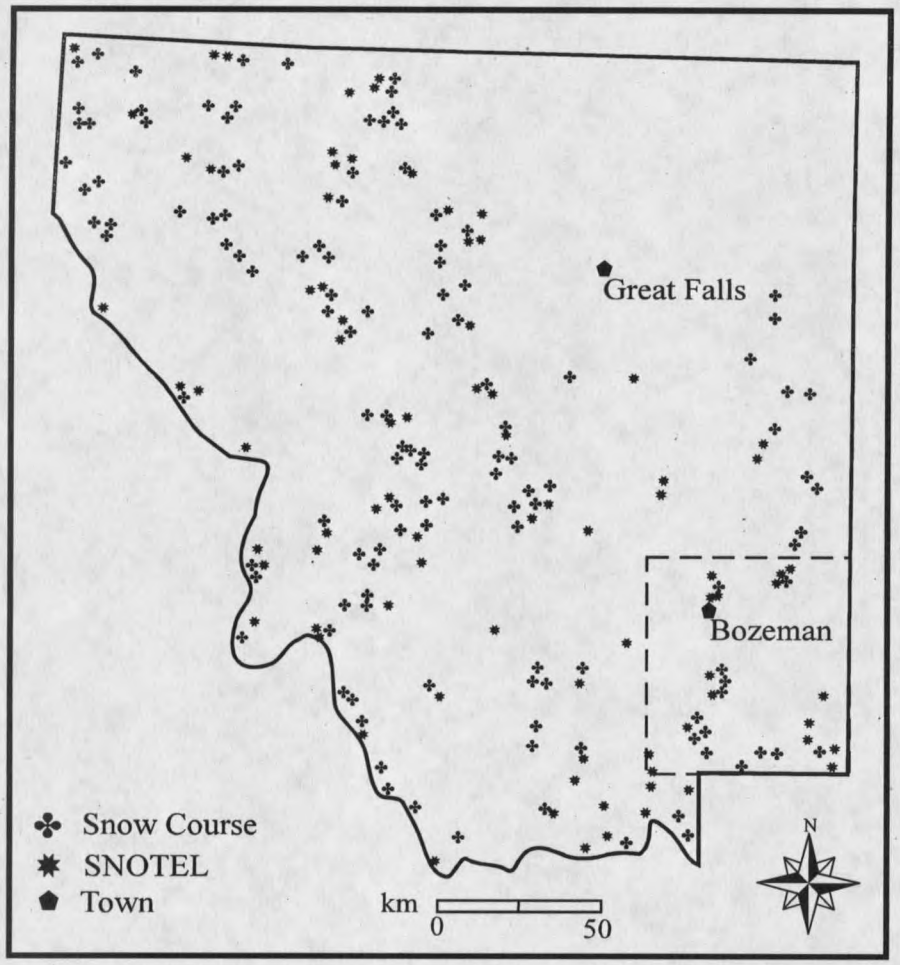

Figure 2. NRCS snow survey network in western Montana as of 1993 representing the regional scale. The dashed square represents the meso-scale depicted in Figure 3.

(Alford 1985; Barry 1992b).

An important component of precipitation models is validation. Since snow accumulation trends are consistent within meso-scale ranges but highly variable at regional scales (Locke 1989), use of the existing measurement network is adequate for validation of meso-scale models in regions of adequate data (Custer et al. 1996). However, the latest generation of high-resolution models operates at a sub-network local-scale and the existing measurement network is inadequate

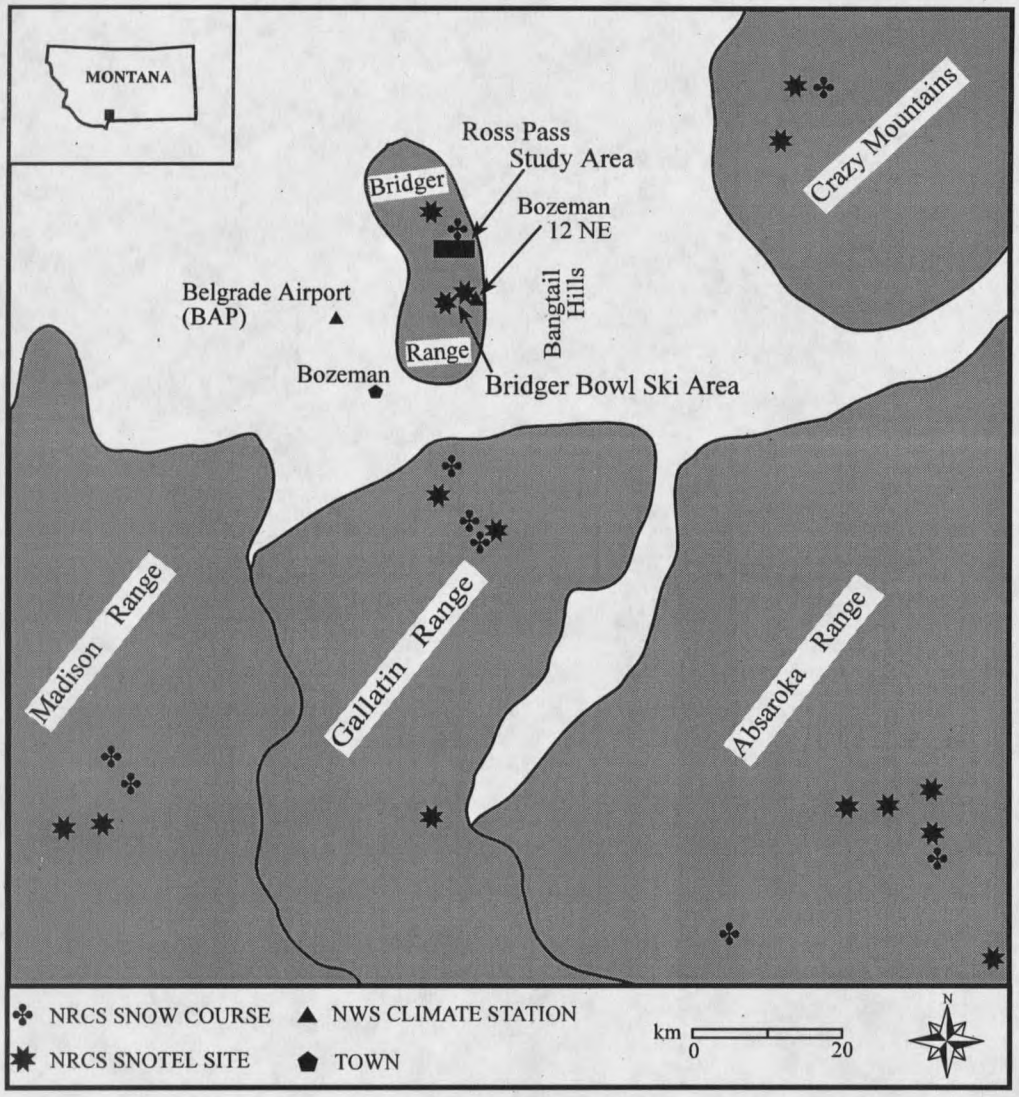

Figure 3. Present distribution of NRCS snow survey sites, NWS climate stations (used for this study), and location of the Ross Pass Study Area in southwest Montana. Shaded areas are elevations above 1,830 m (6,000 ft) in ranges with summit elevations exceeding 2,500 m (8,200 ft).

for model control (Barros and Lettenmaier 1994). Therefore, empirical investigation of local-scale snow distribution would help clarify the nature of local-scale variability. This improved understanding will help develop local-scale snow accumulation trends necessary for the calibration and validation of large-scale snow distribution models.

Study Objectives

1) Assess the ability of NRCS Snow Survey measurements in a single mountain range to predict the snow-elevation gradients within the mountain range.

2) Explore factors that control storm snowfall distribution in a montane area from a meteorological and geographic perspective.

Research Questions

1) Will NRCS Snow Survey sites in a mountain range accurately (± 10%) predict the seasonal snow accumulation gradient for an area of less than 100 km^2 within the mountain range?

2) Are atmospheric variables (wind azimuth, wind velocity, air temperature, and relative humidity) significant in explaining snowfall distribution for individual storms within a montane area of less than 100 km^2?

3) Are geographic variables (distance from a ridge and distance from a pass) significant in explaining snowfall distribution for individual storms within a montane area of less than 100 km^2?

Hypotheses

1) Ho: The NRCS measured snow-elevation gradient in the Bridger Range will not predict the measured snow accumulation gradient in the Brackett Creek area.

Ha: The NRCS measured snow-elevation gradient in the Bridger Range will predict the measured snow accumulation gradient in the Brackett Creek area.

2) Ho: Elevation will not account for the predominance of the storm snowfall distribution with a lesser amount of the variance accounted for by wind azimuth, wind velocity, air temperature, humidity, distance from a ridge, and/or distance from a pass.

Ha: Elevation will account for the predominance of the storm snowfall distribution with some amount of the variance accounted for by storm wind azimuth, wind velocity, air temperature, humidity, distance from a ridge, and/or distance from a pass.

Hb: Elevation will account for the predominance of storm snowfall distribution with a significant amount of the variance accounted for by other contributing variables.

Anticipated Outcomes

Based on past studies of the complex nature of airflow and precipitation in complex terrain (Hayes 1984; 1986; Daley and Neilson 1992; Barros and Lettenmaier 1993), the snow accumulation gradient based on NRCS snow survey data for the Bridger Range will differ significantly from the small montane area (accepting H1o and rejecting H1a). Elevation will account for the predominance of the storm snowfall distribution, but wind azimuth, wind velocity, air temperature, relative humidity, and distances from the ridge and pass will improve the predictions (rejecting H2o, H2b, and accepting H2a).

Study Area

Ross Pass Study Area

The Ross Pass Study Area (Figure 4) is in the Brackett Creek Basin in the Bridger Range, in southwest Montana (Figure 3). The Bridger Range is nearly linear and extends roughly north-south, with a slight northwest bias, and is 31 km long x 10 km wide x 1.3 km high (19 mi x 6 mi x 0.8 mi). It is at the eastern end of the Gallatin Valley, which is a large east-west intermontane valley approximately 85 km long x 45 km wide (53 mi x 28 mi). To the east of the range is the Great Plains. Only the circular massif of the Crazy Mountains and the low Bangtail Hills influence airflows from the east.

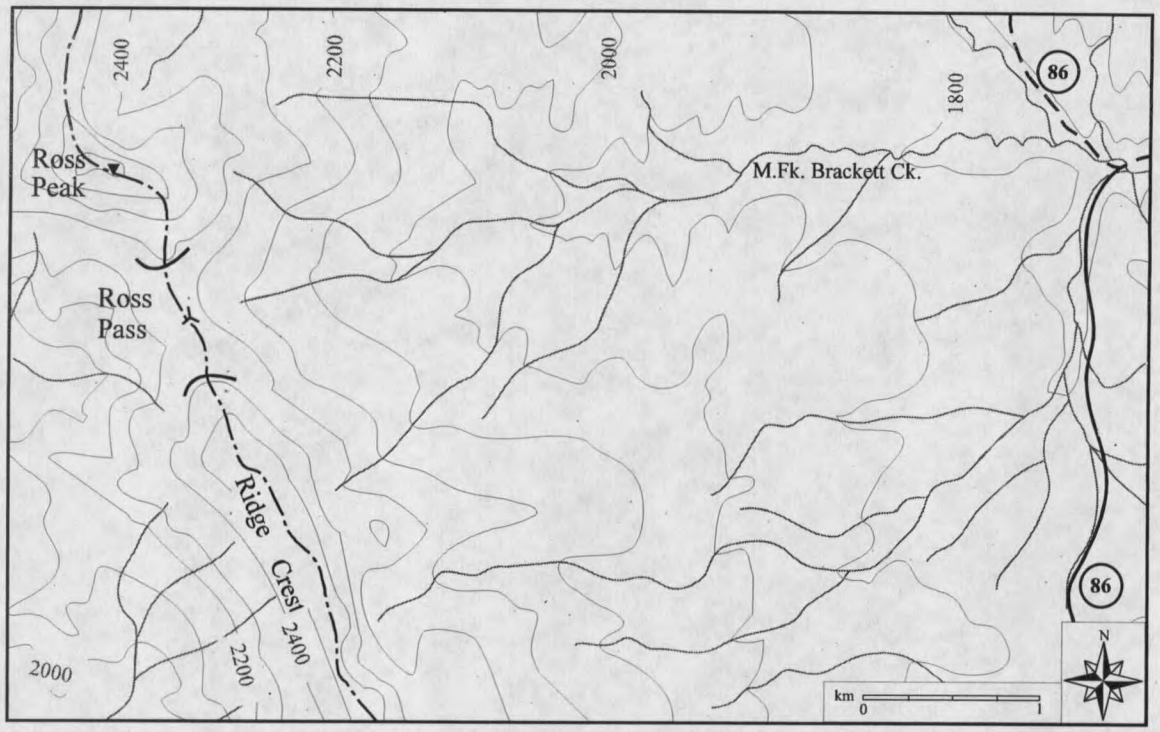

Figure 4. Topography of the Ross Pass Study Area, Bridger Range, MT. Solid and long dashed line is MT state highway 86. Refer to Figure 3 for location. Contour Interval = 100 m.

The geographic position of the Bridger Range -- in the zone of westerly airflow and at the eastern edge of the Gallatin Valley -- offers an ideal site for the study of simple topographic effects on snow distribution. The length of the Gallatin Valley should dampen wind flow disturbances caused by ranges to the west. Since none of these ranges are within 15 km (9 mi) of the Bridger Range, the airflow should be effectively undisturbed (Rhea 1978; Tremper et al. 1983). Influence of the Bridger Range and Ross Pass on the wind flow, and resultant snow distribution, should be evident if such features have an effect on the accumulation of snow.

From MT highway 86 to the 2,200 meter elevation, slopes in the study area are low to moderate (< 10% to ~ 35%). The slope then increases to nearly 130 percent below the ridge crest with many avalanche paths. This topography restricts ski and snowmobile travel after storm events

to the moderate slopes beyond avalanche path run-out zones.

The Ross Pass Study Area is bounded by four NRCS snow survey sites -- three SNOTEL and one snow course (Figure 3). The SNOTEL sites are measured monthly from January to April or May with a standard Federal Snow Sampler and continuous measurements of SWE (snow water equivalent) from the snow pillows. The snow course is measured monthly from December to April with a Federal Snow Sampler.

The Bridger Bowl Ski Area is 6 km (4 mi) south of Ross Pass (Figure 3) and is the source of surface weather data. This data is collected at the ridge crest with a data logger and provides information on wind azimuth and velocity, air temperature, and snowfall at hourly intervals.

Climate

Winters in southwest Montana are characterized by a mid-latitude continental climate, with significant influence from mountain ranges. Winter precipitation at these latitudes is primarily due to frontal and convergent lifting mechanisms (Tremper et al. 1983) which can be greatly enhanced by orographic barriers. The ranges may block or slow movement of regional air masses (Birkeland and Mock 1996) and create temperature and humidity differences.

The period from 1964-1993 was used to compute the 30-year averages for monthly snowfall, minimum, and maximum temperature (Table 2). Average monthly (October - April) snowfall in the Gallatin Valley (Belgrade Airport) at 1,355 m (4,450 ft) range from five to 22 cm (two to seven inches). Average monthly (October - April) snowfall on the east slope of the Bridger Range (Bozeman 12NE) at 1,815 m (5,950 ft) range from 32 to 101 cm (13 to 40 inches). Average monthly minimum and maximum temperatures however, have low variability ($< 4\,^{\circ}C$) between stations indicating a limited influence of the Bridger Range on regional-scale air masses.

Table 2. 30-year average climate, 1964-1993. (Refer to Figure 3 for station locations.)

	Belgrade Airport (BAP)			Bozeman 12NE		
Month	Snowfall (cm)	Min. Temp. (degrees Celsius)	Max. Temp.	Snowfall (cm)	Min. Temp. (degrees Celsius)	Max. Temp.
Oct.	5	-1	15	32	-3	12
Nov.	14	-7	5	72	-8	4
Dec.	17	-13	0	90	-12	1
Jan.	19	-13	-1	97	-13	0
Feb.	13	-10	2	72	-12	2
Mar.	22	-6	6	101	-9	5
Apr.	16	-1	12	80	-5	9

CHAPTER 2

LITERATURE REVIEW

The distribution of snow in mountainous terrain is influenced by many geographic and meteorologic variables. Among the most important variables are terrain and wind fields (Price 1981; Barry 1992a, b). Elevation is generally considered the most important factor controlling snow distribution (McKay and Gray 1981).

Elevation

Although the relationship of snow accumulation (SWE) to elevation is well established, it varies across time and space as illustrated by Meiman (1968). This relation is also true for 24 snow courses in southwest Colorado (Caine 1975) where an overall gradient for the San Juan Mountains of 655 mm SWE per vertical kilometer (mm km^{-1}) ($R = 0.66$) showed a slightly greater snow accumulation gradient occurred on the windward (Colorado River) side than the leeward (Rio Grande) side. The difference in gradient was not statistically significant. There is also a decrease in annual variability of snow accumulation with elevation (Caine 1975). This trend is attributed to greater annual variation at lower elevations during both wet and dry winters.

In an evaluation of snow accumulation at 265 sites in western Montana, Idaho, and Wyoming, Locke (1989) noted the snow-elevation relationship was very low ($R = 0.16$). However, when the gradient is limited to a subregion (one or two mountain ranges) the relationship becomes highly significant (Bozeman, MT: $R = 0.95$; $n = 6$). For 45 subregions in western Montana, gradients range from 330 ± 100 mm to 2050 ± 210 mm km^{-1} (Locke 1989).

Snow accumulation relationships have been further explained for specific geographic

areas with supporting meteorologic and geographic variables. Meteorological variables include wind azimuth and velocity, and upper atmosphere temperature, dew point, and vapor content (Hjermstad 1970; Super et al. 1972; 1974; Storr 1973; Barros and Lettenmaier 1993). Geographic variables include slope, aspect, local topography, and coordinate space (e.g., latitude and longitude) (Hjermstad 1970; Super et al. 1972; 1974; Locke 1989; Elder et al. 1991; Troendle et al. 1993; Custer et al. 1996).

Seasonal Snow Distribution

Much of the literature on snow distribution focuses on seasonal snow accumulation for water supply forecasts or defining basin hydrology. Research basins have been extensively monitored with snow courses and precipitation gauges (Golding 1968; Troendle and King 1987). Traditionally, snow course sampling is done with snow cores that average depth and density recorded at several points. This method produces reliable estimates of snow water equivalent for the snowpack, but is time consuming and thus limits the number of sample points (Rovansek et al. 1993).

Double sampling of the snowpack (Rovansek et al. 1993) involves a greater number of depth measurements for each depth-density pair, but is faster because fewer density measurements are made. Snow depth can be highly variable across short distances, but can be measured rapidly. Density is conservative across space and requires more time than depth to measure. By averaging a larger number of depth measurements for each density, the variance of the estimate can be reduced. A 20 percent improvement in sample variance was realized using the double sampling method (Rovansek et al.1993).

Recent trends in seasonal snow distribution analysis is the use of computer technologies and geographic information systems (GIS). Studies have coupled GIS technology and

computerized classification methods with field surveys of snow distribution (Elder et al. 1991; Davis et al. 1993), hand-drawn annual precipitation maps (Custer et al. 1996; Stillman 1996), geostatistical interpolation techniques (Hosang and Dettwiler 1991), and remotely sensed imagery (Cooley and Rango 1991; Davis et al. 1993) to validate computer modeled snow distribution maps.

Elder et al. (1991) used a simple random sampling scheme with 86 to 354 depth measurements, along with eight density measurements, to calibrate their model of snow water storage in an alpine basin. The model incorporated elevation, slope, and insolation parameters smoothed over a 5-minute (9.3 km latitude-longitude) digital elevation model (DEM) of the basin. The basin was divided into zones of similar characteristics and values for elevation, slope, and insolation were determined and clustered. Clustered images of the basin were classified into 72 different combinations. All classifications proved significant at the 95 percent level and three were significant at the 99 percent level. Estimated total basin water volume was consistently different from true basin water volume, but by only a negligible amount. Elder states that this showed a stratified random sample design, based on physical parameters, would be superior to a simple random sample for estimating average basin SWE. Insolation was the most important variable in the clustering routine, but overall, a majority of the variance was not explained by the three parameters alone. This suggests other important variables are involved in seasonal snow distribution.

Hand-drawn, average-annual precipitation contour maps by Phillip Farnes for the period 1961 to 1990 using standard techniques (Farnes 1971; SCS 1977), were digitized and compared with a computer-generated map (Custer et al. 1996). The computer-generated, average-annual precipitation map, using the same 96 station data set, was produced using ANUSPLIN (Hutchinson and Bischof 1983) and a DEM grid surface with 90 m north-south and 65 m east-west

grid cells. Precipitation distribution was classified into 14 classes of equal precipitation ranging from 5 to 75 inches. Maps were compared on a cell-by-cell basis using a GIS and were rarely different by more than one classification interval. However, in areas where the data input stations are sparsely located, ANUSPLIN tended to incorrectly estimate precipitation values when compared with the hand contoured map (Custer et al. 1996).

Hosang and Dettwiler (1991) developed a seasonal SWE map for a 2.1 km^2 basin with a geostatistical approach. Snow accumulation measurements were recorded at 33 snow courses with average course values plotted on a Cartesian grid system. All but one snow course were aligned along the main basin axis. Multiple linear regression of SWE vs. elevation, potential insulation (slope), and presence/absence of forest cover produced a correlation coefficient of $R = 0.66$. The regression formula was valid, however only during snowmelt and failed completely during snow accumulation. Point-kriging interpolation was used to estimate SWE values from the regression residuals. Results indicate elevation as the most significant variable and that the distribution of the measurement network is critical in reducing the variance of interpolated values.

Cooley and Rango (1991) found similar results in a 0.3 km^2 basin using a 30 m x 30 m sampling grid. Snow cores from all 282 grid points with snow cover were used to generate SWE distribution maps using varying numbers of sample points. These maps were verified with aerial photos of the basin. Results showed the variance between sample and population means decreased as the number of sample points increased, with a 40% standard deviation of error for 30 points to 0% for all 282 points.

Davis et al. (1993) tested various interpolation methods and mapping strategies to develop snow accumulation maps for a 4.4 km^2 cirque basin coupling satellite imagery and manual snow courses. Sixty snow courses, aligned up the center of the basin, were sampled near peak snow accumulation. Sampling dates were established to corresponded with the timing of satellite

imagery. Sample points were registered on a 30-minute DEM and snow accumulation (SWE) was interpolated over the basin using a simple mean and a nearest neighbor technique with 5, 10, and 50 points. Snow-covered area (SCA) maps were developed using Landsat Thematic Mapper imagery and two classification methods -- Bayesian Maximum Likelihood (binary) and Spectral Mixture Analysis (fractional percent). Classification results showed the binary method had a 10% greater SCA than the fractional method. Basin SWE values were calculated by combining SWE interpolation methods with SCA maps. Results showed the binary SCA maps with 11.4% to 11.6% greater basin SWE volumes than fractional SCA maps. When compared against annual stream discharge below the basin, volumes produced by the fractional SCA maps were closer than the binary SCA maps. Preferred SWE interpolation schemes were the simple mean and 50-point nearest neighbor, although this appeared to be influenced by the narrow distribution of sample points along the basin axis (Davis et al. 1993).

Summary

Empirical snowpack measurements can have improved estimate variances by using double sampling techniques. Variables influencing seasonal snow accumulation include elevation, insolation (encompassing aspect, latitude, and slope), and forest cover. Also, density and distribution of the measurement network are important. Measurement network distribution and density affects the ability to estimate snow accumulation. As the study area deviates (large or small) from measurement resolution, standard deviation of the estimate increases. Regardless of the estimating method used, adequate spatial distribution of sampling points -- at the scale of study -- is critical to minimizing estimation errors.

Storm Snow Distribution

In Colorado, Hjermstad (1970) investigated the average distribution of precipitation with elevation as influenced by 500 mb (millibar) meteorological parameters (wind azimuth, wind velocity, and air temperature). He used a measurement network of 45, 24-hour snowboards extending up the west side of Vail Pass and the north side of Fremont Pass. Snowboards were placed at one-mile intervals, and recording precipitation gages were stationed at three sites along Fremont Pass. Precipitation data from 26 NWS precipitation gages along east-west and north-south transects (17 gages/225 mi and nine gages/140 mi, respectively) were also collected. Data were collected from these networks between 1960 and 1968. Hjermstad's results showed that precipitation increased consistently with elevation with the maxima below the topographic crest, precipitation totals were larger for 500 mb winds perpendicular to the topographic barriers, precipitation totals increased with strong 500 mb winds (velocity > 25 ms^{-1}), and precipitation totals decreased with low 500 mb temperatures (-20°C to -30°C).

Meteorologic, physiographic, and terrain parameters were evaluated during a cloud seeding project in southwest Montana (Holman 1971; Super et al. 1972; 1974). A network of 27 weighing type precipitation gages, fitted with Alter shields, was established for a study area of 780 km^2 with the western edge the Bridger Range (Figure 3). Upper atmosphere data collected from the Great Falls, MT, National Weather Service rawinsonde, 187 km to the north (Figure 2) was complimented by local radiosonde launches when a seeding operation was in progress. Super et al. (1972) reported a strong correlation of wind azimuth, R = 0.95 for 10,000 ft and R = 0.97 for 14,000 ft, between Great Falls, MT and the Bangtails Hills, 8 miles east of the Bridger Range. However, wind velocity was only moderately correlated, R = 0.75 for 10,000 ft and R = 0.85 for 14,000 ft. Wind velocity was the third most important variable behind cloud thickness and cloud

top temperature in explaining storm snowfall distribution (Super et al. 1972; 1974).

Holman (1971) analyzed a subset of Super's data and found a similar correlation between 700 mb (~10,000 ft) winds in the Bridger/Bangtail area with Great Falls rawinsonde data. Results suggested that cloud-base temperatures were significant and positively related to precipitation amounts. Also significant was the 500 mb air temperature, which related inversely to precipitation.

Troendle et al. (1993) compared snow accumulations from storms on opposing hill slopes (north and south) to assess accumulation as a function of slope and canopy. Based on snowboard measurements and late season snow cores, they found that total storm snowfall agrees with seasonal accumulation if no significant ablation occurs before the melt season. The north slope suffered no ablation losses during the season, while the south slope recorded losses from ablation during March. The difference in snowpack between slopes was attributed to lower canopy densities on the south slope than the north slope. The lower densities resulted in greater insolation and wind velocities at the snow surface facilitating ablation and erosional losses of the snowpack.

Summary

Storm snowfall distribution is dependent on local and meso-scale topography, upper atmosphere and surface meteorological variables, and forest cover. Reported relationships between snowfall and these variables are generally direct, except for temperature which is inversely related. Specific for southwest Montana, the relationship of atmospheric winds above the Bridger Range and Great Falls, MT is strong for 700 mb and 500 mb azimuths and moderate for 700 mb velocities.

Modeling of Snow Distribution

Scale Models

Snow distribution patterns generated by various barriers, such as snow fences and shelter belts, have been investigated using scaled models of various designs. Tabler and Jairell (1980) tested several configurations and types of scale model snow fences in perpendicular winds. Their results showed that snow distribution downwind of the 1:30 scale model snow fences were exactly proportional to full scale snow fences. Additionally, a model with a gap between fences displayed an erosional zone immediately downwind and to the sides of the gap with accumulation displaced at a distance downwind.

Peterson and Schmidt (1984) found similar results using 1:20 scale models of shrub barriers. Gaps were set in the barrier to simulate shrub mortality and investigate the resultant distribution pattern. They also found a pattern of snowdrift erosion below and to the downwind sides of the gap with augmentation at a distance downwind of the barrier. The downwind influence of the gap on snow depletion was determined to be $2.5W$, where W is the width of the gap. Such patterns may exist at the scale of mountain ranges, but have not been tested.

Computer Models

Computer models of precipitation have been developed for various spatial and temporal scales -- a function of the variability in the precipitation process itself. Global Circulation Models or GCMs (e.g., Giorgi and Bates 1989) model atmospheric processes at the synoptic and regional scales. The topographic surface the Giorgi and Bates model runs on is a digital elevation model (DEM) of the western United States, smoothed to 60 km x 60 km grid cells. Within each cell containing high-elevation regions, several snow measurement sites should be represented. If so, the model would be reasonable if it used, in part, the measurement network represented in Figure 1

for input and validation. However, in their model, Giorgi and Bates use only 72 NWS climate stations that regularly report snow depths (which are strongly biased toward lower elevation and valley locations and are not density corrected). Regardless, for the one-month simulation period reported, modeled snow depths compared well with observed depths. This result may have been fortuitous however, given the coarseness of the validation network.

PRISM (Precipitation-elevation Regressions on Independent Slopes Model) is a regional to synoptic scale model for monthly averaged precipitation (Daley and Neilson 1992). PRISM's framework uses a 5-minute (9.3 km) DEM surface smoothed to 10 km x 10 km grid cells. Distribution of precipitation is calculated for topography using a precipitation-elevation gradient adjusted to the "orographic elevation" of each measurement point. Orographic elevation of a measurement point is the smoothed elevation of the DEM grid cell in which it resides. Orographic elevation incorporates the larger scale topographic factors that influence orographic precipitation and improved estimates of actual precipitation compared to estimates using the station elevation alone (Daley and Neilson 1992). The PRISM methodology enhances model sensitivity to local and regional landforms, while compensating for potential gaps in the measurement network (Daley and Neilson 1992).

Meso- to local-scale models attempt to resolve a complex array of physical and atmospheric processes that drive mountain precipitation events (Barros and Lettenmaier 1993). Barros and Lettenmaier (1993) developed a three-dimensional model on a ½-minute (90 m) DEM surface, smoothed to 10 km x 10 km horizontal resolution with six vertical layers for atmospheric processes. Temporal scales range from ten minutes to one hour with the capability of calculating annual precipitation. For model validation, monthly average precipitation was compared against eight NWS climate stations and three NRCS snow courses. Annual precipitation totals were compared against U.S. Geologic Survey (USGS) discharge measurements in three basins.

Individual storms were compared with the eight NWS precipitation stations. Model results supported validation measurements for seasonal and annual totals with a standard error of 10 to 15 percent. However, for storm distribution, the measurement network used for validation (and represented in Figure 3) is unable to resolve spatial distribution with a high level of confidence (Barros and Lettenmaier 1993).

Summary

Scale models of snow distribution downwind of barriers (snow fences and shelter belts) have proportional characteristics to full scale models. Gaps in barriers cause erosion of the snow drift behind the barrier (and to the downwind sides) to a distance of 2½ times the gap width.

Accurate computer modeling of precipitation distribution over synoptic and regional spatial scales rest in the ability to nest local-scale models of complex terrain into regional and meso-scale models (Giorgi and Bates 1989). Model development and validation is contingent on a measurement network that can capture the variability of precipitation at the local-scale. However, the probability of achieving such a physical measurement network is low. This posses a serious measurement problem for model validation and calibration process (Alford 1985; Barry 1992b).

The research described here for the Bridger Range may improve the validation process through empirical measurement of local-scale storm snow distribution. The local-scale network is nested within and compared with a meso-scale measurement network typical of mountainous regions in the western United States.

CHAPTER 3

METHODS

Measurement Transects

Three transects were measured and analyzed to determine snow distribution in the Ross Pass area and to test the influence of pass topography (Figure 5). Transect one (T1) is below Ross Pass and was established to measure the downwind influence of the Pass. Transect two (T2) is between one and two kilometers south of transect one and established to measure any eddying effects generated by westerly airflow through Ross Pass. Transect three (T3) is between two and three kilometers south of transect one and was established to measure snow distribution influenced by the Bridger Range Ridge Crest.

Sampling Sites

Selection criteria for measurement sites followed NRCS standard guidelines for SNOTEL site locations (Farnes 1967; 1971) and were inspected by Philip Farnes. Sites were located in small forested openings with negligible canopy influence in a 30° cone from vertical above the measurement point. Canopy densities of 10 percent or less in this 30° cone have a negligible influence on snow accumulation at the ground (Farnes 1994). Other site criteria established for this study included variable distances from the topographic divide and as great an elevational distribution as possible. These two criteria were constrained by logistic and safety concerns, which included land access, travel to sites via snowmobile and/or skis, access to all sites within a six-hour period, and exposure to avalanche tracks and run out zones.

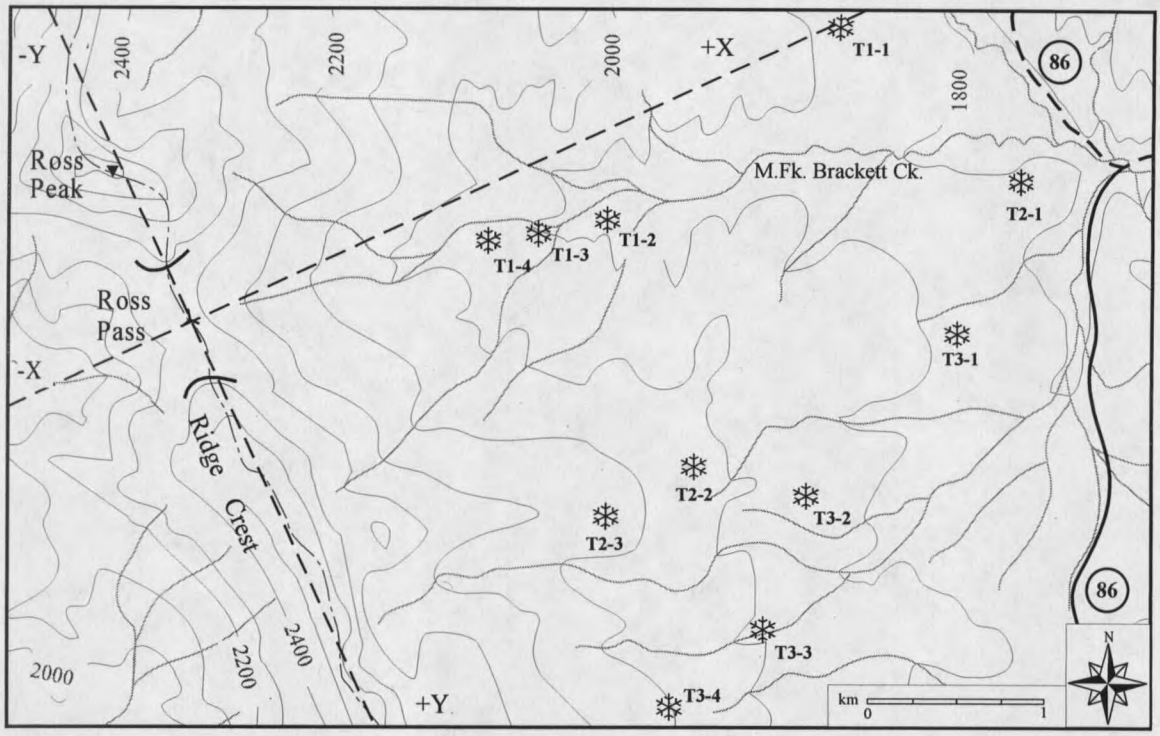

Figure 5. Measurement transects (T1, T2, and T3), sampling sites (snowflakes), and XY baselines (long dashes) in the Ross Pass Study Area.

The selection process of potential sites involved map analysis of land ownership and travel routes in the Brackett Creek Basin on a Gallatin National Forest map and USGS 7½' quadrangle map (Saddle Peak, MT). Travel corridors were assessed on skis during the winter of 1993. During this period, standard USFS 9 in. x 9 in. aerial photos of the Ross Pass area were analyzed for forest openings of appropriate size and locations along the three proposed transect lines. Potential sites were marked on the photos, and field reconnaissance was conducted during the summer of 1994. Final sampling sites were selected and flagged for later measurement. The selection procedure resulted in eleven sampling sites which are marked as snowflakes and labeled by transect with increasing elevation (Figure 5). Transects one and three have four sites each and transect two has only three sites.

Sampling Design

Snow distributions were measured on a seasonal basis and for individual storms. Seasonal snowpack accumulation was measured on March 1 and April 1. April 1st snowpack is generally considered the peak accumulation of the winter and was used to characterize seasonal snow distribution. Individual storms were measured from early November 1994 through March 1995.

Seasonal Samples

Double sampling, i.e., recording multiple depth measurements for each density measurement of the snowpack (Rovansek et al. 1993), requires knowledge of the time required for both depth and density measurements to determine an optimal depth-to-density ratio. Snow cores taken at seven sites in the Ross Pass Study Area (RPSA) on March 1 were used to determine the optimal depth-to-density ratio for the double sampling method. A depth-to-density sampling ratio of 4:1 was determined using March 1 data and double sampling formulae (Rovansek et al. 1993) (Appendix A).

Seasonal snowpack at the eleven RSPA sites was measured on April 1 using the double sampling procedure and a standard Federal Snow Sampler. Measured snow core weights were adjusted for oversampling (Farnes et al. 1982) (Appendix B, Table B-1).

Storm Samples

Storm periods were monitored from the Gallatin Valley and by an observer five miles east of the Bridger Range. Weather observations on the onset and abatement of snowfall and storm track were recorded to help with delineation of the storm period for compiling the storm meteorological data set. Storm sampling occurred when first possible after the cessation of snowfall.

Sampling sites consist of three storm boards placed such that a third of the opening was represented with less than 10 percent canopy influence. The purpose of this pattern was to obtain a representative average snowfall from each opening.

Snow accumulations on the storm boards were measured with a modified bulk sampler (USGS 1977). Storm boards were constructed with 5/8 in. plywood and were 40 cm x 40 cm (16 in. x 16 in.) square. Each board was painted white, as was a centered, vertical 1 in. x 1½ in. stake, 60 cm or 90 cm (24 in. or 36 in.) high.

Modified bulk snow samplers were constructed from #10 coffee cans and have an average inner diameter of 15.3 cm (Table 3). The diameter of the can, along with the narrowness of the can edge, reduces the sampling error to ≤1 percent (Beard 1994; Farnes 1994).

Table 3. Modified bulk sampler measurements.

can #	tare (gm)	cutter edge (cm)	outside dia. (cm)	inside dia. (cm)	inside rad. (cm)	cutter area (sq cm)
1	520	0.1	15.6	15.2	7.6	181.0
2	510	0.1	15.6	15.3	7.7	184.0
3	525	0.1	15.7	15.3	7.7	184.0
4	520	0.1	15.6	15.3	7.7	184.0
5	515	0.1	15.6	15.2	7.6	181.0
6	525	0.1	15.7	15.3	7.7	184.0
7	515	0.1	15.7	15.3	7.7	184.0
8	510	0.1	15.6	15.3	7.7	184.0
9	515	0.1	15.6	15.2	7.6	181.0
10	760	0.1	15.7	15.3	7.7	184.0
11	745	0.1	15.7	15.3	7.7	184.0
12	735	0.1	15.7	15.3	7.7	184.0
mean	-----	0.1	15.7	15.3	7.6	183.3
std dev	-----	0.01	0.05	0.04	0.02	1.11

A 2-kg hand-held spring scale, with a 30 percent zeroing capacity, was used to weigh snow core samples. Bulk sampler tare weights were recorded before measuring each sample. Spring accuracy was assessed twice during the season by weighing 100 ml, 200 ml, 300 ml, 500 ml, 700 ml, and 1500 ml of water at 70° F. All measurements were exactly at the specified weight

(i.e., one ml = one gm), with a scale accuracy of ± five grams.

Storm board measurements were taken by recording snow depth on the vertical stake to the nearest ½ cm and then inserting the bulk sampler in front of the stake down to the board. The board was inverted and a core removed from the board. Snow cores were weighed to the nearest five grams. Storm boards were cleaned and reset after each measurement. If snow depth exceeded the height of the bulk sampler, cores were sampled in sections. Snow was first removed from in front of the storm board and a folding ruler placed to measure the depth of snow. A thin sheet of aluminum was inserted horizontally as an intermediate base and a core removed to this level. The remaining snowfall was sampled in a similar way down to board level. All storm SWE measurements are reported in Appendix B, Table B-2.

Site Mensuration

Each sampling site was measured in the field for canopy influence, opening length, opening width, slope, aspect, and elevation (Table 4). Site location was also reconfirmed on aerial photos for determination of spatial coordinates using a Saltzman Projector.

Canopy influence for each storm board location was measured with a photocanopyometer (Codd 1959). Measurement sites with less than 4.5 m (15 ft) between storm boards required only one photograph to characterize the site (Farnes 1994). A dot overlay, with 15°, 30°, and 45° radii marked off the center, is placed over the photos and the number of dots covered by canopy within the 30° radii are counted. The sum of the dots counted are converted to percent canopy coverage for the site or measurement location (Codd 1959). Canopy influence for a site is the averaged value if more than one photograph was taken. Measurement sites showed less than 10 percent canopy influence (Table 4).

Site dimensions were measured by pacing, with length measured along the slope axis and

Table 4. Sampling site variables. Refer to text for explaination.

Site	Elev. km	Length m	Width m	Slope %	Aspect deg.	Canopy %	*Theta deg.	*Phi m	*Easting m	*Southing m	Ridge m	Pass m
T1-1	1.85	17	10	10	73	7.1	91.5	4030	4010	70	4322	1650
T1-2	1.88	42	21	6	55	0.9	100.5	2400	2340	450	2555	590
T1-3	1.90	47	13	11	91	3.2	102.0	2030	1980	410	2160	470
T1-4	1.94	9	16	8	50	1.2	100.5	1780	1730	310	1885	470
T2-1	1.80	17	11	12	346	0	106.0	4780	4560	1286	5010	780
T2-2	2.04	17	21	5	90	6.8	131.0	2880	2230	1960	2595	840
T2-3	2.16	25	20	16	60	1.5	140.0	2600	1680	1960	1875	1080
T3-1	1.87	17	12	14	32	0	116.0	4340	3880	1930	4225	90
T3-2	1.98	19	12	12	134	4.9	131.0	3620	2740	2380	3090	1000
T3-3	1.99	13	15	15	115	5.4	143.5	3640	2180	2950	2465	1750
T3-4	2.11	15	11	13	27	6.2	156.0	3500	1570	3140	1775	2200

*Origin at Ross Pass (Figure 5)

width measured perpendicular to the slope axis. The edge of the opening was where the conifer boughs were at a 90° angle to the pacer. Slopes were measured using a two-person clinometer method. Aspect was measured facing down the slope axis with a hand-held compass and azimuths adjusted for local magnetic declination (N15°E).

Elevations were measured with a hand-held altimeter adjusted at the Belgrade Airport at the start of each field day. During these measurements no storm fronts passed, however, afternoon convection potentially influenced measurement accuracy. Because of this, elevations were later recalculated using a Saltzman Projector. Aerial photos with site locations were projected onto the Saddle Peak quadrangle to place sites and elevations estimated from the map. Map elevations were assumed to have better accuracy than the field measurements and these values are reported in Table 4.

Spatial coordinates for each site were determined off the Saddle Peak quadrangle using the Saltzman Projector. Local baselines were established with the origin set at Ross Pass and rotated N25°W (Figure 5). This aligned the Y baseline with the Bridger Range in the Ross Pass Study Area. Polar coordinates were determined to assess any radial influence of Ross Pass on downwind

snow deposition. Phi (ϕ) is the linear distance in meters from the pass origin and Theta (θ) is the angle in degrees off an east-west line running through Ross Pass to the line defining Phi. A second coordinate set, easting (X) and southing (Y), is based on the local Cartesian grid centered at Ross Pass. The third set, ridge distance (X) and pass distance (Y), was determined by measuring the distance east from the ridge crest to the site and the absolute distance north-south of an east-west line running through Ross Pass (Table 4).

Meteorological Data

Upper air data was collected from the nearest NWS rawinsonde station at Great Falls, MT. This station is approximately 187 km (116 mi) north of Bozeman (Figure 2). Rawinsondes are launched at 0Z and 12Z (1700 hrs and 0500 hrs, local time respectively). Hard copy output of the Rawinsonde data was received at the end of each month from November 1, 1994 to April 1, 1995. Super et al. (1972) reported R values of 0.95 and 0.97 for 10,000 ft and 14,000 ft wind azimuths, respectively, over the Bridger Range as compared with Great Falls rawinsonde data. Because of these correlations, the 700 mb and 500 mb wind azimuths were used to characterize conditions over the Ross Pass area. Air temperatures and relative humidities were used from these, as well as the 850 mb pressure heights. Wind velocities did not correlate as well in Super's study with reported R values of 0.75 at the 700 mb and 0.85 at the 500 mb pressure heights. As a result, upper air wind velocities were only used from the 500 mb height.

Surface weather data was recorded 6 km (4 mi) south of the Ross Pass area on the ridge crest above the Bridger Bowl Ski Area (Figure 3). A data logger was in operation from November 4, 1994 to April 11, 1995 and recorded wind azimuth, velocity, air temperature, and snowfall at one-hour intervals, 24 hours per day. Wind velocity and air temperature were the variables used from this data set. Azimuths were not used because the topographic influence of the ridge crest

created a dominate westerly airflow with little variation during the winter. Snowfall data was also not used because it did not contain a density measure and was not directly comparable to the data collected in the Ross Pass Study Area.

CHAPTER 4

RESULTS

Weather Summary

Winter weather patterns in the continental interior of North America tend to have a wide range of variability (Barry and Chorley 1992). This variability is increased for mountainous regions where regional scale topographies may create distinctive weather and climatic regimes (Barry 1992a). Given this potential variability, the 1994-95 winter weather is compared with the 30-year climate to assess whether the 1994-95 winter was representative for the study area.

Monthly total snowfall was assessed at two National Weather Service (NWS) cooperative climate stations (Figure 3). Belgrade Airport (Gallatin Field) is in the Gallatin Valley 18 km (11 mi) west of the Bridger range crest at an elevation of 1,360 m (4,460 ft). Bozeman 12NE is 3½ km (2 mi) east of the Bridger range crest at an elevation of 1,825 m (5,990 ft). The period 1964 to 1993 was used to compute 30-year monthly averages for October to April.

Snowfall recorded at NWS climate stations is a depth measurement and does not include a measure of density (water content). Densities of newly fallen snow can vary from 30 kg m^{-3} to 300 kg m^{-3} (McClung and Schaerer 1993) depending upon temperature and wind characteristics at the time of deposition (McKay and Gray 1981). Also, new snow densities generally decrease with elevation due to adiabatic cooling of the atmosphere (Grant and Rhea 1973). The depth of new snowfall is further influenced by settlement due to gravitational effects on ice grains (McClung and Schaerer 1993) and temperature trends during and after snowfall. McClung and Schaerer (1993) report settlement densification as great as 10 cm day^{-1} for alpine settings. Timing

of snowfall, relative to measurement, can therefore influence the reported depth of new snow.

1994-95 Snowfall

Monthly cumulative snowfall for the 1994-95 winter was above the 30-year average every month except February at Belgrade Airport, while Bozeman 12NE recorded above average snowfalls during three months and below average snowfalls during four months (Table 5). In terms of 30-year variability, monthly snowfall exceeded +/- one standard deviation of the 30-year average on six of fourteen measurements -- March and April at Belgrade Airport and January, February, March, and April at Bozeman 12NE. Snowfall at Belgrade Airport was consistently above average except in February, and this kept the 1994-95 cumulative snowfall well above

Table 5. Monthly and seasonal snowfalls totals.

	Belgrade Airport (BAP)				
	Snowfall 1964-1993 (cm)	Snowfall 1994-1995 (cm)	Departure from 30-year average (cm)	Stnd deviation 30-year (cm)	Percent of 30-year average (%)
Oct.	5	12	7	8.6	240
Nov.	14	18	4	8.9	129
Dec.	17	25	8	10.0	147
Jan.	19	22	3	14.3	116
Feb.	13	5	-8	9.4	38
Mar.	22	52	30	14.0	236
Apr.	16	28	12	10.1	175
Seasonal	106	162	57	34.0	153

	Bozeman 12NE				
	Snowfall 1964-1993 (cm)	Snowfall 1994-1995 (cm)	Departure from 30-year average (cm)	Stnd deviation 30-year (cm)	Percent of 30-year average (%)
Oct.	32	31	-1	24.5	97
Nov.	72	101	29	34.1	140
Dec.	90	69	-21	38.5	77
Jan.	97	54	-43	30.6	56
Feb.	72	27	-45	28.1	38
Mar.	101	148	47	45.9	147
Apr.	80	117	37	36.6	146
Seasonal	544	547	3	119.1	101

average, exceeding one standard deviation of the 30-year average cumulative snowfall from November through April (Figure 6).

Bozeman 12NE had monthly snowfall variability that included both high and low totals compared with the 30-year average (Table 5). This opposing variability balanced the 1994-95 cumulative snowfall total to be nearly identical with the 30-year average cumulative snowfall for the station (Figure 6).

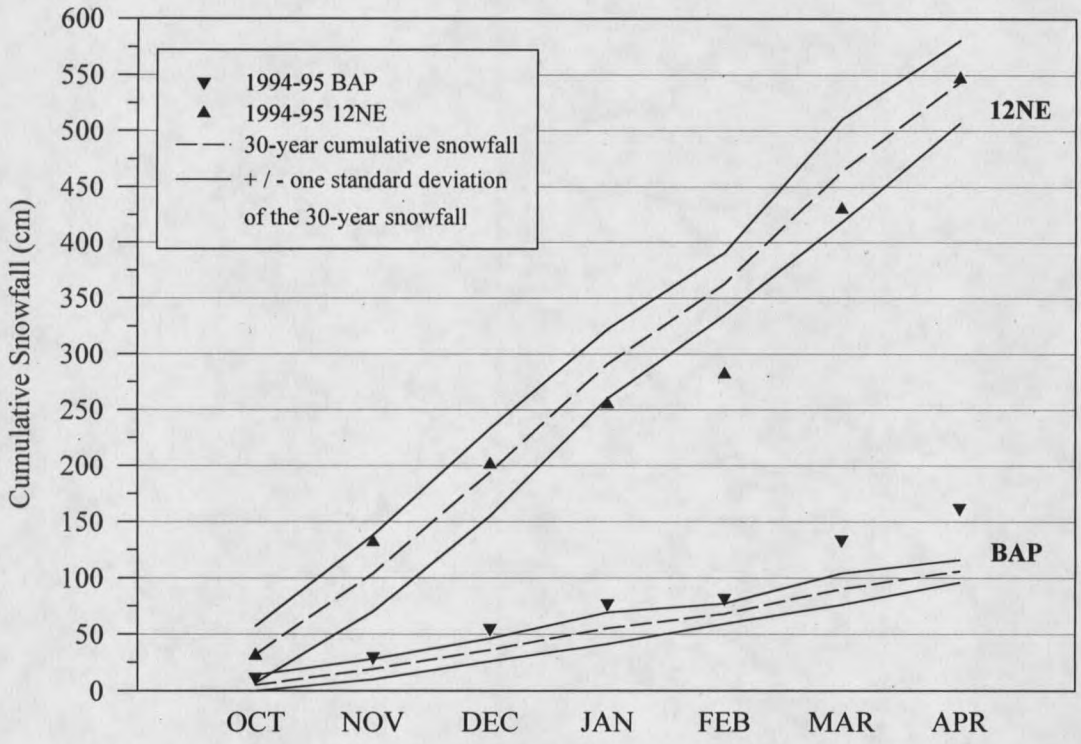

Figure 6. 1994-95 cumulative snowfall at Belgrade Airport (BAP) and Bozeman 12NE climate stations relative to 30-year monthly average cumulative snowfall.

Summary

Assessment of the 1994-95 winter snowfall indicates that the Gallatin Valley conditions recorded above average seasonal snowfall while mountain conditions (more relevant to the Ross Pass Study Area) recorded seasonally average snowfall. However, only the slightly higher than

average spring snowfall for the area differentiated 1994-95 from the average winter.

Seasonal Snow Distribution

The 1994-95 winter snowpack was measured at four NRCS snow survey sites and the eleven Ross Pass Study Area (RPSA) sites (Figure 7) on or near April 1. NRCS sites consist of high-low pairs, north (Brackett Creek [BC] and Sacajawea [SAC]) and south (Bridger Bowl [BB] and Maynard Creek [MC]) of Ross Pass. RPSA sampling sites are located along the middle and south forks of the Brackett Creek basin along three transects (Figure 7). Snow measurement sites sampled during the 1994-95 season span 430 m (1,400 ft) of elevation ranging from 1,800 to 2,230 m (5,900 to 7,315 ft). April 1 snowpack ranged from 244 to 607 mm (9.6 to 23.9 inches) of snow water equivalent (SWE) (Table 6).

Table 6. April 1 snowpack in the Bridger Range, MT.

Site name	Elevation (km above msl)	SWE (mm)
BC	2.23	485
BB	2.21	607
T2-3	2.16	374
T3-4	2.11	528
T2-2	2.04	300
SAC	2.00	305
T3-3	1.99	351
T3-2	1.98	374
T1-4	1.94	376
T1-3	1.90	378
MC	1.89	244
T1-2	1.88	353
T3-1	1.87	254
T1-1	1.85	239
T2-1	1.80	269

The NRCS has a 27-year record of April 1 snowpack at Bridger Bowl, Maynard Creek, and Sacajawea from 1968 and 1995. In 1992, Brackett Creek was added to the NRCS network.

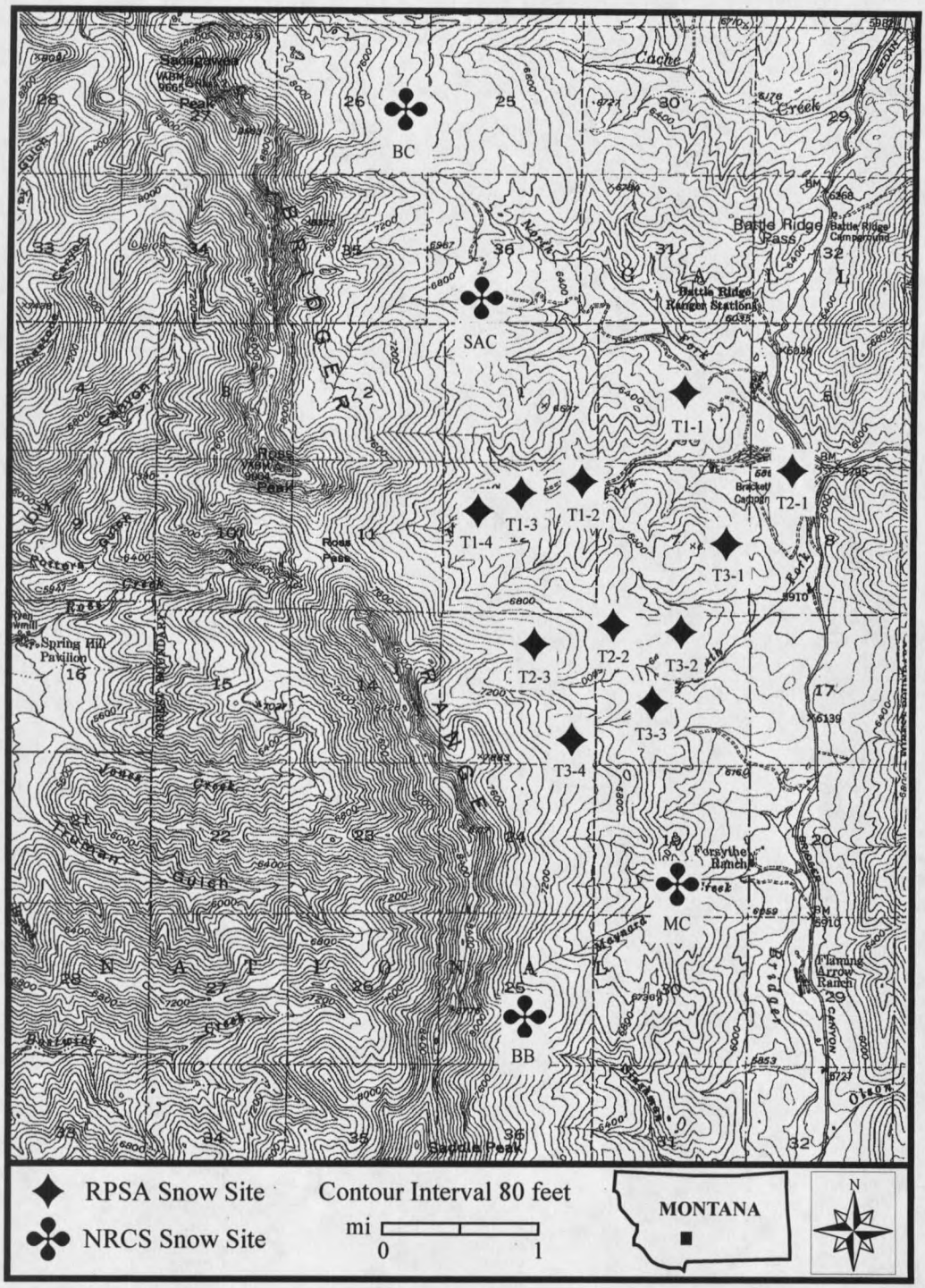

Figure 7. Ross Pass Study Area (RPSA) and Natural Resources Conservation Service (NRCS) snow measurement sites in the central Bridger Range, MT.

Bridger Range SNOTEL sites are ground truthed monthly using snowcores taken near the snow pillow and these are the data for BB, MC, and BC in Table 6. Snowcores were taken on or near April 1 with an unsharpened standard Federal Snow Sampler and cores adjusted for oversampling (Farnes et al. 1982).

The 27-year snow-elevation gradient for the Bridger Range of 879 mm km^{-1} was determined with an ordinary least squares regression and is plotted with 95% confidence intervals (CI) (Figure 8). Plotted against the 1968-95 data are the NRCS and RPSA snow-elevation gradients for April 1, 1995. Neither of the 1995 snow-elevation gradient lines fall completely within the 95% CI for the 27-year average. The NRCS 1995 snow-elevation gradient (1174 mm km^{-1}) is drier at low elevations and average at the high elevation site, while the RPSA snow-elevation gradient (468 mm km^{-1}) is much smaller, with greater SWE accumulation at low elevation and less at higher elevation. NRCS data indicate a smaller-than-average low elevation snowpack and average high elevation snowpack during the 1994-95 winter.

Snow-elevation data for the four-year period 1992-95 (Figure 9), which include the Brackett Creek SNOTEL, show overall drier winters with a smaller snow-elevation gradient (876 mm km^{-1}) compared with the 27-year period 1968-95 (Figure 8). The addition of the Brackett Creek SNOTEL, which is a higher elevation, yet drier, site than the Bridger Bowl SNOTEL, moderates the overall snow-elevation gradient for the range. All NRCS sites, except Bridger Bowl, represented the four-year average snow-elevation gradient in 1995. Bridger Bowl was well above the 95% confidence interval for average snow accumulation. Although the Maynard Creek and Sacajawea sites typified the four-year average, these low elevation sites were consistently drier when compared against the 27-year record (Figure 8).

Comparing the 1995 snow-elevation gradients for the NRCS and RPSA with the four-year average (Figure 9), the NRCS (937 mm km^{-1}) falls within the upper bound while the RPSA

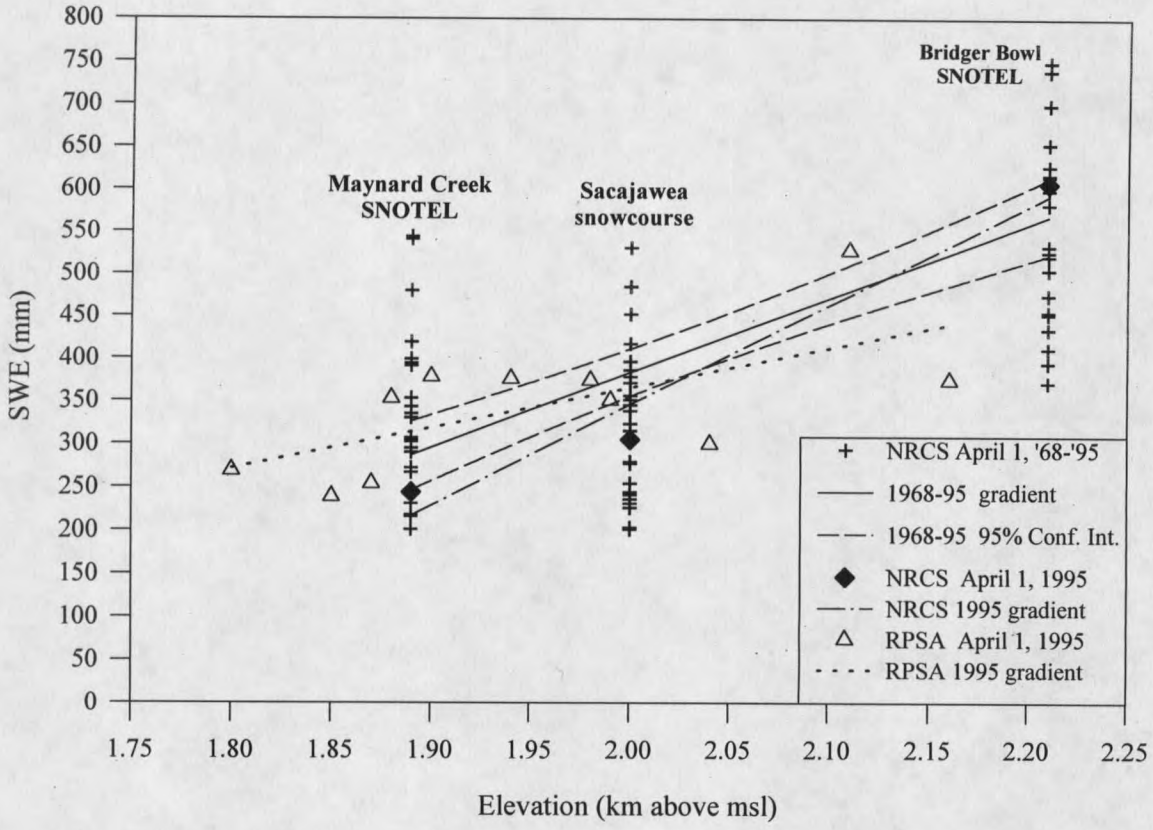

Figure 8. SWE vs elevation for Natural Resources Conservation Service (NRCS) 27-year and 1995 April 1 snowpack and Ross Pass Study Area (RPSA) 1995 April 1 snowpack.

(468 mm km^{-1}) falls outside the 95% confidence intervals bounds. This suggests that the 1995 NRCS April 1 snow-elevation gradient would be representative of recent winter snowpacks. However, the RPSA snow-elevation gradient differs at high elevations, and probably low elevations, compared with the 27-year average (Figure 8) but only at low elevations when compared with the 4-year NRCS data (Figure 9).

NRCS vs. RPSA

The predictive strength of the NRCS snow-elevation gradient for 1995 April 1 SWE is assessed using individual transects within the RPSA (Figure 10). All three of the transect lines fall within the 95% confidence interval (CI) of the NRCS gradient (938 mm km^{-1}) for their respective

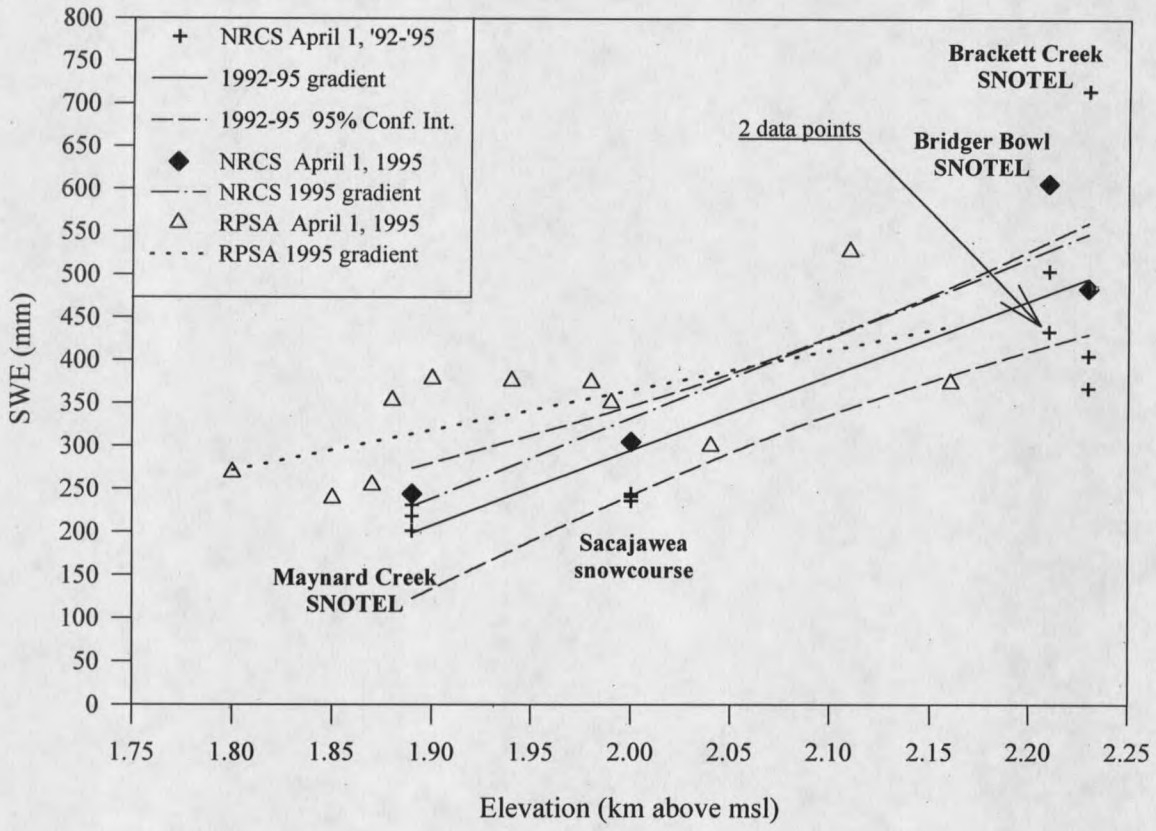

Figure 9. SWE vs elevation for Natural Resources Conservation Service (NRCS) 4-year and 1995 April 1 snowpack and Ross Pass Study Area (RPSA) 1995 April 1 snowpack.

elevational distributions. However, since Transect 1 does not include any true high elevation sites, it eludes rigorous testing of whether its snow-elevation gradient (1432 mm km^{-1}) would continue across higher elevations taking it out of the 95% CI. Depressed SWE accumulation at the upper site on Transect 1 suggests that this would not be the case. Transect 2 has a much smaller snow-elevation gradient (268 mm km^{-1}) compared with the other gradients. Transect 2 is drier than expected at high elevation and wetter than expected at low elevation sites, but remains within the 95% CI. Transect 3 has an snow-elevation gradient (1139 mm km^{-1}) similar to, although wetter, than the NRCS gradient. The NRCS gradient can "predict" both the snow-elevation gradients for individual transects and data points within the RPSA, however, this is mostly a product of the

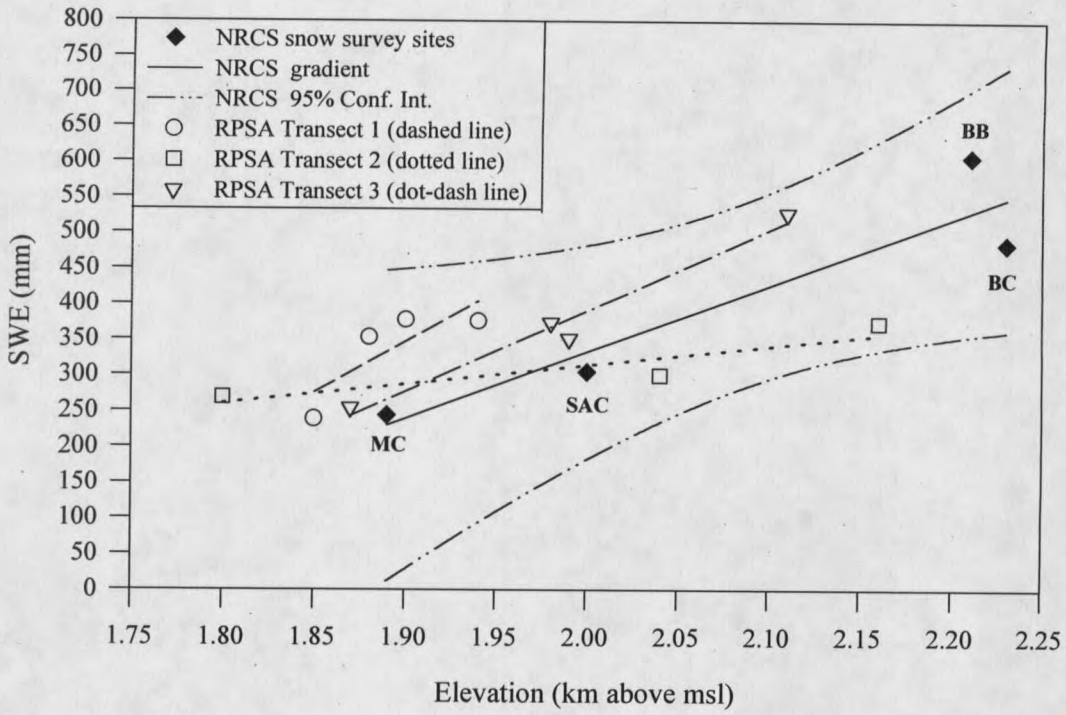

Figure 10. SWE vs elevation for Ross Pass Study Area (RPSA) transects compared to Natural Resources Conservation Service (NRCS) Bridger Range snow-elevation gradient for April 1, 1995.

small NRCS sample size (n = 4).

Inherent in a small sample is a large standard error of the estimate and consequently larger confidence intervals. Thus, it is improbable that the NRCS snow-elevation model would not predict the observed SWE and snow-elevation gradient(s) in the RPSA. Also, since the data set is small, assessing the residual distribution is difficult (Graham 1996) making it difficult to detect whether these data violate standard regression assumptions (Griffith and Amrhein 1991). However, since the NRCS sampling sites are not randomly distributed across elevation, but are set in high-low elevation pairs they would be unlikely to satisfy standard regression assumptions.

April 1 NRCS data plotted against RPSA data and snow-elevation gradient (Figure 11) shows that the NRCS snow-elevation gradient fails to fall within the 95% CI of the RPSA

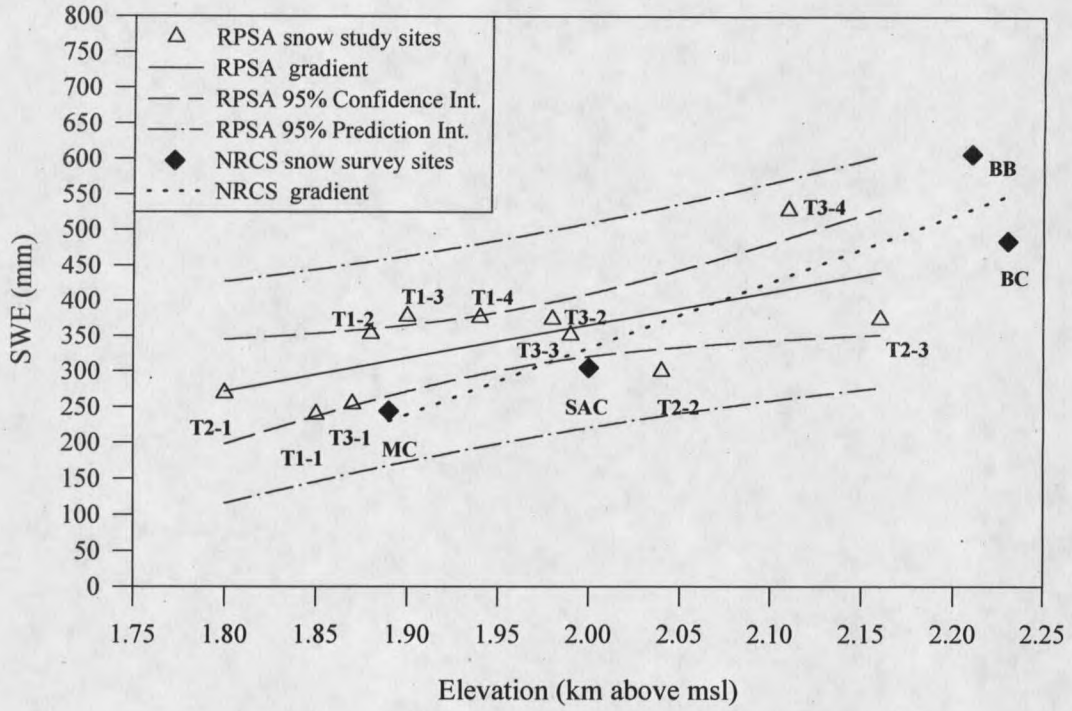

Figure 11. Natural Resources Conservation Service (NRCS) snow-elevation gradient compared with Ross Pass Study Area (RPSA) snow-elevation gradient, April 1, 1995. The dashed line is the 95% confidence interval of the RPSA snow-elevation gradient (solid line), the dot-dashed line is the 95% prediction interval of the RPSA data points, and the dotted line is the NRCS gradient.

gradient. However, the NRCS data appear to fall within the 95% prediction interval (PI). Although both high elevation sites (BB and BC) are beyond the elevational range predicted by the RPSA, if the 95% PI were extrapolated, they would likely fall within the interval. Note also that the RPSA data are not randomly distributed across elevation but are skewed toward lower elevations.

Conclusion

Interpretation of Figures 10 and 11 suggest that the null hypothesis -- NRCS measured snow accumulation gradient in the Bridger Range will not predict the measured snow accumulation gradient in the Brackett Creek area (RPSA) -- is rejected. Constrained by the small NRCS data set (n = 4), construction of a linear regression model resulted in a large standard error

of the estimate (74.1 mm), a large 95% CI, and an insignificant relationship with elevation ($p = 0.069$). The size of the 95% CI makes it improbable, or at least difficult, for NRCS data to contradict snow-elevation gradients measured in the RPSA (Figure 10). Conversely, the RPSA data set ($n = 11$) has a smaller standard error of the estimate (64.0 mm) and 95% CI and a significant relationship with elevation ($p = 0.029$). Although the RPSA snow-elevation relationship does not differ significantly from the NRCS, the NRCS snow-elevation relationship does differ significantly from the RPSA.

Storm Snow Distribution

The 1994-95 winter season produced 23 precipitation events (storms with measurable snowfall) between October and April 1. Field measurements of storm snow distribution were accomplished 20 times during this period, with 18 of the 23 storms recorded as individual storms. Samples were dropped from subsequent analysis if they did not contain individual storms or if melting was observed on the storm board prior to sampling. Seven storms met these criteria; five storms were contained in two samples and two storms where melting was observed at low elevation prior to sampling. A complete record of storm snow measurements in the RPSA during the 1994-95 season is reported in Appendix B, Table B-2.

The sixteen storms used for analysis are listed in Table 7. Storm SWE ranged from 1.3 mm to 46.5 mm at low elevation sites (T1-1, T2-1, and T3-1) and from 5.5 mm to 122.0 mm at high elevation sites (T1-4, T2-3, and T3-4). Storm SWE values were normalized (Table 8) by dividing storm SWE values with the largest storm value. Normalizing eliminated absolute variation and allowed for trend assessment between storms.

Table 7. Storm SWE (mm), number (#), and beginning date.

Site	#1 Nov. 12	#2 Nov.17	#3 Nov. 26	#4 Nov. 28	#5 Dec. 1	#6 Dec. 26	#7 Jan. 7	#8 Jan. 11
T1-1	2.4	12.4	6.6	10.8	19.1	6.5	7.3	12.6
T1-2	7.4	16.3	13.2	9.5	34.3	6.8	6.9	16.2
T1-3	9.4	17.3	14.1	9.8	36.3	7.3	7.0	16.2
T1-4	10.2	20.6	17.2	10.5	37.0	7.3	7.3	17.7
T2-1	1.3	10.8	8.5	10.4	27.6	9.6	7.8	12.8
T2-2	5.3	11.6	7.4	9.1	35.3	10.2	6.4	17.5
T2-3	7.8	13.8	8.1	8.6	40.4	10.2	7.0	17.5
T3-1	3.2	11.7	7.5	11.2	30.1	10.0	6.7	13.3
T3-2	5.7	13.2	8.9	10.1	35.1	10.7	7.5	16.3
T3-3	9.8	15.8	11.8	12.2	35.1	12.2	7.5	17.2
T3-4	13.1	19.7	14.3	12.7	43.3	12.8	9.1	20.8

Site	#9 Jan. 12	#10 Jan. 14	#11 Jan. 26	#12 Feb. 9	#13 Feb.	#14 Mar. 3	#15 Mar.	#16 Mar.
T1-1	3.3	12.2	10.7	6.8	4.4	18.4	4.8	46.5
T1-2	4.3	13.8	18.3	6.9	5.3	20.7	6.9	98.3
T1-3	4.4	15.0	12.1	6.7	5.3	21.4	11.2	106.1
T1-4	4.8	16.6	27.2	7.3	5.7	21.0	13.5	122.0
T2-1	3.2	12.6	11.5	6.2	4.2	16.6	4.2	52.0
T2-2	3.9	17.8	13.0	6.1	6.7	18.3	9.0	68.6
T2-3	3.7	20.8	23.5	7.4	7.5	18.6	10.8	87.3
T3-1	3.8	16.5	12.8	5.7	4.3	17.4	6.5	65.7
T3-2	4.8	20.4	19.0	7.1	7.5	19.8	9.7	69.9
T3-3	4.7	21.9	22.3	7.2	8.1	19.9	9.7	100.9
T3-4	5.5	25.8	27.8	9.5	9.1	19.5	17.7	115.5

Storm Meteorologic Data

Meteorological data for each storm (Appendix D, Tables D-1 - 4) was cut from the full data set to the nearest atmospheric sounding based on local observations for the beginning and end of each storm. Arithmetic average storm values for air temperature and relative humidity were calculated for each storm (Table 9). Averaged storm temperatures ranged by 12.3° C at the surface, 21.5° C at 850 mb, 14.5° C at 700 mb, and 10.0° C at 500 mb. Relative humidities varied by

Table 8. Normalized storm snow values, storm number (#), and beginning date.

Site	#1 Nov. 12	#2 Nov.17	#3 Nov. 26	#4 Nov. 28	#5 Dec. 1	#6 Dec. 26	#7 Jan. 7	#8 Jan. 11
T1-1	0.18	0.60	0.39	0.85	0.67	0.51	0.79	0.61
T1-2	0.57	0.79	0.77	0.75	0.79	0.53	0.75	0.78
T1-3	0.72	0.84	0.82	0.77	0.84	0.57	0.76	0.78
T1-4	0.78	1.00	1.00	0.82	0.85	0.57	0.80	0.85
T2-1	0.10	0.55	0.49	0.82	0.64	0.75	0.85	0.62
T2-2	0.40	0.57	0.43	0.72	0.81	0.80	0.71	0.77
T2-3	0.60	0.67	0.47	0.68	0.93	0.80	0.76	0.84
T3-1	0.25	0.57	0.44	0.90	0.69	0.78	0.74	0.64
T3-2	0.44	0.64	0.52	0.80	0.81	0.83	0.82	0.78
T3-3	0.75	0.77	0.69	0.96	0.81	0.95	0.82	0.83
T3-4	1.00	0.96	0.83	1.00	1.00	1.00	1.00	1.00

Site	#9 Jan. 12	#10 Jan. 14	#11 Jan. 26	#12 Feb. 9	#13 Feb.	#14 Mar. 3	#15 Mar.	#16 Mar.
T1-1	0.60	0.47	0.39	0.72	0.48	0.86	0.27	0.38
T1-2	0.77	0.53	0.66	0.73	0.58	0.97	0.54	0.81
T1-3	0.79	0.58	0.76	0.71	0.58	1.00	0.63	0.87
T1-4	0.87	0.65	0.98	0.76	0.63	0.98	0.76	1.00
T2-1	0.58	0.49	0.41	0.65	0.46	0.77	0.24	0.43
T2-2	0.71	0.69	0.47	0.64	0.74	0.85	0.51	0.56
T2-3	0.66	0.81	0.85	0.78	0.82	0.87	0.61	0.72
T3-1	0.69	0.64	0.46	0.60	0.47	0.81	0.37	0.54
T3-2	0.87	0.79	0.68	0.75	0.82	0.92	0.55	0.57
T3-3	0.84	0.85	0.80	0.75	0.88	0.93	0.55	0.83
T3-4	1.00	1.00	1.00	1.00	1.00	0.91	1.00	0.95

50% at 850 mb, 39% at 700 mb, and 44% at 500 mb.

Wind fields (velocity and azimuth) were averaged similar to temperatures and humidities and then classified into nominal groups (Table 10). Velocity classifications, based on snow entrainment, transport, and crystal habitat (Kind 1981; McClung and Schaerer 1993), were delineated into five classes: low, low-moderate, moderate, moderate-strong, strong (Table 11).

Table 9. Storm averaged air temperatures and relative humidity. Temperatures in degrees Celcius.

Storm #	Storm date	surface air temp.	850 mb air temp.	700 mb air temp.	500 mb air temp.	850 mb RH (%)	700 mb RH (%)	500 mb RH (%)
1	Nov. 12	-7.0	1.5	-10.0	-23.5	49	62	72
2	Nov. 17	-12.3	-7.0	-15.7	-31.7	85	77	48
3	Nov. 26	-11.0	-6.3	-13.0	-31.3	71	73	53
4	Nov. 28	-10.5	-4.0	-15.5	-30.5	44	54	55
5	Dec. 1	-6.0	-7.8	-12.2	-27.6	59	68	37
6	Dec. 16	-5.0	2.5	-7.5	-24.5	50	51	43
7	Jan. 7	-5.5	-4.0	-10.0	-24.5	61	72	73
8	Jan. 11	-3.0	6.0	-6.5	-24.5	50	64	55
9	Jan. 12	-6.0	3.5	-9.0	-27.5	52	72	59
10	Jan. 14	-5.0	2.3	-8.5	-27.0	62	63	52
11	Jan. 26	-4.0	3.0	-8.0	-25.3	66	84	71
12	Feb. 9	-15.3	-10.0	-21.0	-33.5	81	62	52
13	Feb. 26	-7.8	-12.4	-15.2	-28.4	83	77	29
14	Mar. 3	-8.0	-15.5	-13.3	-29.8	92	90	67
15	Mar. 15	-3.0	5.0	-8.0	-25.5	42	68	48
16	Mar. 24	-7.2	-3.6	-11.8	-24.6	69	68	64

Table 10. Storm averaged wind velocity and azimuth classes.

Storm #	Storm date	Surface velocity	500 mb velocity	700 mb azimuth	500 mb azimuth
1	Nov. 12	II	III	NW	SW
2	Nov. 17	I	I	**N**	- - -
3	Nov. 26	II	II	NW	**NW**
4	Nov. 28	II	III	NW	W
5	Dec. 1	II	IV	W	W
6	Dec. 16	III	IV	W	NW
7	Jan. 7	III	III	W	W
8	Jan. 11	II	II	W	W
9	Jan. 12	II	II	W	W
10	Jan. 14	II	II	W	**W**
11	Jan. 26	II	I	W	SW
12	Feb. 9	II	IV	N	NW
13	Feb. 26	II	III	N	W
14	Mar. 3	II	III	SW*	W
15	Mar. 15	II	III	W*	SW
16	Mar. 24	III	II*	**N**	**N***

Velocity Class Boundaries	
I	0 - 3 m/s
II	4 - 7 m/s
III	8 - 16 m/s
IV	17 - 25 m/s
V	> 25 m/s

Azimuth Class Boundaries	
NE	23 - 67
E	68 - 112
SE	113 - 157
S	158 - 202
SW	203 - 247
W	248 - 292
NW	293 - 337
N	338 - 22

* storm record incomplete **Bolded:** most common azimuth class assigned

Table 11. Velocity class characteristics.

Class	Speed	Description	Characteristics
I	0 - 3 m/s	Low	Light winds, no crystal entrainment,
II	4 - 7 m/s	Low-moderate	minimal snow displacement
III	8 - 16 m/s	Moderate	Crystal entrainment and displacement occurs,
IV	17 - 25 m/s	Moderate-strong	crystal transport becomes significant
V	> 25 m/s	Strong	High plumes, destructive habitat - i.e., evaporation and sublimation of crystals

Wind azimuths were classed with eight cardinal directions (Table 10). If winds did not vary by more than one azimuth class during the storm then a simple arithmetic average of azimuths was calculated. When storm winds varied by more than one class, the most common azimuth class during the storm was assigned as the storm value (bolded values in Table 10). (Storm #2 recorded no similar azimuth classes during the storm and thus could not be categorized).

Geographic Variables

Storm SWE distributions were correlated against the April 1 snowpack and the set of geographic variables measured for each site (Table 12). April 1 snowpack was only significantly related to one storm (#6) and then, the relationship was moderate with a correlation coefficient (R) of 0.74. Elevation was significantly related in eight of 16 storms with correlation coefficients ranging from 0.61 to 0.87. Radial coordinates, theta and phi, were significantly related in five and six storms, respectively, while the Y-coordinate set, southing and pass distance, were only significant in three storms each. The X-coordinate set, easting and ridge distance, was the most relevant of all geographic variables, with significance in 13 of 16 storms. Correlation coefficients ranged from -0.63 to -0.93 for easting and from -0.61 to -0.91 for ridge distance. Aspect and slope were not significant in any storm.

Table 12. Correlation coefficients for storm SWE vs. April 1 SWE and geographic variables. Aspect and slope were not significant in any storm. Two-tailed significance, bolded values are significant at the p = 0.05 level.

Storm	April 1	Elev.	Theta	Phi	Easting (X)	Southing (Y)	Ridge (X)	Pass (Y)
1	.2111	**.6099**	.4845	**-.6240**	**-.9040**	.2961	**-.9101**	.3530
	p= .533	**p= .046**	p= .131	**p= .040**	**p= .000**	p= .377	**p= .000**	p= .287
2	-.0146	.2856	.1066	**-.6568**	**-.7364**	-.0577	**-.7579**	.1904
	p= .966	p= .395	p= .755	**p= .028**	**p= .010**	p= .866	**p= .007**	p= .575
3	-.0327	.0773	-.0378	**-.6450**	**-.6289**	-.1515	**-.6481**	-.0091
	p= .924	p= .821	p= .912	**p= .032**	**p= .038**	p= .657	**p=.031**	p= .979
4	.4417	-.0566	.3123	.4433	.0818	.4353	.0783	.5457
	p=.174	p= .869	p= .350	p= .172	p= .811	p= .181	p= .819	p= .083
5	.1512	**.8699**	**.6555**	-.5893	**-.9249**	.4186	**-.9222**	.3741
	p= .657	**p= .001**	**p= .029**	p= .056	**p= .000**	p= .200	**p= .000**	p= .257
6	**.7368**	.5983	**.9365**	.3892	-.2062	**.9891**	-.1727	.5049
	p= .010	p= .052	**p= .000**	p= .237	p= .543	**p= .000**	p= .612	p= .113
7	.2196	.2158	.4217	.2820	-.1081	.4160	-.1093	**.7008**
	p= .517	p= .524	p=.196	p= .401	p= .752	p= .203	p= .749	**p= .016**
8	.2545	**.7787**	**.6634**	-.5333	**-.9052**	.4688	**-.9003**	.4275
	p= .450	**p= .005**	**p= .026**	p= .091	**p= .000**	p= .146	**p= .000**	p= .190
9	.1535	.4545	.4996	-.3926	**-.7181**	.4264	**-.7148**	.3241
	p= .652	p= .160	p= .118	p= .232	**p= .013**	p= .191	**p= .013**	p= .331
10	.5455	**.8448**	**.9437**	-.0625	**-.6344**	**.8598**	**-.6146**	.5644
	p= .083	**p= .001**	**p= .000**	p= .855	**p= .036**	**p= .001**	**p= .044**	p= .070
11	.2217	**.6164**	.4541	**-.6013**	**-.8529**	.2682	**-.8625**	.2767
	p= .512	**p= .043**	p= .161	**p= .050**	**p= .001**	p= .425	**p= .001**	p= .410
12	.1375	**.6083**	.5526	-.2053	**-.6026**	.3896	**-.6082**	**.7243**
	p= .687	**p= .047**	p= .078	p=.545	**p= .050**	p= .236	**p= .047**	**p= .012**
13	.4868	**.8680**	**.9004**	-.1848	**-.7188**	**.7704**	**-.6961**	**.6548**
	p= .129	**p= .001**	**p= .000**	p=.586	**p= .013**	**p= .006**	**p= .017**	**p= .029**
14	-.2589	.1556	-.0784	**-.8054**	**-.7245**	-.2322	**-.7415**	-.0099
	p= .442	p= .648	p= .819	**p= .003**	**p= .012**	p= .492	**p= .009**	p= .977
15	.1033	**.6764**	.5263	.-5783	**-.8740**	.3354	**-.8767**	.3222
	p= .762	**p= .022**	p= .096	p= .062	**p= .000**	p= .313	**p= .000**	p= .334
16	.1315	.4176	.2622	**-.7217**	**-.8507**	.0931	**-.8640**	.0859
	p= .700	p= .201	p= .436	**p= .012**	**p= .001**	p= .785	**p= .001**	p= .802

Linear regression of storm SWE against site elevation showed the large variability in elevational control of storm-scale snow distribution, with coefficients of determination (r^2) ranging

from 0.00 to 0.76 (Figures D-1 - 16). Regression residuals were correlated with the remaining geographic variables (Table 13) and no variable showed a consistent relationship with the residuals suggesting other variable(s) may be important in storm-scale snow distribution.

Table 13. Correlation coefficients for storm SWE-Elevation residuals vs. geographic variables. Two-tailed significance, bolded values are significant at p = 0.05 level.

Storm	Theta	Phi	Easting (X)	Southing (Y)	Ridge (X)	Pass (Y)
1	-.0262	-.5322	-.5602	-.1043	-.5812	.0955
	p= .939	p= .092	p= .073	p= .760	p= .061	p= .780
2	-.1356	-.5865	-.5436	-.2453	-.5712	.0631
	p= .691	p= .058	p= .084	p= .467	p= .066	p= .854
3	-.1022	**-.6212**	-.5723	-.2001	-.5929	-.0444
	p=.765	**p= .041**	p= .066	p= .555	p= .055	p= .897
4	.3597	.4253	.0391	.4712	.0367	.5723
	p= .277	p= .192	p= .909	p= 143	p= .915	p= .066
5	-.1322	**-.6098**	-.5447	-.2466	-.5698	-.0435
	p= .698	**p= .046**	p= .083	p= .465	p= .067	p= .899
6	.5501	**.7334**	.3059	**.7706**	.3348	.2905
	p= .080	**p= .010**	p= .360	**p= .006**	p= .314	p= .386
7	.2488	.3621	.0560	.2888	.0509	**.6172**
	p= .461	p= .274	p= .870	p= .389	p= .882	**p= .043**
8	.0291	-.4383	-.5066	-.0236	-.5202	.1170
	p= .932	p= .178	p= .112	p= .945	p= .101	p= .732
9	.1382	-.2715	-.4213	.1618	-.4264	.1318
	p= .685	p= .419	p= .197	p= .635	p= .191	p= .699
10	.4555	.4069	.0053	**.6263**	.0151	.3369
	p= .159	p= .214	p= .988	**p= .039**	p= .965	p= .311
11	-.0718	-.5040	-.4926	-.1456	-.5183	-.0046
	p= .834	p= .114	p= .124	p= .669	p= .102	p= .989
12	.0613	-.0045	-.1811	.0149	-.2015	.5640
	p= .858	p= .990	p= .594	p= .965	p= .552	p= .071
13	.3652	.2074	-.1289	.4659	-.1135	.5237
	p= .269	p= .541	p= .706	p= .149	p= .740	p= .098
14	-.2098	**-.7631**	**-.6147**	-.3328	**-.6346**	-.0817
	p= .536	**p= .006**	**p= .044**	p= .317	**p= .036**	p= .811
15	-.0462	-.4087	-.4939	-.1149	-.5134	.0199
	p= .893	p= .135	p= .123	p= .736	p= .106	p= .954
16	-.0922	**-.6419**	-.5895	-.1830	**-.6122**	-.1144
	p= .787	**p= .033**	p= .056	p= .590	**p= .045**	p= .738

Meteorological Variables

Meteorological variables elude statistical significance testing in this study because of the small sample size and only one value per storm. However, it is believed that wind azimuth and velocity are significant environmental variables in determining storm snow distribution. Air temperatures and relative humidity are also factors influencing snowfall -- temperature on crystal habit and fall velocities and relative humidities on rates of growth and secondary crystal features (Schemenauer et al. 1981) -- however, these variables are believed to be less significant in controlling spatial distribution of storm snowfall.

Conclusion

Based on the 1994-95 storm data collected and analyzed with correlation matrices (Tables 12 and 13), the null hypothesis -- site elevation will not account for the predominance of storm snowfall distribution with a lesser amount of the variance accounted for by wind azimuth, wind velocity, air temperature, relative humidity, distance from a ridge, and distance from a pass -- is accepted. It was found that the measure of distance from the ridge crest was significant in 81% of storms as opposed to elevation that was significant in only 50% of storms. Moreover, distance from the ridge accounted for a larger (or equal) portion of variance for six of the eight storms when elevation was also significantly related (Table 12).

CHAPTER 5

DISCUSSION

Seasonal Snow Distribution

Snow vs. Elevation

Seasonal snow distributions are described using using linear equations with elevation (Washichek and McAndrew 1967; Caine 1975; Locke 1989) and elevation combined with geographic coordinates (Locke 1989; Custer et al. 1996). Rationale for this may reside in the computational simplicity of linear models and in the general strength and significance of the seasonal snow-elevation relationship, with reported r^2s from 0.43 (Caine 1975) to 0.91 (Locke 1989). However, seasonal snowpacks do not consistently conform to linear models and may display nonlinear traits in their distributions (Barry 1992a).

More importantly however, is the reality of sample size and distribution generally available for snow-elevation determination. Snow measurement networks are rarely greater than four to six per range and generally in high-low sets. This constrains the use of nonlinear models that would require larger data sets with measurement points at intermediate elevations to construct a relationship with meaningful confidence intervals.

Second-order equations may better explain seasonal snowpack accumulation gradients when compared with linear equations. The mechanics of the precipitation process generally produce greater precipitation at higher elevations due to the decrease in water holding capacity of the atmosphere (Barry and Chorley 1992; Barros and Lettenmaier 1994) with precipitation maxima below summit elevations in higher ranges (Hjermstad 1970; Barry 1992a). Additionally,

mid-season ablation and erosion from warm temperatures, wind, and rain events may further enhance the elevational bias by differentially affecting lower elevations. Moreover, boundary layer wind fields entrain and displace snow crystals in high gradient areas (ridges and passes) and deposit them in low gradient areas such as lee slope wind shadows below ridge crests (Alford 1980; Barry 1992a; McClung and Schaerer 1993). Both linear and second-order equations were investigated and applied to the Bridger Range 1994-95 snowpack to analyze the snow-elevation relationship.

Bridger Range 1994-95 Snow Distribution Models

Linear regression of April 1 SWE with elevation (Figure 12), using the combined Bridger Range snow sites in Figure 7, produced the model:

$$\text{SWE (mm)} = -887 + 628 * \text{Elevation (km)} \quad (1)$$

with a r^2 of 0.62 and standard error of 67.7 mm. Elevation was highly significant with $p = 0.0004$.

Multiple linear regression, including distance from the ridge (X), absolute distance north-south of the Pass (Y), and elevation (Z), returned a model with a r^2 of 0.67 ($p = 0.005$), but an increased standard error to 69.0 mm. Although all variables are significantly correlated to April 1 SWE individually, none of the variables were significant when combined in a multivariate model. Multiple stepwise linear regression failed to enter any variable into the model after elevation. The lack of significance for individual variables in the multivariate model is a product of the strong covariance between elevation and both distance east of the ridge (X) and distance north-south of the Pass (Y).

A second-order linear regression (Figure 13), also using the combined Bridger Range snow sites, produced the model:

$$\text{SWE (mm)} = 1963 - (2204 * \text{Elev.}) + (700 * \text{Elev.}^2) \quad (2)$$

with a r^2 of 0.64 and standard error of 69.4 mm. Only one additional site (SAC) was encompassed

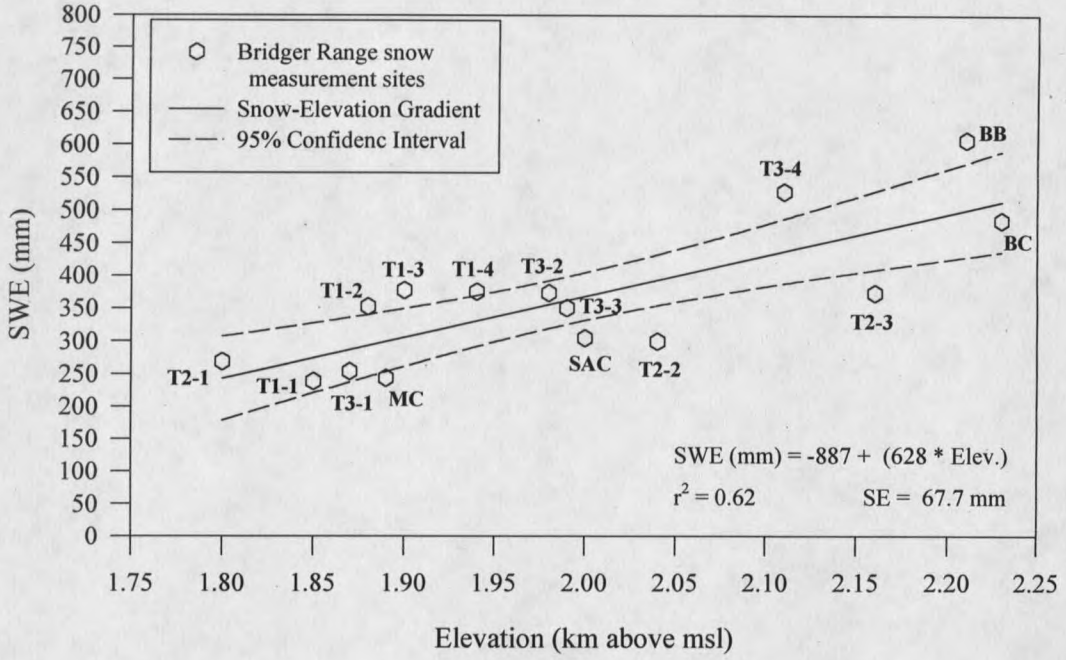

Figure 12. Linear regression of snow and elevation for the central Bridger Range, MT (n = 15) April 1, 1995. SE refers to standard error.

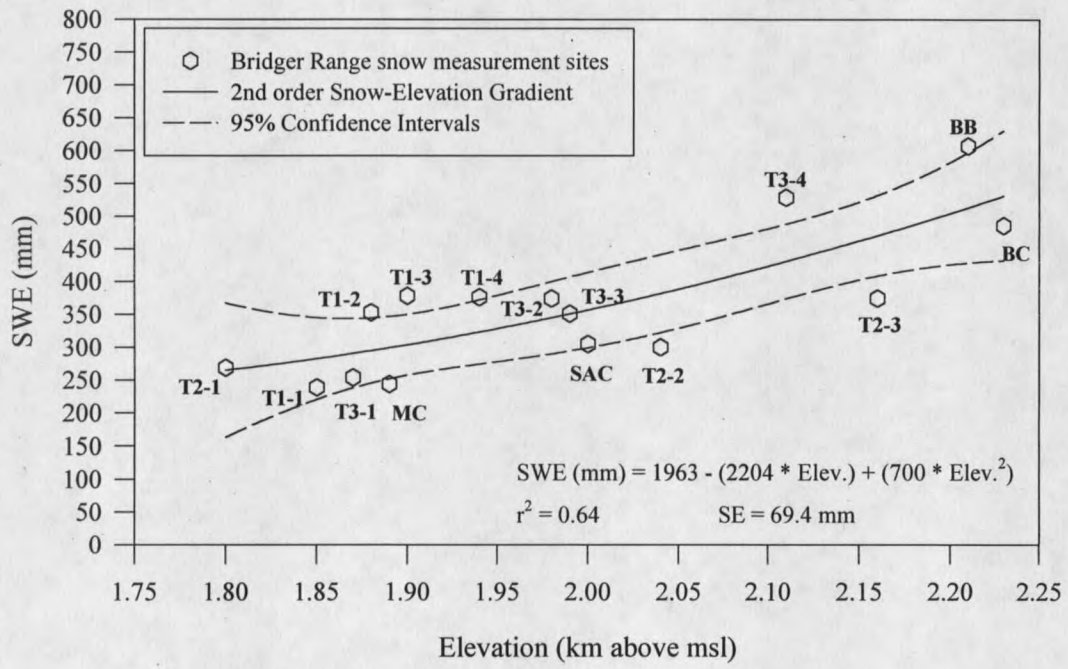

Figure 13. Second-order regression of snow and elevation for the central Bridger Range, MT (n = 15) April 1, 1995. SE refers to standard error.

by the 95% confidence intervals.

Apparent in Figures 12 and 13 is the nonlinear pattern of snow (SWE) with elevation. This pattern appears to have a sinusoidal function and is not a log-linear or log-log function. Given that the snow-elevation relationship follows an unknown, complex function, and a second-order regression produced minimal improvement on the snow-elevation relationship, the linear model with elevation is used for investigating the spatial distribution of snow in the Bridger Range.

Spatial Controls of Seasonal Snowpack

Residuals of the linear snow-elevation model do not correlate significantly to any set of XY variables and scatter plots do not reveal any inherent trends. A residual map (Figure 14) does present some potential trends and insight as to remaining controls on seasonal snow distribution in the central Bridger Range. The residual map has a "-", "+", or "**0**" next to the site name based on whether the site was below, above, or inside the 95% confidence interval in Figure 12.

The spatial distribution of dry (-) and wet (+) sites in Figure 14 can be interpreted as two distinct patterns generated by the ridge and the pass. First, the influence of the Bridger ridge, with high relief over a short distance and perpendicular to prevailing winds, augments snow accumulation closer to the ridge, indicated by sites T3-4 and BB, than would be predicted by elevation alone. This observed accumulation is consistent with snow drift patterns behind snow fences and topographic features (Tabler and Jairell 1980) and snow distribution patterns over sharp ridge lines (McClung and Schaerer 1993).

Second, the influence of Ross Pass on snow distribution augments snow accumulation at a greater distance downwind of the ridge crest and at lower elevations, indicated by sites T1-2, T1-3, and T1-4, than would be predicted by elevation alone. Additionally, lateral depletion zones were observed both north and south of Ross Pass, indicated by sites T2-3, T2-2, and SAC, which are

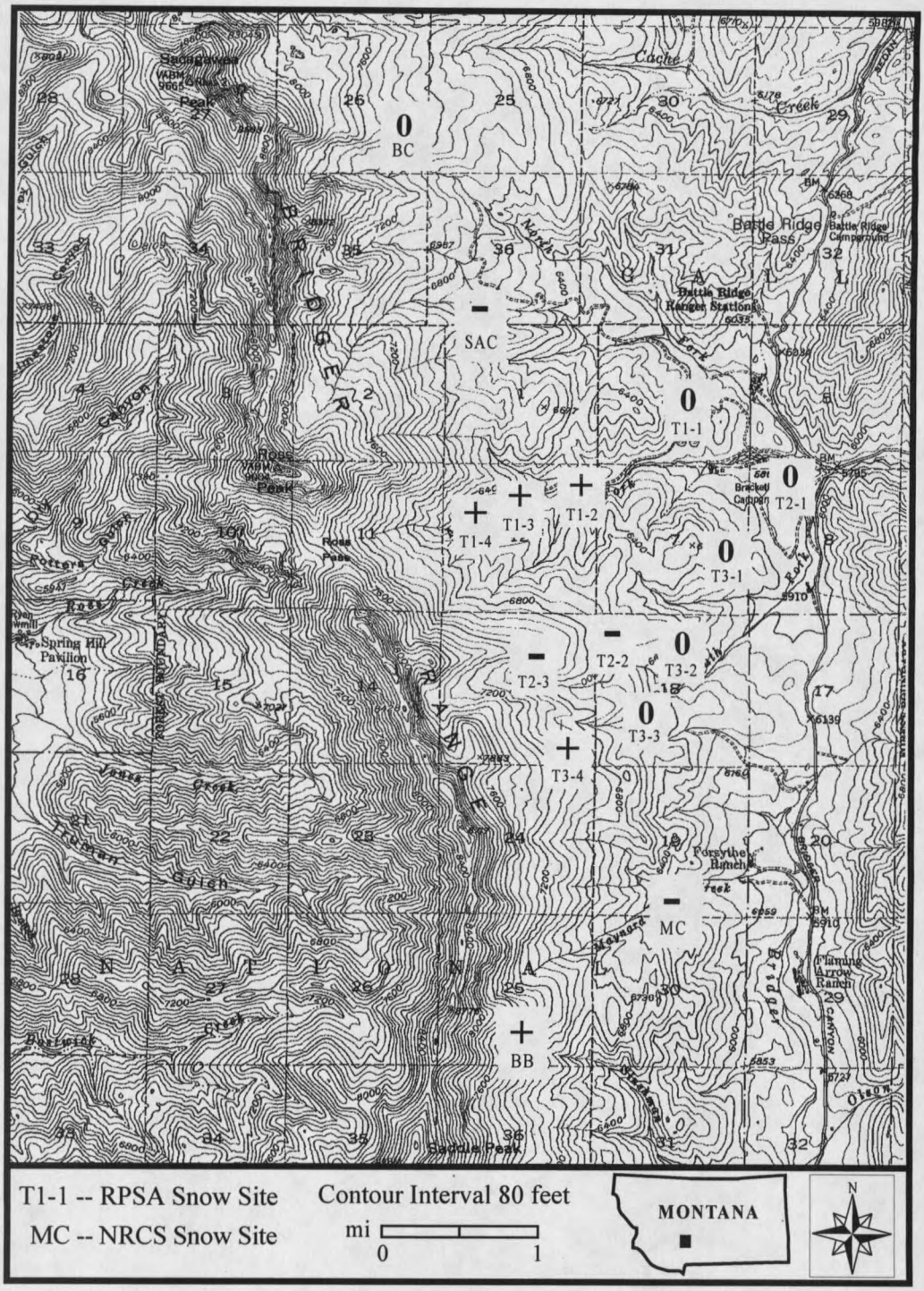

Figure 14. Residual map of the April 1 snow-elevation regression (Figure 12) for the Bridger Range, MT. Sites with "-" have less than average accumulation, "+" have greater than average accumulation, and "**0**" have average accumulation as predicted by the snow-elevation relationship.

both closer to the ridge and/or at a higher elevation than predicted by the model. Again, a snow fence analogy can be used (Peterson and Schmidt 1984). Given an averaged gap size (W) of 400 m (1,300 ft) for Ross Pass, a depletion zone would be expected to extend 1,000 m (3,280 ft) downwind ($2.5W$), with an augmentation zone below that (Peterson and Schmidt 1984). Site T1-4 is located roughly 1,600 m downwind of Ross Pass.

Seasonal snow distribution in the central Bridger Range is diagrammatically illustrated in Figure 15. Controlling factors of this pattern are found by increased wind velocities through topographic constrictions (Oke 1987; Barry 1992a), entrainment of snow crystals in strong wind fields (Kind 1981; McClung and Schaerer 1993), and by conditional flow separation of air stream lines over barriers (McKay and Gray 1981; Barry 1992a) which create eddies in the meso-scale wind field over the Bridger Range. The increased wind velocities through Ross Pass entrain snow crystals further downwind creating areas of relative snowfall depletion below and to the sides of the pass and an area of relative snowfall augmentation further downwind than is observed downwind of the ridge crest.

Observed snow distribution on April 1 conform to these theories at all but one site -- Maynard Creek SNOTEL (MC). The relative depletion of April 1 snow accumulation at Maynard Creek is mostly likely attributable to site location and forest influence factors. The snow course used for ground truthing is placed along one edge of the opening and has canopy interception potentially reducing snowfall. This factor, which was not adjusted for in this study, may have reduced April 1 SWE below the predicted level.

Forestry practices in the Brackett Creek Basin during the 1980's and earlier have left several clear cut and partial cut harvest areas. A clear cut area is located east of Ross Pass, north of Transect 2 and upwind of Transect 1. During high wind events, redistribution of snow is possible along the upper portions of these transects and may have led to seasonal accumulation different

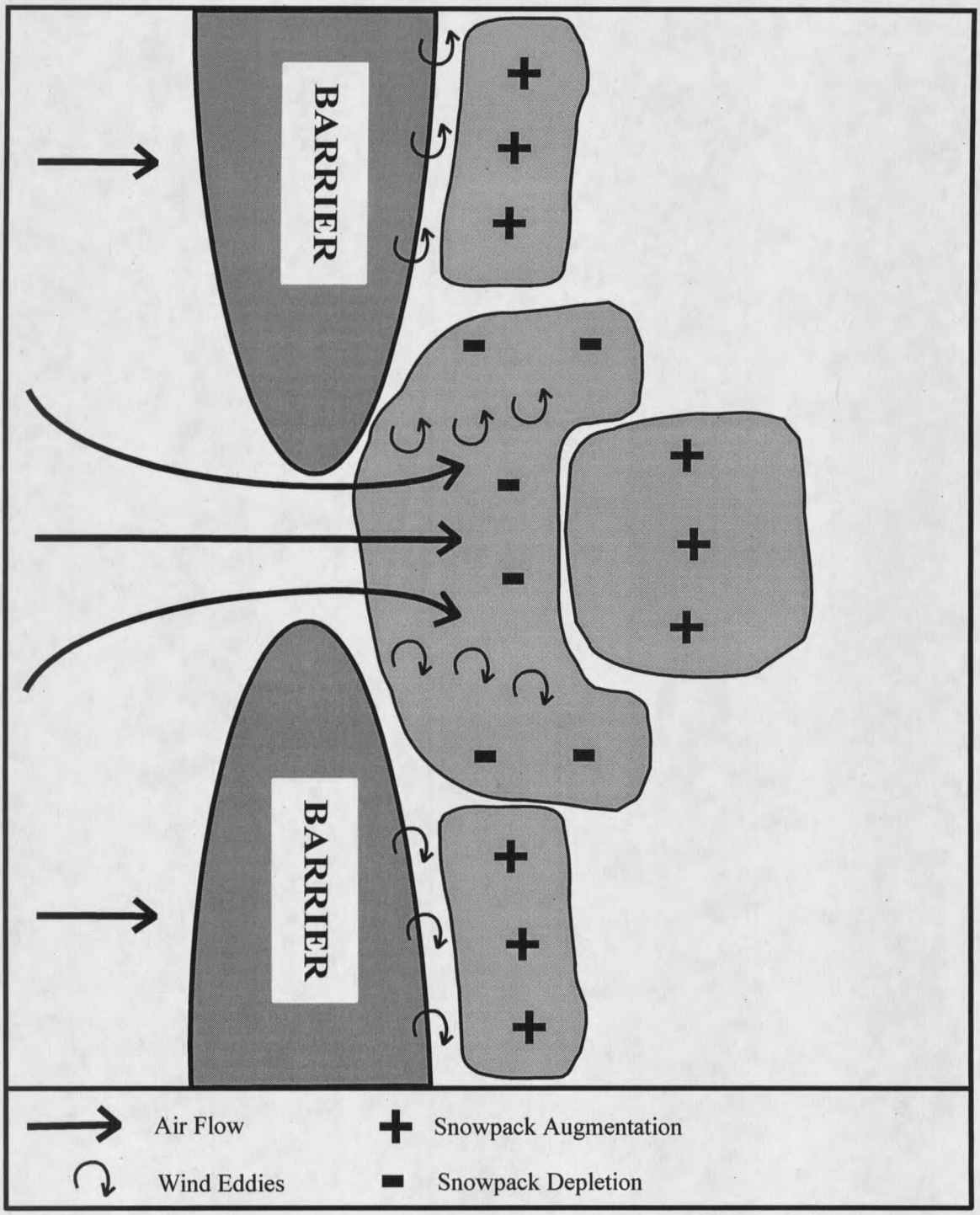

Figure 15. Conceptual model of snow distribution downstream of a wind barrier. Adapted from Tabler and Jairell (1980), Peterson and Schmidt (1984), and Oki (1987).

than predicted by elevation. If this were the case, then seasonal accumulations at sites T2-3, T2-2 and T1-4 would be greater than expected. However, a lower than expected accumulation was observed at sites T2-3 and T2-2 and, although site T1-4 was greater than expected, it had less accumulation than sites T1-3 and T1-2, which are both at greater distances from the clear cuts. The overall influence of forestry practices on snow distribution in this study is thought to be minimal, was not controlled for, and is considered part of the unexplained variance.

The existence of a variable(s) other than elevation that strongly influence seasonal snow accumulation may be seen by comparing interpolated surfaces of topography (Figure 16) and April 1 SWE (Figure 17) in the Ross Pass Study Area. The mesh surfaces were produced with a 15 X 15 grid interpolation scheme in SigmaPlot (Jandel 1994) using sampling site northing and easting as XY data, and site elevation and April 1 SWE as Z data.

Comparison of maximum elevation along upper ends of the three transects (Figure 16) shows that Transect 2 is about 10% higher than Transect 1 and 2% higher than Transect 3. By comparison, April 1 SWE (Figure 17) shows an accumulation at the upper end of Transect 2 about 30% less than Transect 3 and generally equivalent to Transect 1. These differences in the topographic and April 1 SWE surfaces add graphical support to the idea that snow accumulation is not solely controlled by elevation.

Storm Snow Distribution

Topography influences storm-scale snow distribution by modifying boundary layer wind fields and establishing localized wind jets and eddies (Oke 1987). Local-scale, topographic predictors of storm snow distribution are primarily a combination of elevation and distance downwind of the barrier. Although ridge distance was a better predictor of the 1994-95 storm distributions in the RPSA (Table 12), strong covariance with elevation hinders isolation of a

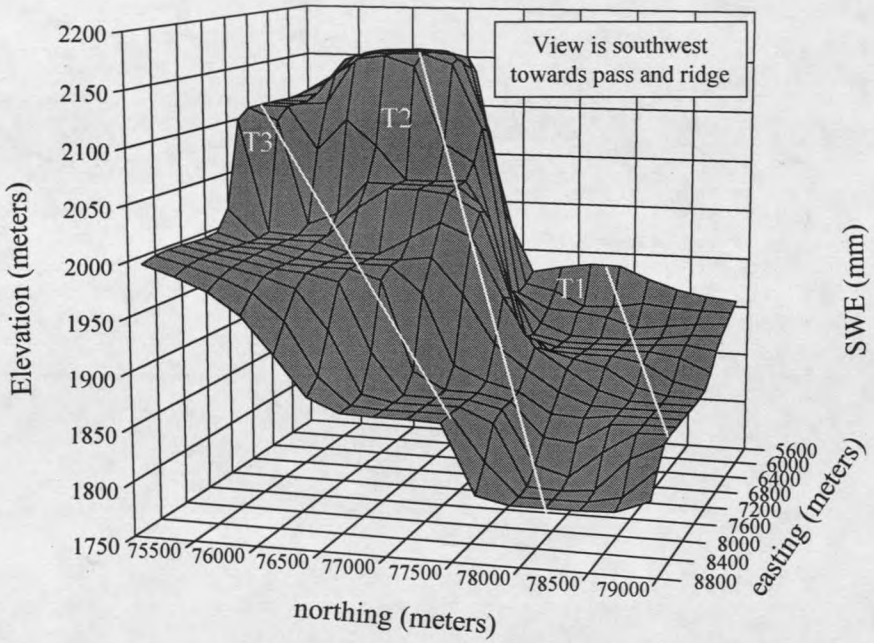

Figure 16. Interpolated surface of topography in the Ross Pass Study Area (RPSA).

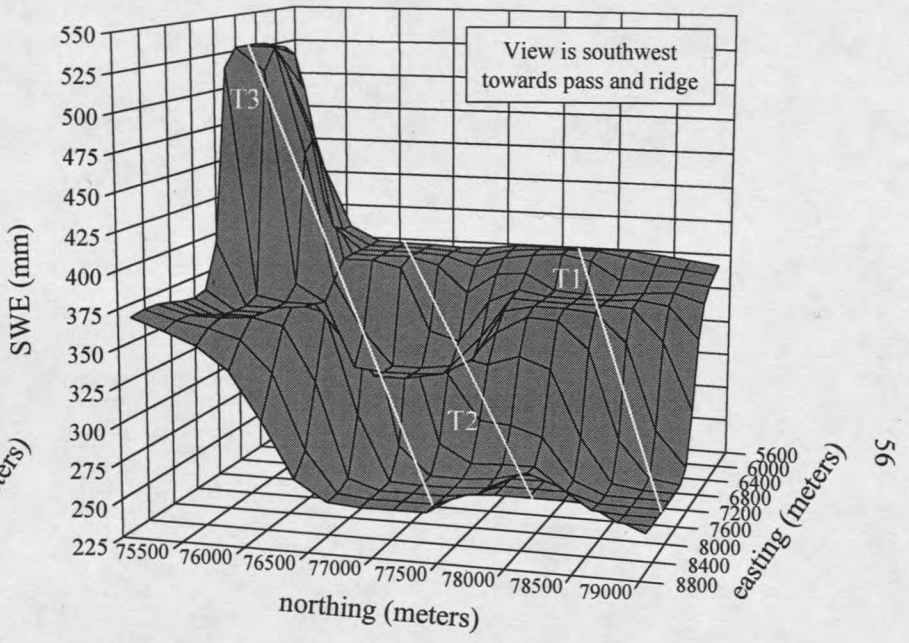

Figure 17. Interpolated surface of April 1, 1995 snowpack (SWE) in the Ross Pass Study Area (RPSA).

unique signal. Thus, elevation and ridge distance are considered equally competent as linear predictors of storm-scale snow distribution in this study.

Of the remaining geographic variables assessed, only theta and phi were significantly related to SWE in more than a couple of storms (Table 12). Their predictive ability however was inconsistent, with significance in only five (theta) and six (phi) storms, respectively. Additionally, use of these variables is limited to areas downstream of topographic constrictions. No other geographic variable offered any consistent or reliable explanation of storm-scale snow distribution.

Downwind (east side) depositional patterns in the RPSA appear to strongly mimic those found with snow fence and shrub barrier models (Tabler and Jairell 1980; Peterson and Schmidt 1984). Snow depletion and augmentation zones were consistently evident along each transect line as described by the barrier models and conceptually illustrated in Figure 14. These regions also exhibited strong internal consistency throughout the sixteen storm events (Figures D-1-16) which suggests the possibility of applying snow fence models to the mountain barrier level for determination of snow distribution.

Storm Class Analysis

Normalized snow distribution and interpolated surfaces of snow distribution (Figures D-1 -16) were plotted and visually grouped into clusters of similar patterns. Clustering identified four primary storm classes with similar distributions and two sub-class distributions. Storm classes were characterized by the nature of elevational SWE distribution along transect lines; magnitude of high elevation SWE depletion on Transect 2; differences between low and high elevation accumulation; and whether Transect 1 or 3 recorded the largest high elevation SWE (Table 14).

Initial storm groupings were validated using Pearson correlation coefficients (Table 15). Refinements were made to Classes 2 and 2a based on R values that indicated a better groupings. Of the sixteen storms, three storms each were classified as Class 1 and Class 1a (Figure 18), and

Table 14. Storm classifications.

Class	Storm Distribution Characterisitics
1	Elevational increase of SWE along transects. Large relative difference between low and high elevation accumulation. Weak high elevation SWE depletion along T2. T3-4 maximum accumulation.
1a	Elevational increase of SWE along transects. Large relative difference between low and high elevation accumulation. Strong high elevation SWE depletion along T2. T1-4 maximum accumulation.
2	Elevational increase of SWE along transects is inconsistant. Moderate to strong SWE vs Elevation relationship. T3-4 maximum accumulation.
2a	General elevational increase of SWE along transects. Moderate to strong SWE vs Elevation relationship. T3-4 maximum accumulation.
3	Elevational increase of SWE along transects is inconsistant. Weak high elevation SWE depletion along T2.
4	T1, T2 low elevations have greater accumulation than high elevations. Weak high elevation SWE depletion along T2.

Class 2 and Class 2a (Figure 19) and two storms each as Class 3 and Class 4 (Figure 20). All storms within classes were significantly related (bolded values, Table 15), however, they may have also shown stronger correlations with other storms. In these situations, a lower correlation was accepted if the storm distribution fit better into characteristics described in Table 14 and the storms remained significantly related.

Meteorological Influences

Zones of snow depletion and augmentation varied in magnitude between storms (Figures D-1 - 16) that implies a degree of meteorological influence on storm distributions. Grouping meteorological parameters by storm class allowed for class-averaged values to be estimated. Wind

Table 15. Correlation coefficients for storm vs. storm SWE distributions. Two-tailed significance at the p = 0.05 level. Bolded values are members of the storm class for that column.

	Class 1	Class 1a		Class 4	Class 2	Class 2a			Class 3						
Storm #	**1**	**2**	3	**4**	**5**	**6**	7	8	**9**	10	11	12	13	14	15
2	.8975														
	p=.000														
3	.7994	**.9486**													
	p=.003	**p=.000**													
4	.3053	.3302	.2689												
	p=.361	p=.321	p=.424												
5	.8863	.6846	.5207	.0510											
	p=.000	p=.020	p=.101	p=.882											
6	.2942	-.0416	-.1233	.4713	.4043										
	p=.380	p=.903	p=.718	p=.143	p=.217										
7	.4268	.4348	.3502	**.6989**	.3683	.4794									
	p=.190	p=.181	p=.291	**p=.017**	p=.265	p=.136									
8	.9426	.7752	.6516	.2273	**.9593**	.4626	.4889								
	p=.000	p=.005	p=.030	p=.502	**p=.000**	p=.152	p=.127								
9	.8862	.7960	.7306	.4718	.7321	.4039	.5185	.8561							
	p=.001	p=.003	p=.011	p=.143	p=.010	p=.218	p=.102	p=.001							
10	.6865	.3821	.2111	.4070	.7930	**.8439**	.5109	.8177	.7171						
	p=.020	p=.246	p=.533	p=.214	p=.004	**p=.001**	p=.108	p=.002	p=.013						
11	**.9382**	.8814	.7580	.2328	.8695	.2778	.4600	9147	.8106	.6766					
	p=.000	p=.000	p=.004	p=.491	p=.001	p=.408	p=.155	p=.000	p=.002	p=.022					
12	.7743	.7020	.5205	.4629	**.7870**	.4054	.8157	.8375	.7251	.7130	.7766				
	p=.005	p=.016	p=.101	p=.152	**p=.004**	p=.216	p=.002	p=.001	p=.012	p=.014	p=.005				
13	.7172	.4047	.2409	.2753	.8237	**.7488**	.4826	.8549	.7135	.9467	.6837	.7467			
	p=.013	p=.217	p=.476	p=.413	p=.002	**p=.008**	p=.133	p=.001	p=.014	p=.000	p=.020	p=.008			
14	.7382	.8010	.7943	-.0131	.5270	-.2749	.0820	.5789	**.6854**	.1722	.6766	.3874	.2965		
	p=.009	p=.003	p=.003	p=.969	p=.096	p=.413	p=.935	p=.062	**p=.020**	p=.613	p=.022	p=.239	p=.376		
15	**.9442**	.8538	.7338	.2594	.9340	.3359	.4929	.9652	.8775	.7298	.9129	.8240	.7284	.6243	
	p=.000	p=.001	p=.010	p=.441	p=.000	p=.313	p=.123	p=.000	p=.000	p=.011	p=.000	p=.002	p=.011	p=.040	
16	.9465	**.9409**	.9164	.2148	.7650	.0975	.2869	.8403	.7983	.4854	.9170	.6124	.4992	.7908	.8730
	p=.000	**p=.000**	p=.000	p=.526	p=.006	p=.776	p=.392	p=.001	p=.003	p=.130	p=.000	p=.045	p=.118	p=.004	p=.000

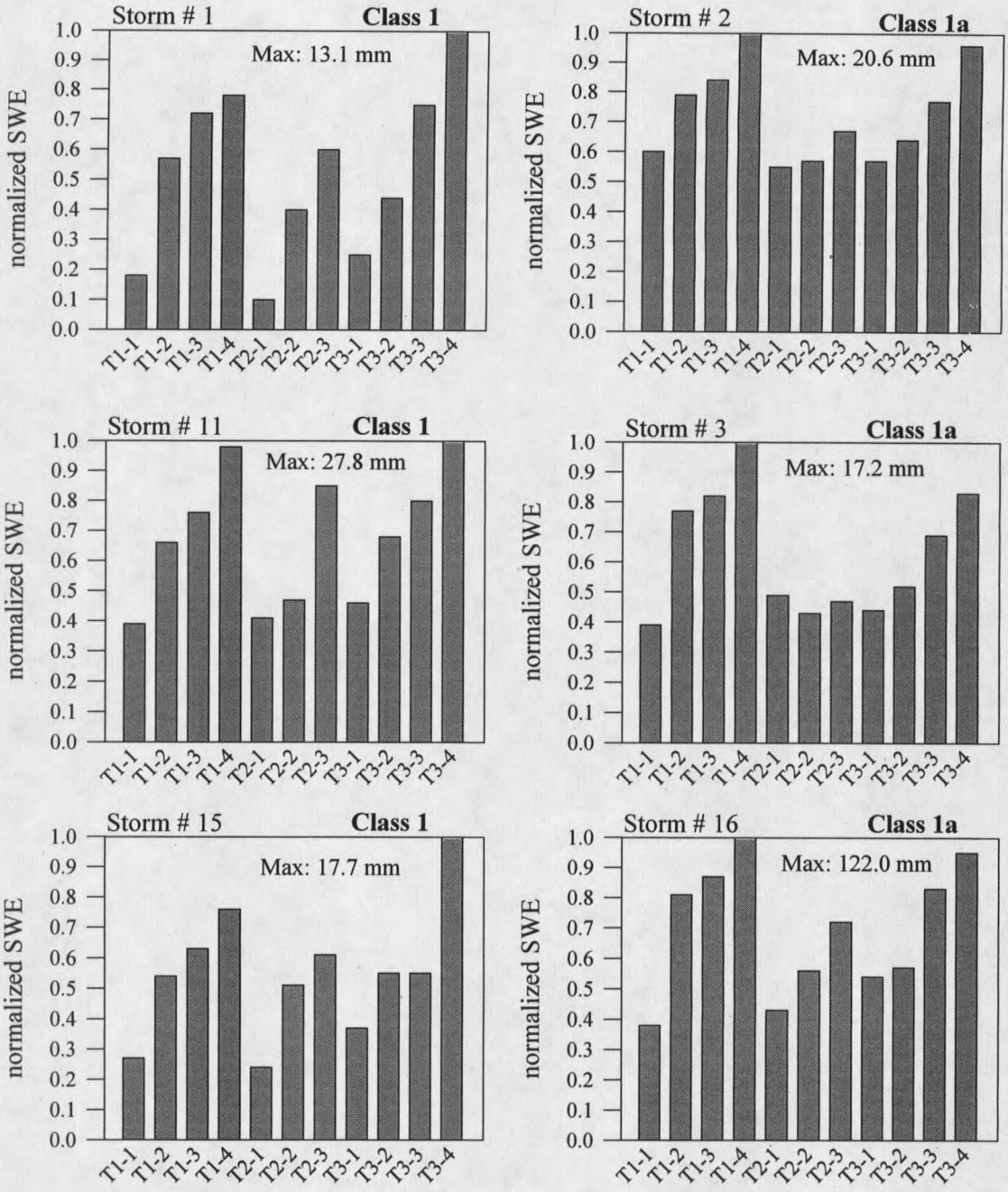

Figure 18. Nomalized SWE for Class 1 and Class 1a snow distributions.

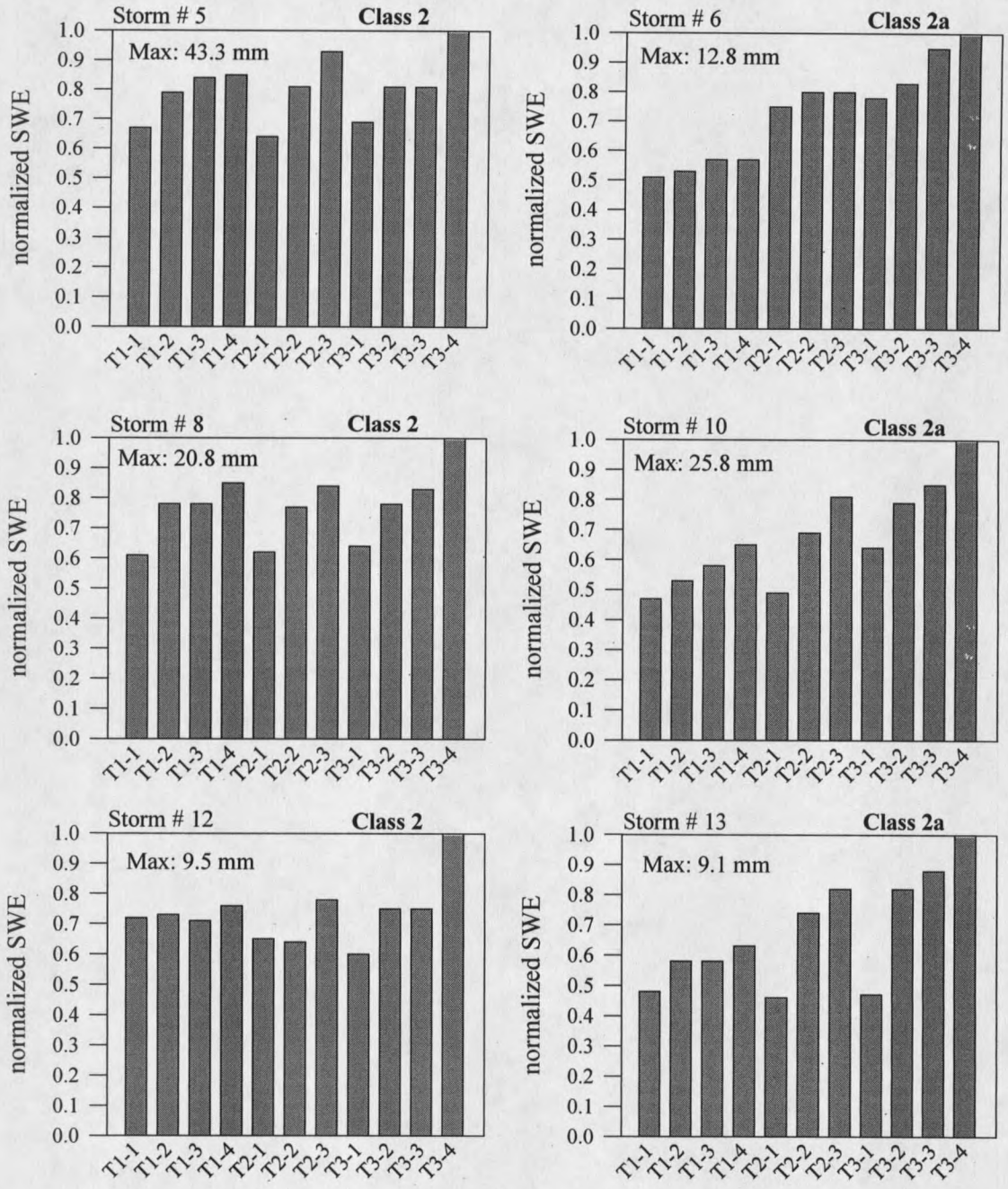

Figure 19. Normalized SWE for Class 2 and Class 2a snow distributions.

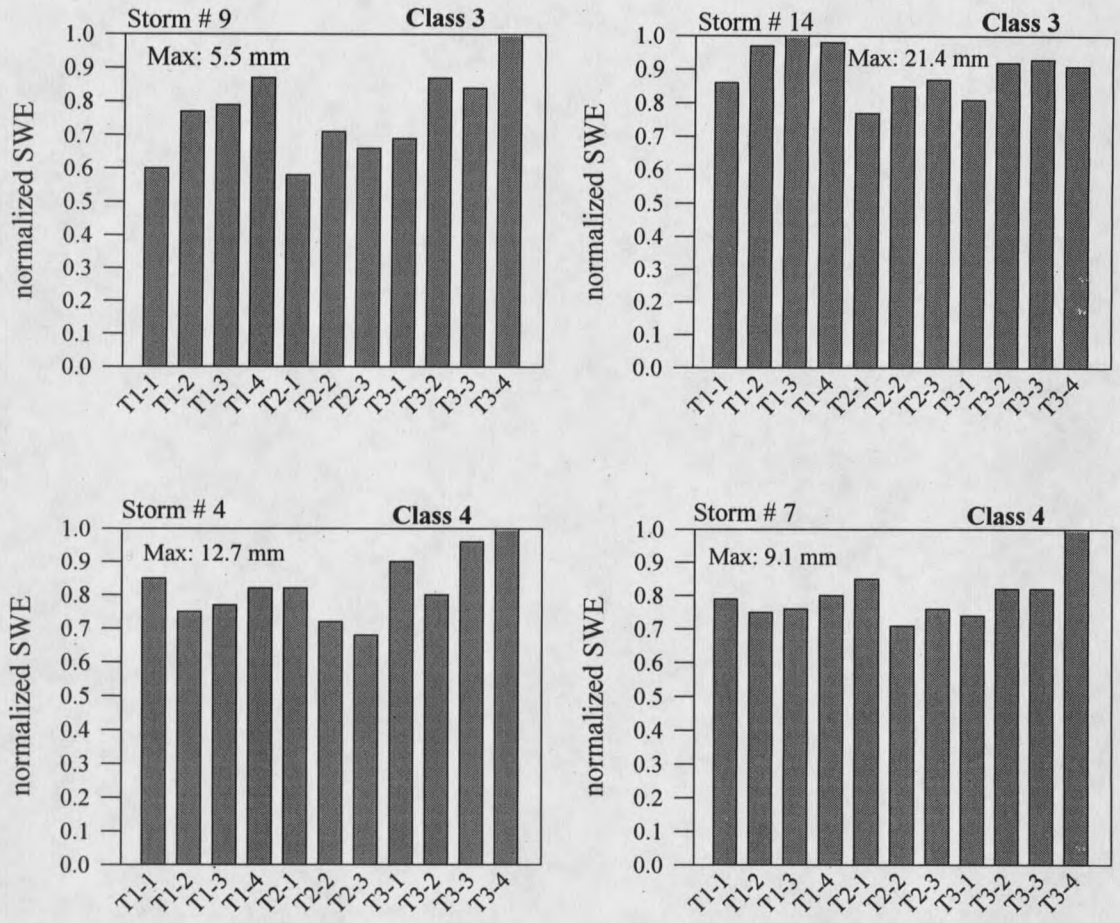

Figure 20. Normalized SWE for Class 3 and Class 4 snow distribution.

velocities and azimuths at the 500 mb level (Table 16) were used due to velocity's larger between-class variability than at the surface and azimuth's within-class consistency compared with the 700 mb level.

Storm class temperature ranges were determined from averaged temperatures (Figure 21) at the 700 mb pressure height. Temperatures at this level were consistently appropriate for snow crystal formation and production. Moreover, averaged relative humidities (Figure 22) consistently favored snowfall production at the 700 mb level, but otherwise failed to show trends at any atmospheric level for storm classes and were dropped from further consideration.

Table 16. Storm averaged wind velocity and azimuth classes grouped by storm class.

Storm	Storm date	Surface velocity	500 mb velocity	700 mb azimuth	500 mb azimuth
Class 1					
#1	Nov. 12	II	III	NW	SW
#11	Jan. 26	II	I	W	SW
#15	Mar. 15	II	III	W*	SW
Class 1a					
#2	Nov. 17	I	I	**N**	- - -
#3	Nov. 26	II	II	NW	**NW**
#16	Mar. 24	III	II*	**N**	**N***
Class 2					
#5	Dec. 1	II	IV	W	W
#8	Jan. 11	II	II	W	W
#12	Feb. 9	II	IV	N	NW
Class 2a					
#6	Dec. 16	III	IV	W	NW
#10	Jan. 14	II	II	W	**W**
#13	Feb. 26	II	III	N	W
Class 3					
#9	Jan. 12	II	II	W	W
#14	Mar. 3	II	III	SW*	W
Class 4					
#4	Nov. 28	II	III	NW	W
#7	Jan. 7	III	III	W	W

Velocity Class Boundaries	
I	0 - 3 m/s
II	4 - 7 m/s
III	8 - 16 m/s
IV	17 - 25 m/s
V	> 25 m/s

Azimuth Class Boundaries	
NE	23 - 67
E	68 - 112
SE	113 - 157
S	158 - 202
SW	203 - 247
W	248 - 292
NW	293 - 337
N	338 - 22

* storm record incomplete **Bolded:** most common azimuth class assigned

Table 17 outlines general snow distributions by storm class with interpreted topographic and meteorological influences with class-averaged meteorological conditions.

Wind velocity controls the entrainment and downwind transport of snow crystals. Class 1 and 1a storms have lower velocities and large accumulation differences along transect lines indicative of orographically enhanced snowfall and minimal crystal transport or the existence of a ridge eddy augmenting snow accumulation close to the ridge. Class 2 and 2a storms have greater wind velocities and a less pronounced difference in transect accumulation suggesting increased entrainment and transport of snow crystals downwind. Class 3 and 4 storms exhibit no elevational or distance from the ridge signature with moderate wind velocities suggesting the absence of a

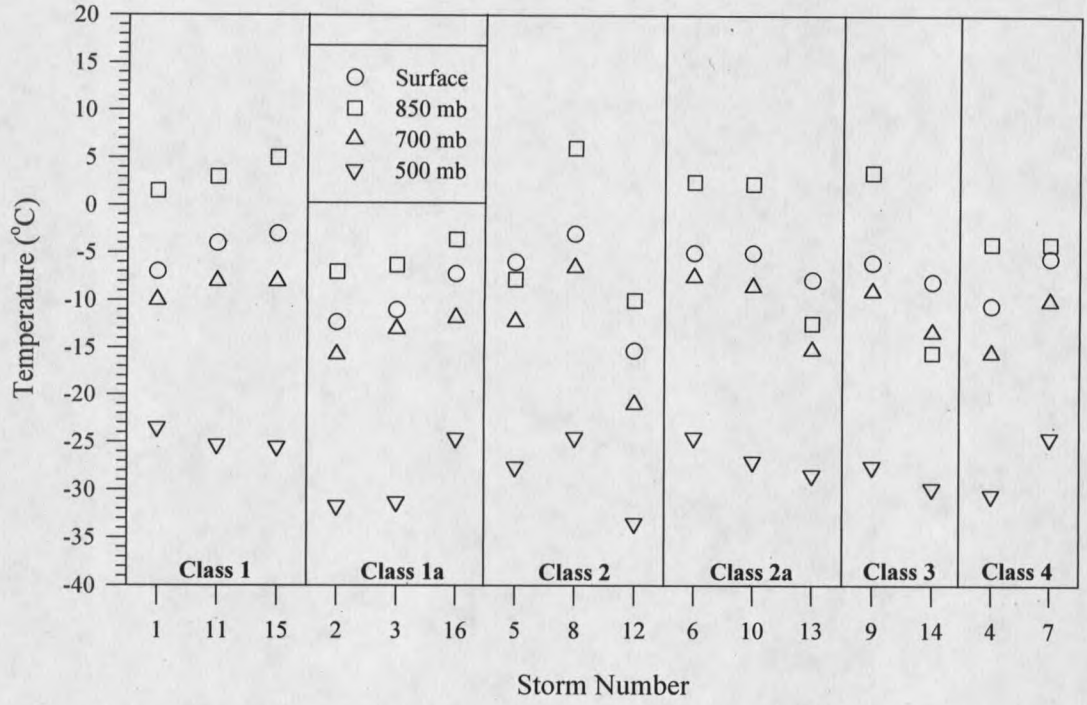

Figure 21. Averaged storm air temperatures.

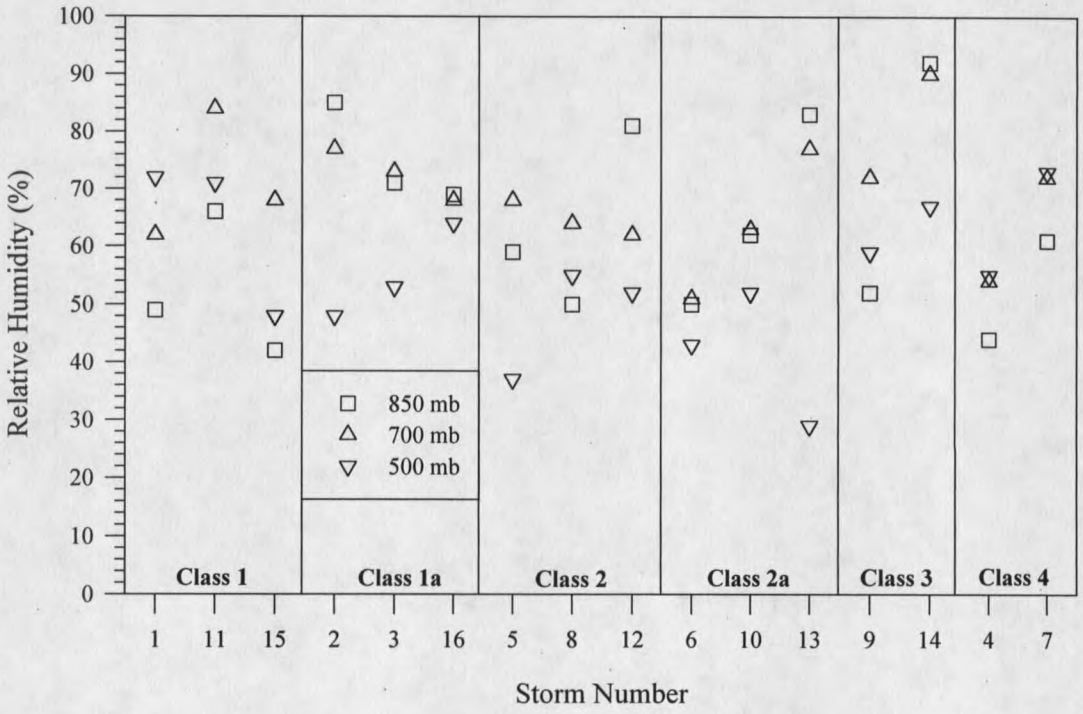

Figure 22. Averaged storm relative humidities.

Table 17. Storm class meteorological parameters with distributional and inferred atmospheric trends.

Storm Class	Storm class snow distribution and suggested atmospheric characteristics	500 mb Vel. Class	500 mb Azimuth	700 mb Temp. (deg. C)	* Crystal Habit
1	Pass Effect shifted north; strong T2 depletion and strong T1 augmentation. Minimal crystal displacement. Atmospheric instability and/or strong orographic enhancement.	III	SW	-4 to -10	Prisms
1a	Pass Effect shifted south; very strong T2 depletion and very strong T1 augmentation. Minimal crystal displacement. Atmospheric instability and/or strong orographic ehancement.	II	NW / N	-10 to -20	Plates
2	Increased T2 depletion with NW wind component. Atmospheric instability but crystal entrainment due to stong winds.	IV	W / NW	-7 to -22	Prisms Plates Columns
2a	Pass Effect strengthens with increasing velocities. Moderate instability and crystal entrainment.	III	W / NW	-7 to -15	Prisms / Plates
3	Ridge Effect minimized, crystal displacement east of ridge crest. Pass Effect moderate: T2 depletion, T1 augmentation. No elevational influence on snow distribution. Atmospheric stability and crystal entrainment.	III	W	-8 to -14	Prisms / Plates
4	Ridge Effect minimized, crystal displacement east of ridge crest. Pass Effect moderate: T2 depletion, T1 augmentation. No elevational influence on snow distribution. Atmospheric stability and crystal entrainment.	III	W	-10 to -16	Plates

* Inferred habit from storm class temperature regime (Schermenauer et al. 1981)

ridge eddy and increased crystal entrainment and transport downwind.

Wind azimuth offers an explanation for locational shifts during Class 1 and 1a storm types. With a SW flow in Class 1 storms, the pass influence appears to shift the southern eddy northward, reducing the depletion of Transect 2, while the pass jet augments deposition along Transect 1 (Figures D-1, 11, and 15). The NW flow predominant during Class 1a storms shifts the pass effect south, creating a very strong Transect 2 depletion and strengthening Transect 1 augmentation (Figures D-2, 3, and 16). Azimuths are generally westerly during Class 2, 2a, 3, and 4 storms and the strong high elevation differences between transects evident in Class 1 and 1a storms are either small or absent (Figures D-4 - 10 and 12 - 14).

Snow crystal habit, inferred from storm temperature regimes (Table 17), offers little insight into depositional patterns between storm classes. Additionally, 700 mb storm temperatures are internally consistent within storm classes only during Class 1 and 1a storms (Figure 22) which diminishes the predictive ability of temperature for snow distribution.

Atmospheric instability (Barry 1992a), which was not measured during the 1994-95 season, is strongly suspected as a meteorological control on local-scale storm snow distribution. Class 1 and 1a storm types exhibit strong depositional differences along transect lines, suggesting either air flow separation (Barry 1992a) at the ridge line and a ridge eddy that enhances accumulation, or strong orographic snowfall with minimal downwind transport of snow. Class 2 and 2a storm distributions show a differential accumulation along transect lines inferring the presence of a ridge eddy from air flow separation over the ridge or moderate atmospheric instability. Atmospheric stability is suggested during Class 3 and 4 type storms where snow accumulation differences between sites closer to the barrier and further downwind were minimized. This implies that ridge level air flow separation is reduced, the ridge eddy is absent, or there is no orographic lift during the storm.

Storm-Seasonal Snowpack

Development of the seasonal snowpack is strongly influenced by the winter storm track and the depositional patterns characteristic of each storm class. Dominance of a particular storm class will influence the seasonal snowpack to a greater extent than will any individual, disproportionately large storm event (e.g., storm 16, Figure D-16). Moreover, dominance of an extreme high gradient storm class (1 and 1a) or extreme low gradient storm class (3 and 4) could develop a seasonal snowpack that varies substantially from "normal".

During 1994-95, four primary storm classes and two subclasses were distinguished in the central Bridger Range (Table 14). Equal representation of all storm class types (Figures 18 - 19) during the season developed an April 1 snowpack (Figure 17 and D-17) which resembled a Class 2a storm type (storm #6, Figure D-6) with a moderate snow-elevation relationship. The agglomeration of the two extreme storm class types -- 1, 1a and 3, 4 -- muted individual class signatures and combined with class 2 and 2a storm distributions to resemble a snowpack with an "average" snow-elevation relationship by April 1.

Locational Bias

The existence of topographic forcing on boundary layer wind fields, and the resultant depositional patterns of snowfall, makes measurement site location a significant issue for seasonal and storm snow accumulation measurements. Elevation has been historically used as the most efficient predictor of snow accumulation, and as such, representative seasonal snowpacks have been determined from stations that are widely spaced.

Locational bias, however, can strongly influence the snow-elevation relationship on any given year, as in the Bridger Range when comparing April 1 snowpack at the Bridger Bowl and Brackett Creek SNOTEL sites (Figure 9). Elevations at the sites are effectively equal, with the Brackett Creek only 20 m (65 ft) higher than the Bridger Bowl, yet Brackett Creek has

accumulated less snowpack (SWE) in three of four years. Accumulation differences are a product of ridge-augmented snowfall at the Bridger Bowl SNOTEL, which is located closer to the ridge line. This location bias diminishes the predictive strength of the NRCS snow-elevation model for the Bridger Range.

Local-scale influences on snow distribution effect seasonal snow distribution models used for calculating precipitation distribution. Bridger Range locations that avoid a 2 -3 km radius of Ross Pass and are not within 2 km of the ridge crest should accumulated seasonally average snowpacks more representative of the Range.

Summary

Seasonal Snow Distributions

Prediction of a local-scale snow-elevation gradient in the Ross Pass Study Area (RPSA) using Natural Resources Conservation Service (NRCS) data was possible and thus, the null hypothesis that the NRCS measured snow accumulation gradient would not predict the snow accumulation gradient in the RPSA was rejected. This was however, a product of a small sample size for the NRCS data set. The large statistical uncertainty of this data set lowers the resolution for seasonal snow-elevation gradient prediction in the Bridger Range. Conversely, predicting the Bridger Range gradient with the larger RPSA data set was also not possible. This was a result of the topographic influence of the pass on snowfall distribution.

Seasonal snow distribution in the central Bridger Range is a product of an undefined, complex nonlinear function, with zones of depletion and augmentation related to storm wind azimuths, velocities, atmospheric stability conditions (inferred), and distances from the ridge crest and pass. In lieu of a nonlinear model, elevation provides a good linear prediction of seasonal snow distribution in the Bridger Range, explaining 62% of the variance with a standard error of

67.7 mm in snow water equivalent, for the 1994-95 snowpack.

Seasonal snow distribution, and the snow-elevation gradient, is an average of the winter's storm patterns. Influence of the pass topography and range crest on meteorological conditions during storms creates areas of high local-scale variability and "non-normal" snow accumulations. Measurement sites located to avoid these areas will provide a more realistic snow-elevation relationship for the mountain range. In the central Bridger Range, areas of "non-normal" snow accumulation are located 2-3 km radially east of Ross Pass and within 2 km downwind of the range crest. Above-average accumulations are located 2½ km downwind of the pass and within 2 km the range crest and below-average accumulations are located north and south of the pass. The extent of area influenced by the pass would be a function of the size of the pass and the directions and velocity of winds during storm events.

Areas of "non-normal" accumulation caused the local snow-elevation gradient in the Ross Pass area to be significantly different from the Bridger Range gradient. The importance of this measured local-scale variability is to offer some explanation for differences in basin runoff when compared with forecasted runoff based on modeled seasonal snow accumulation.

Snow distributions in the Ross Pass area appear to resemble accumulation patterns created by snow fences and shrub barriers. This suggests that snow fence models may be extended to explain local-scale snow distributions at the mountain barrier level. If so, nesting snow fence models within meso-scale precipitation models could enhance local-scale predictive accuracy and precision without increasing the measurement network.

Storm Snow Distributions

Elevation was significant in explaining storm snow distribution in only 50% of storms with R values ranging from 0.61 to 0.87 and the distance from the range crest was significant in 81% of storms with R values ranging from -0.60 to -0.92. Moreover, distance from the ridge

accounted for a larger (or equal) portion of variance for 75% of the eight storms in which elevation was also significantly related. Therefore, the null hypothesis that elevation will not account for the predominance of variance in storm snow distributions was accepted.

Additional factors influencing storm snow distributions are wind azimuth, wind velocity, and atmospheric stability. Atmospheric stability is suspected as being an integral factor influencing storm distributions, but was not measured in this study. Storms with NW, SW, and W components created very different snow distributions. Wind velocities influence snow entrainment and transport, as well as, windflow separation at the range crest as velocities increase. The degree of instability also effects windflow separation at the range crest, with unstable conditions favoring flow separation and eddy formation and stable conditions reducing eddy formation. The existence of the range crest eddy has an affect on the downwind distribution of storm snowfall.

Stormwise distribution of snowfall allowed the definition of four storm classes and two subclasses, each representing two or more events. Elevation was not significant in storm classes 1a, 3, and 4, and distance east of the ridge crest was only not significant during class 4 storms. Neither variable was significant during storm #6 (storm class 2a). Distance east of the ridge crest explained more variance in storm classes 1 and 2, and elevation explained more variance in storm class 2a.

Forecasting storm snow distributions would be improved by knowledge of the 500 mb wind azimuth (storm track), wind velocity, and atmospheric stability during storm events. Snow distributions in this study suggest that storms with instability have increased accumulations closer to the ridge crest on the steeper slopes and avalanche terrain. It appears that in storms with a more stable atmosphere, snow distributions are more equally distributed across elevations and distances from the ridge crest. Also, in concurrence with Birkeland and Mock (1996), a northwest flow at the 500 mb level produced the largest snowfall totals during the season (storms #5 and #16).

Suggested Future Research

Not all questions and issues that evolved during the course of this project were addressed or resolved completely. The following issues are potentially important when attempting to further refine snow distribution models at the local-scale.

1) Construction of a nonlinear mathematical model for the Bridger Range which describes snow distribution below the ridge crest and pass saddle for both the seasonal snowpack and storm class snow distributions.

2) Analyze the 1995 April 1 snowpack measurements with the summed storm SWE measurements for the 1994-95 season to assess the magnitude of mid-season ablation events on the April 1 snow-elevation gradient.

3) Application of snow fence accumulation models to mountain barrier and mountain pass settings using scale models or empirically measured snow distributions.

4) Analysis of the 1994-95 winter season synoptic climate charts during the storm periods to identify global-scale controls associated with the various storm tracks and distributional patterns.

5) Determine the meso-scale atmospheric structure over the Bridger Range during storm events to assess and quantify the influence of atmospheric stability/instability on the meso-scale wind fields, ridge/pass eddy formations, and subsequent storm snow distribution.

REFERENCES CITED

Alford, D., 1980. The orientation gradient: regional variations of accumulation and ablation in alpine basins. In *Geoecology of the Colorado Front Range: A Study of Alpine and Subalpine Environments*, ed. Jack D. Ives, pp. 214-223.

_____ . 1985. Mountain hydrology systems. *Mountain Research and Development* 5**(4)**:349-363.

Barros, A. P., and Lettenmaier, D. P., 1993. Dynamic modeling of the spatial distribution of precipitation in remote mountainous areas. *Monthly Weather Review* **121**:1195-1214.

_____ . 1994. Dynamic modeling of orographically-induced precipitation. *Reviews of Geophysics* 32**(3)**:265-284.

Barry, R. G., 1992a. *Mountain Weather and Climate*. 2nd edition. Routledge, New York. 402 p.

_____ . 1992b. Mountain climatology and past and potential future climatic changes in mountain regions: A review. *Mountain Research and Development* 12**(4)**:71-86.

Barry, R. G. and Chorley, R. J., 1992. *Atmosphere, Weather, and Climate*. 6th ed. Routledge, London. 392 p.

Beard, J., 1994. Personnel Communication. Supervisor, NRCS Snow Survey, Bozeman, Montana.

Birkeland, K. W. and Mock, C. J., 1996. Atmospheric circulation patterns associated with heavy snowfall events, Bridger Bowl, Montana, U.S.A. *Mountain Research and Development* 16**(3)**:281-286.

Caine, N., 1975. An elevational control of peak snowpack variability. *Water Resources Bulletin* 11**(3)**:613-621.

Codd, A. R., 1959. The photocanopyometer. Proceedings of the 27th Western Snow Conference. pp. 197-203.

Cooley, K. R., and Rango, A., 1991. Effects of sampling density on estimations of snowpack characteristics. Proceedings of the 59th Western Snow Conference. pp. 109-118.

Custer, S. G., Farnes, P., Wilson, J. P., and Synder, R. D., 1996. A comparison of hand- and spline-drawn precipitation maps for mountainous Montana. *Journal of the American Water Resources Association* 32**(2)**:393-405.

Daly, C. and Neilson, R. P., 1992. A digital topographic approach to modeling the distribution of precipitation in mountainous terrain. In *Interdisciplinary Approaches in Hydrology and Hydrogeology* American Institute of Hydrology, pp. 437-454.

Davis, R. E., Elder, K., Rosenthal, W., Melack, J., and Sickman, J., 1993. Estimating total snow volume in a small alpine watershed using remotely sensed data and ground-based surveys. Proceedings of the 50th Western Snow Conference. pp. 197-203.

Dingman, S. L., 1994. *Physical Hydrology.* Macmillian College Publishing Co., New York, 575 p.

Elder, K., Dozier, J., and Michaelsen, J., 1991. Snow accumulation and distribution in an alpine watershed. *Water Resources Research* 27(7):1541-1552.

Farnes, P. E., 1967. Criteria for determining mountain snow pillow sites. Proceedings of the 35th Western Snow Conference. pp. 59-62.

_____ . 1971. Mountain precipitation and hydrology from snow surveys. Proceedings of the 39th Western Snow Conference. pp. 44-49.

_____ . 1994. Personal Communication. Consulting Hydrologist - Snow Cap Hydrology. Bozeman, Montana.

Farnes, P. E., Peterson, N. R., Goodison, B. E., and Richards, R. P., 1982. Metrication of manual snow sampling equipment. Proceedings of the 50th Western Snow Conference. pp.120-132.

Giorgi, F., and Bates, G. T., 1989. A regional climate model for the western United States. *Monthly Weather Review* **117**:2325-2347.

Golding, D. L., 1968. Snow measurement on Marmot Creek Experimental Watershed. *Canadian Forestry Research Laboratory* Report A-X-18. 16 p.

Goodison, B. E., Ferguson, H. L., and McKay, G. A., 1981. Measurement and Data Analysis. In *Handbook of Snow: Principles, Processes, Management, and Use*, ed. D.M. Male and D.H. Gray, Pergamon Press, New York. 776 p.

Graham, J., 1996. Personal Communication. Asst. Professor, Mathematical Sciences, University of Montana, Missoula, Montana.

Grant, L. O. and Rhea, J. O., 1973. Elevation and meteorological controls on the density of new snow. In *Advanced Concepts and Techniques in the Study of Snow and Ice Resources.* Compiled by: Henry S. Santeford and James L. Smith. National Academy of Sciences, Washington, D.C. 1974.

Griffith, D.A and Armhein, C.G., 1991. *Statistical Analysis for Geographers.* Prentice-Hall, New Jersey. 478 p.

Hayes, S. P., 1984. Diagnosis of precipitation in mountainous terrain. International Snow Science Workshop, Aspen, Colorado. pp. 36-41.

———— . 1986. A simple orographic precipitation model for the pacific northwest. International Snow Science Workshop, Lake Tahoe, California. pp. 46-55.

Hjermstad, L. M., 1970. The influence of meteorological parameters on the distribution of precipitation across central Colorado mountains. *Master's Thesis*, Department of Atmospheric Science, Colorado State University, Fort Collins, Colorado. 78 p.

Holman, L. E., 1971. Some meteorological and physiographic aspects of winter precipitation variation in mountainous southwestern Montana. *Master's Thesis*, Department of Earth Sciences, Montana State University, Bozeman, Montana. 62 p.

Hosang, J. and Dettwiler, K., 1991. Evaluation of a water equivalent of snow cover map in a small catchment area using a geostatistical approach. *Hydrological Processes* **5**:283-290.

Hutchinson, M. F. and Bischof, R. J., 1983. A new method for estimating the spatial distribution of mean seasonal and annual rainfall applied to the Hunter Valley, New South Wales *Australian Meteorological Magazine* **31**:179-184.

Jandel, 1994. *SigmaPlot Scientific Graphing Software - User's Manual.* Jandle Corp., 494 p.

Kind, R. J., 1981. Snow drifting. In *Handbook of Snow: Principles, Processes, Management, and Use,* ed. D.M. Male and D.H. Gray, Pergamon Press, New York, 776 p.

Linacre, E., 1992. *Climate data and Resources: A Reference Guide.* London: Routledge. 366 p.

Locke, W. W., 1989. Present climate and glaciation of western Montana, U.S.A. *Arctic and Alpine Research* 21**(3)**:234-244.

McClung, D. and Schaerer, P., 1993. *The Avalanche Handbook.* The Mountaineers/Seattle. 272 p.

McKay, G. and Gray, D. M., 1981. The Distribution of Snowcover. In: *Handbook of Snow: Principles, Processes; Management, and Use,* ed. D.M. Male and D.H. Gray, Pergamon Press, New York. 776 p.

Oke, T. R., 1987. *Boundary Layer Climates.* London: Methuen. 372 p.

Peterson, T. C., and Schmidt, R. A., 1984. Outdoor scale modeling of shrub barriers in drifting snow. *Agricultural and Forest Meteorology* **31**:167-181.

Price, L. W., 1981. *Mountains and Man.* University of California Press. Berkeley. 506 p.

Rhea, J. O., 1978. Orographic precipitation model for hydrometeorological use. *Atmospheric Science Paper No. 287.* Department of Atmospheric Science, Colorado State University, Ft. Collins, Colorado. 198 p.

Rovansek, R. J., Kane, D. L., and Hinzman, L. D., 1993. Improving estimates of snowpack water equivalent using double sampling. Proceedings of the 61st Western Snow Conference. pp. 157-163.

Schemenauer, R. S., Berry, M. O., and Maxwell, J. B., 1981. Snowfall Formation. In *Handbook of Snow: Principles, Processes, Management, and Use,* ed. D.M. Male and D.H. Gray, Pergamon Press, New York. 776 p.

SCS, 1972. Snow Survey and Water Supply Forecasting. *SCS National Engineering Handbook* Sect. 22.

SCS, 1994. Central Forecasting System (CFS). U.S. Department of Agriculture, Portland, Oregon.

SCS, 1977. Average annual precipitation, Montana, based on the 1941-1970 base period. United States Department of Agriculture Soil Conservation Service, Bozeman, Montana, 16 p.

Stillman, S., 1996. Comparison of three automated precipitation models: ANUSLPIN, MTCLIM-3D, and PRISM. *Master's Thesis.* Department of Earth Sciences, Montana State University, Bozeman, Montana, 98 p.

Storr, D., 1973. Wind-snow relations at Marmot Creek, Alberta. *Canadian Journal of Forest Research* **3**:479-485.

Super, A. B., Grainger, C. A., McPartland, J. T., Mitchell, V. L., and Yaw, B. H.,1972. Bridger Range cloud seeding experiment, Final Report, Part I. *Atmospheric Water Resources Management Program,* Montana State University, Bozeman, Montana. 425 p.

_____ . 1974. Bridger Range cloud seeding experiment, Final Report, Part II. *Atmospheric Water Resources Management Program,* Montana State University, Bozeman, Montana. 198 p.

Tremper, W. B., Dawson, P. J., and Yaw, R. H., 1983. A meteorological and climatological approach in determining snowpack accumulation at snow course sites in a Montana watershed. Final report, Project No. A-132-MONT, Montana Water Resources Research Center, Montana State University, Bozeman, Montana. 29 p.

Tabler, R. D., and Jairell, R. L., 1980. Studying snow drifting problems with small-scale models outdoors. Proceedings of the 48th Western Snow Conference. pp. 1-13.

Troendle, C. A. and King, R. M., 1987. The effect of partial clear cutting on streamflow at Deadhorse Creek, Colorado. *Journal of Hydrology* **90**:145-157.

Troendel, C. A., Schmidt, R. A., and Martinez, M. H., 1993. Partitioning the deposition of winter snowfall as a function of aspect on forested slopes. Proceedings of the 50th Western Snow Conference. pp. 373-379.

USGS, 1977. National handbook of recommended methods for water data acquisition. Office of Water Data Coordination, Geologic Survey, United States Department of Interior, Reston, Virginia.

Vuglinski, V. S., 1972. Methods for the study of laws for the distribution of precipitation in medium-high mountains (Illustrated by the Vitim River basin). In *Distribution of Precipitation in Mountainous Areas,* Geilo Symposium, Norway, July 1972. WMO Publication 326.

Washichek, J. N. and McAndrew, D. W., 1967. Snow measurement accuracy in high density snow course network in Colorado. Western Snow Conference, Boise, Idaho. pp. 43-49.

Whaley, B., 1983. SNOTEL - Operations and Uses. Presented at the Westside Snow Survey Training School, Big Sky, Montana. Jan. 16-21. 22 p.

APPENDICES

APPENDIX A

DOUBLE SAMPLING CALCULATION

Double Sampling Measurement Determination

Definition of Terms

w	snow water equivalent (cm)
x	depth measurement (cm)
n_w	number of density samples
n_x	number of depth measurements
C_w	estimate of time per density measurement
C_x	estimate of time per depth measurement
$S^2\rho$	variance of SWE values about a line defined by the product of average density (ρ) and depth
S^2	sample variance of SWE
$\bar{\rho}$	average density of snow

$$\bar{\rho} = \frac{\sum_{i=1}^{n_w} w_i}{\sum_{i=1}^{n_w} x_i} \qquad (3)$$

$$s^2\rho = \frac{1}{n_w - 1} \sum_{i=1}^{n_w} (w_i - \bar{\rho} x_i) \qquad (4)$$

$$\frac{n_w}{n_x} = \sqrt{\left(\frac{c_x}{c_w}\right)\left(\frac{S^2\rho}{S^2 - S^2\rho}\right)} = \frac{1}{4} \qquad (5)$$

Table A-1. March 1 snow cores in the RPSA.

Site	Depth (cm)	SWE (mm)	Density (%)
T3-1	68.6	208	30.4
	58.4	173	29.6
	63.5	208	32.8
	66.0	196	29.6
T3-2	94.0	290	30.8
	80.0	244	30.5
	86.4	277	32.1
	86.4	254	29.4
T3-3	95.3	358	37.6
	81.3	231	28.4
	83.8	277	33.0
	82.6	277	33.5
T3-4	144.8	475	32.8
	132.1	417	31.5
	125.7	404	32.1
	125.7	417	33.1
T2-1	80.0	218	27.3
	76.2	208	27.3
	72.4	185	25.6
	81.3	208	25.6
T1-1	81.3	196	24.1
	86.4	208	24.1
	88.9	208	23.4
	87.6	173	19.7
T2-2	88.9	218	24.6
	101.6	218	21.5
	97.8	208	21.3
	101.6	231	22.8
sum	2518.4	718.6	Ave. = 28.4
var. (s^2)	425.93	67.39	

Values for equations (3), (4), and (5):

$\bar{\rho}$ = 0.284 n_w ; n_x = 28

C_w = 5 min $S^2\rho$ = 2.92

C_x = .75 min S^2 = 10.44

APPENDIX B

RAW SNOW MEASUREMENT DATA

Table B-1. April 1 snow cores in the RPSA.

Site T1-1								Site T1-2							
Core #	Depth (in.)	Length (in.)	Weight	Tare	SWE (in)	SWE (adj)	Density (%)	Core #	Depth (in.)	Length (in.)	Weight	Tare	SWE (in)	SWE (adj)	Density (%)
1	26.50							1	35.00						
	26.75								33.50						
	29.00	27.00	22.0	12.5	9.5	8.6	30		33.25	31.00	23.5	12.5	11.0	10.0	30
	26.00								34.00						
	25.00								25.00						
2	29.50							2	50.00						
	30.25								52.00						
	29.00	28.00	21.0	12.5	8.5	7.7	27		51.00	42.00	46.5	30.0	16.5	15.0	29
	29.75								54.50						
	29.00								55.25						
3	30.75							3	61.00						
	29.00								60.00						
	30.50	28.00	25.0	12.5	12.5	11.4	37		58.50	48.00	47.5	30.0	17.5	15.9	27
	29.25								59.00						
	28.75								58.00						
4	32.50							4	55.00						
	33.00								55.50						
	36.00	33.50	25.5	12.5	13.0	11.8	33		57.00	45.00	46.0	30.0	16.0	14.6	26
	35.00								58.00						
	32.00								58.00						
5	31.50							5	55.00						
	31.25								57.00						
	32.50	30.50	22.5	12.5	10.0	9.1	28		56.50	38.00	44.5	30.0	14.5	13.2	23
	30.50								56.50						
	35.00								55.00						
Ave.	30.3					9.4	30.9	Ave.	51.3					13.9	27.1
Std - s	2.8					1.8	4.2	Std - s	10.2					2.3	2.8

* Ave. SWE (adj.) = (ave. sample density) * (ave. depth for all measurements)
SWE (adj.) - correction factor of 0.91 applied

Table B-1 (cont.). April 1 snow cores in the RPSA.

Site T1-3								Site T1-4							
Core #	Depth (in.)	Length (in.)	Weight	Tare	SWE (in)	SWE (adj)	Density (%)	Core #	Depth (in.)	Length (in.)	Weight	Tare	SWE (in)	SWE (adj)	Density (%)
1	57.00							1	63.00						
	56.00								60.00						
	55.00	42.00	46.0	30.0	16.0	14.6	26		59.50	51.75	46.5	30.0	16.5	15.0	25
	55.50								65.00						
	54.50								59.00						
2	46.00							2	58.75						
	46.00								59.75						
	48.50	47.00	46.5	30.0	16.5	15.0	31		62.00	43.00	40.5	30.0	10.5	9.6	15
	52.00								64.75						
	53.00								65.75						
3	57.25							3	60.00						
	58.25								60.75						
	57.75	48.00	46.5	30.0	16.5	15.0	26		63.00	52.00	50.0	30.0	20.0	18.2	29
	57.25								60.00						
	58.00								61.50						
4	57.00							4	61.50						
	60.00								63.50						
	63.00	37.00	43.0	30.0	13.0	11.8	19		62.00	47.50	47.5	30.0	17.5	15.9	26
	62.00								66.00						
	57.00								62.00						
5	57.50							5	50.00						
	57.50								66.25						
	60.25	56.00	50.0	30.0	20.0	18.2	30		67.00	49.50	47.5	30.0	17.5	15.9	24
	60.00								67.50						
	58.50								68.50						
Ave.	56.2					14.9	26.5	Ave.	62.3					14.8	23.8
Std - s	4.3					2.3	4.8	Std - s	3.8					3.2	5.0

* Ave. SWE (adj.) = (ave. sample density) * (ave. depth for all measurements)
SWE (adj.) - correction factor of 0.91 applied

Table B-1 (cont.). April 1 snow cores in the RPSA.

Site T3-1								Site T3-2							
Core #	Depth (in.)	Length (in.)	Weight	Tare	SWE (in)	SWE (adj)	Density (%)	Core #	Depth (in.)	Length (in.)	Weight	Tare	SWE (in)	SWE (adj)	Density (%)
1	34.75							1	46.50						
	19.50								47.75						
	29.00	26.50	36.5	28.5	8.0	7.3	25		47.25	41.00	44.5	28.5	16.0	14.6	31
	33.00								45.75						
	36.25								46.00						
2	34.50							2	43.50						
	35.70								46.00	44.50	43.5	28.5	15.0	13.7	30
	29.50	29.50	40.5	28.5	12.0	10.9	37		42.50	38.75	41.0	28.5	12.5	11.4	27
	34.50								44.00						
	35.00								48.50						
3	31.25							3	41.75						
	29.50								47.00						
	29.00	27.50	37.5	28.5	9.0	8.2	28		45.00	41.00	42.5	28.5	14.0	12.7	28
	27.50								46.50						
	28.75								46.00						
4	33.25							4	39.25						
	34.50								42.00						
	36.25	34.00	41.5	29.0	12.5	11.4	31		44.50	43.75	43.0	28.5	14.5	13.2	30
	35.50								43.25						
	35.00								44.50						
5	34.50							5	45.75						
	35.50								46.25						
	35.25	35.00	40.5	28.5	12.0	10.9	31		47.00	44.50	46.0	28.5	17.5	15.9	34
	35.25								46.25	42.00	44.0	28.5	15.5	14.1	30
	36.00								46.50						
Ave.	32.7					10.0	30.5	Ave.	45.2					13.5	29.9
Std - s	3.9					1.9	4.4	Std - s	2.2					1.4	2.2

* Ave. SWE (adj.) = (ave. sample density) * (ave. depth for all measurements)
SWE (adj.) - correction factor of 0.91 applied

Table B-1 (cont.). April 1 snow cores in the RPSA.

Site T3-3								Site T3-4							
Core #	Depth (in.)	Length (in.)	Weight	Tare	SWE (in)	SWE (adj)	Density (%)	Core #	Depth (in.)	Length (in.)	Weight	Tare	SWE (in)	SWE (adj)	Density (%)
1	53.50							1	76.50						
	56.75								67.25						
	52.50	47.25	61.5	45.5	16.0	14.6	28		80.50	79.50	75.5	46.0	29.5	26.8	33
	51.00								78.00						
	48.50								74.50						
2	51.25							2	76.00						
	51.50								68.00						
	51.50	45.50	61.0	46.0	15.0	13.7	27		62.00	57.00	61.5	45.5	16.0	14.6	23
	50.00								71.50						
	49.00								70.50						
3	56.00	51.00	65.0	45.5	19.5	17.7	32	3	73.50						
	53.50	42.00	61.0	45.5	15.5	14.1	26		76.50						
	53.00	52.00	61.0	45.5	15.5	14.1	27		77.75	70.50	70.0	45.5	24.5	22.3	29
	49.75								69.50						
	45.00								71.50						
4	45.00							4	69.00	63.50	66.0	45.5	20.5	18.7	27
	46.00								76.50	67.00	71.0	45.5	25.5	23.2	30
	45.50	42.25	60.0	46.0	14.0	12.7	28		77.00	66.50	73.0	45.5	27.5	25.0	33
	46.75								75.25						
	47.00								77.50						
5	48.25							5	78.00	65.00	67.0	45.0	22.0	20.0	26
	46.50								71.25	52.00	66.0	45.0	21.0	19.1	27
	49.50	45.50	61.5	46.0	15.5	14.1	28		74.50	54.00	67.0	45.0	22.0	20.0	27
	45.50								71.25						
	42.00								74.50						
Ave.	49.4					13.8	27.9	Ave.	73.5					20.8	28.3
Std - s	3.7					1.6	1.9	Std - s	4.3					3.7	3.2

* Ave. SWE (adj.) = (ave. sample density) * (ave. depth for all measurements)
SWE (adj.) - correction factor of 0.91 applied

Table B-1 (cont.). April 1 snow cores in the RPSA.

Site T2-1								Site T2-2							
Core #	Depth (in.)	Length (in.)	Weight	Tare	SWE (in)	SWE (adj)	Density (%)	Core #	Depth (in.)	Length (in.)	Weight	Tare	SWE (in)	SWE (adj)	Density (%)
1	40.00							1	39.50						
	40.00								38.50						
	41.50	37.00	42.5	33.5	9.0	8.2	20		41.00	38.50	46.0	33.5	12.5	11.4	28
	39.00								42.00						
	38.50								42.00						
2	33.00							2	43.00						
	42.50								44.00						
	44.00	29.75	45.5	33.5	12.0	10.9	25		44.00	40.75	49.0	33.5	15.5	14.1	32
	41.00								44.25						
	42.00								44.00						
3	44.50							3	42.00						
	40.00								43.00						
	43.00	37.00	47.0	33.5	13.5	12.3	29		43.00	34.00	47.0	35.0	12.0	10.9	25
	40.50								43.00						
	38.25								43.00						
4	43.50							4	45.50						
	43.50								25.00						
	42.00	35.00	46.0	33.5	12.5	11.4	27		43.75	41.00	48.0	33.5	14.5	13.2	30
	43.50								41.00						
	44.00								41.50						
5	43.00							5	42.50						
	42.50								43.50						
	44.50	37.50	47.0	33.5	13.5	12.3	28		43.00	34.00	45.0	33.5	11.5	10.5	24
	43.00								43.50						
	42.5								46.5						
Ave.	41.6					10.6	25.6	Ave.	42.1					11.8	27.9
Std - s	2.6					1.7	3.5	Std - s	3.9					1.6	3.2

* Mean SWE (adj.) = (mean sample density) * (mean depth for all depth measurements)
SWE (adj.) - correction factor of 0.91 applied

Table B-1 (cont.). April 1 snow cores in the RPSA.

Site T2-3

Core #	Depth (in.)	Length (in.)	Weight	Tare	SWE (in)	SWE (adj)	Density (%)
1	49.25						
	49.50						
	50.50	45.00	49.5	33.5	16.0	14.6	29
	50.75						
	50.50						
2	52.00						
	52.75						
	53.50	50.00	53.0	35.0	18.0	16.4	31
	55.00						
	55.00						
3	54.50						
	52.50						
	52.50	50.00	50.0	34.0	16.0	14.6	28
	49.50						
	53.25						
4	52.50						
	52.50						
	51.75	46.50	49.5	33.5	16.0	14.6	28
	53.75						
	52.00						
5	55.00						
	54.00						
	52.00	47.50	49.3	34.0	15.3	13.9	27
	53.00						
	53.00						
Ave.	52.4					14.9	28.4
Std - s	1.7					0.9	1.5

* Ave. SWE (adj.) = (ave. sample density) * (ave. depth for all measurements)
SWE (adj.) - correction factor of 0.91 applied

Table B-2. Storm SWE measurements for each site and storm board.

First 3 storms of season

	SITE T1-1			SITE T1-2			SITE T1-3			SITE T1-4			SITE T2-1			SITE T2-2		
	Bd 1	Bd 2	Bd 3	Bd 1	Bd 2	Bd 3	Bd 1	Bd 2	Bd 3	Bd 1	Bd 2	Bd 3	Bd 1	Bd 2	Bd 3	Bd 1	Bd 2	Bd 3
weight	558	559	600	790	785	830	850	855	850	1000	1105	1045	580	565	635	940	900	930
depth	20.0	20.5	21.0	28.0	27.0	27.0	27.5	28.0	28.0	30.0	32.0	31.0	20.0	20.0	21.0	25.5	24.0	25.5
density	149.8	146.4	153.4	151.5	156.1	156.1	166.0	164.0	163.0	179.0	185.5	181.0	155.7	151.7	162.4	198.0	201.4	195.9
SWE	30.0	30.0	32.2	42.4	42.2	42.6	45.6	45.9	45.6	53.7	59.3	56.1	31.1	30.3	34.1	50.5	48.3	49.9

	SITE T2-3			SITE T3-1			SITE T3-2			SITE T3-3 *						SITE T3-4 **		
	Bd 1	Bd 2	Bd 3	Bd 1	Bd 2	Bd 3	Bd 1	Bd 2	Bd 3	Bd 1-t	Bd 1-b	Bd 2-t	Bd 2-b	Bd 3-t	Bd 3-b	Bd 1	Bd 2-t	Bd 2-b
weight	------	1315	1180	------	681	675	1040	990	955	605	770	510	975	550	860	2330	805	1015
depth	------	33.0	30.0	------	24.0	28.5	32.0	30.0	30.0	20.0	13.0	20.5	19.5	19.0	21.0	50.0	26.5	26.0
density	------	214.0	211.2	------	152.2	127.2	174.5	177.2	171.0	162.5	318.1	133.6	268.5	155.5	219.9	250.3	163.1	209.7
SWE	------	70.6	63.4	------	36.5	36.3	55.9	53.2	51.3	32.5	41.4	27.4	52.4	29.5	46.2	125.1	43.2	54.5

November 12, 1994

	SITE T1-1			SITE T1-2			SITE T1-3			SITE T1-4			SITE T2-1			SITE T2-2		
	Bd 1	Bd 2	Bd 3	Bd 1	Bd 2	Bd 3	Bd 1	Bd 2	Bd 3	Bd 1	Bd 2	Bd 3	Bd 1	Bd 2	Bd 3	Bd 1	Bd 2	Bd 3
weight	45	40	50	140	135	140	180	175	170	210	190	170	20	25	25	95	100	100
depth	3.0	3.0	3.0	9.0	7.5	8.5	10.0	10.0	10.0	11.0	11.0	10.5	2.0	3.0	2.5	6.5	6.5	7.0
density	80.6	71.6	89.5	83.5	96.7	88.5	96.7	94.0	91.3	102.5	92.8	87.0	53.7	44.8	53.8	78.5	82.6	76.7
SWE	2.4	2.1	2.7	7.5	7.3	7.5	9.7	9.4	9.1	11.3	10.2	9.1	1.1	1.3	1.3	5.1	5.4	5.4

	SITE T2-3			SITE T3-1			SITE T3-2			SITE T3-3			SITE T3-4		
	Bd 1	Bd 2	Bd 3	Bd 1	Bd 2	Bd 3	Bd 1	Bd 2	Bd 3	Bd 1	Bd 2	Bd 3	Bd 1	Bd 2	Bd 3
weight	140	160	135	60	65	55	110	110	100	185	180	185	260	250	221
depth	7.5	8.0	8.0	5.0	5.0	5.0	8.0	8.0	8.0	10.0	10.0	11.0	13.0	13.0	12.0
density	100.3	107.4	90.6	64.4	96.8	59.1	73.8	73.8	67.1	99.4	96.7	90.3	107.4	103.3	98.9
SWE	7.5	8.6	7.3	3.2	3.5	3.0	5.9	5.9	5.4	9.9	9.7	9.9	14.0	13.4	11.9

* due to depth of snowpack, cores were taken in two measurements

** bd 1 sampled in zip lock as one bulk sample: bd 2 slpit into two cores; bd 3 tipped over - no sample

weight (gm); depth (cm); density (kg/cm^3); SWE (mm)

Table B-2 (cont). Storm SWE measurements for each site and storm board.

November 17, 1994

	SITE T1-1			SITE T1-2			SITE T1-3			SITE T1-4			SITE T2-1			SITE T2-2		
	Bd 1	Bd 2	Bd 3	Bd 1	Bd 2	Bd 3	Bd 1	Bd 2	Bd 3	Bd 1	Bd 2	Bd 3	Bd 1	Bd 2	Bd 3	Bd 1	Bd 2	Bd 3
weight	225	235	235	320	295	295	335	335	295	365	385	400	200	205	200	220	205	225
depth	13.0	16.0	16.5	21.5	20.0	19.0	23.0	20.5	20.0	28.0	24.5	26.5	14.0	14.0	14.5	13.0	13.0	13.5
density	93.0	78.9	76.5	79.9	79.2	83.4	78.2	87.8	79.2	70.0	84.4	81.1	76.7	78.6	74.0	90.9	84.7	89.5
SWE	12.1	12.6	12.6	17.2	15.8	15.8	18.0	18.0	15.8	19.6	20.7	21.5	10.7	11.0	10.7	11.8	11.0	12.1

	SITE T2-3			SITE T3-1			SITE T3-2			SITE T3-3			SITE T3-4		
	Bd 1	Bd 2	Bd 3	Bd 1	Bd 2	Bd 3	Bd 1	Bd 2	Bd 3	Bd 1	Bd 2	Bd 3	Bd 1	Bd 2	Bd 3
weight	260	255	255	225	220	210	245	250	245	265	310	305	390	355	355
depth	14.5	14.0	14.0	14.5	15.0	14.0	18.5	17.0	16.5	18.0	21.5	21.0	24.0	25.0	25.0
density	96.3	97.8	97.8	83.3	78.8	80.6	71.1	79.0	79.7	79.1	77.4	78.0	87.3	76.3	76.3
SWE	14.0	13.7	13.7	12.1	11.8	11.3	13.2	13.4	13.2	14.2	16.6	16.4	20.9	19.1	19.1

November 26, 1994

	SITE T1-1			SITE T1-2			SITE T1-3			SITE T1-4			SITE T2-1			SITE T2-2		
	Bd 1	Bd 2	Bd 3	Bd 1	Bd 2	Bd 3	Bd 1	Bd 2	Bd 3	Bd 1	Bd 2	Bd 3	Bd 1	Bd 2	Bd 3	Bd 1	Bd 2	Bd 3
weight	125	120	125	255	215	265	255	270	265	300	335	325	150	155	170	160	125	130
depth	11.0	11.5	11.0	24.5	20.0	23.0	22.5	24.0	22.5	24.5	27.0	27.0	12.5	14.0	14.5	23.0	11.0	40.0
density	61.0	56.0	61.0	55.9	57.7	61.9	61.9	60.4	63.3	65.8	66.6	64.6	64.4	59.5	63.0	71.6	61.0	69.8
SWE	6.7	6.4	6.7	13.7	11.5	14.2	13.7	14.5	14.2	16.4	18.0	17.5	8.1	8.3	9.1	8.6	6.7	7.0

	SITE T2-3			SITE T3-1			SITE T3-2			SITE T3-3			SITE T3-4		
	Bd 1	Bd 2	Bd 3	Bd 1	Bd 2	Bd 3	Bd 1	Bd 2	Bd 3	Bd 1	Bd 2	Bd 3	Bd 1	Bd 2	Bd 3
weight	145	145	165	140	135	145	180	165	150	200	260	200	280	265	255
depth	10.5	10.0	12.5	14.0	14.0	14.0	19.0	18.0	17.0	20.0	22.0	20.0	23.0	23.0	21.5
density	74.2	77.9	70.9	53.7	51.8	55.6	50.9	49.2	47.4	53.7	63.5	53.7	65.4	61.9	63.7
SWE	7.8	7.8	7.8	7.5	7.3	7.8	9.7	8.9	8.1	10.7	14.0	10.7	15.0	14.2	13.7

weight (gm); depth (cm); density (kg/cm^3); SWE (mm)

Table B-2 (cont). Storm SWE measurements for each site and storm board.

November 28, 1994

	SITE T1-1			SITE T1-2			SITE T1-3			SITE T1-4			SITE T2-1			SITE T2-2		
	Bd 1	Bd 2	Bd 3	Bd 1	Bd 2	Bd 3	Bd 1	Bd 2	Bd 3	Bd 1	Bd 2	Bd 3	Bd 1	Bd 2	Bd 3	Bd 1	Bd 2	Bd 3
weight	195	205	205	190	160	180	165	175	205	200	200	185	185	190	205	160	160	190
depth	13.0	14.0	14.0	15.0	15.5	12.0	12.5	13.0	14.0	14.0	13.0	14.0	13.5	13.0	13.5	15.0	12.0	12.0
density	80.6	78.6	78.6	68.0	55.4	80.6	70.9	72.3	78.6	76.7	82.6	71.0	73.6	78.5	81.6	57.3	71.6	85.0
SWE	10.5	11.0	11.0	10.2	8.6	9.7	8.9	9.4	11.0	10.7	10.7	9.9	9.9	10.2	11.0	8.6	8.6	10.2

	SITE T2-3			SITE T3-1			SITE T3-2			SITE T3-3			SITE T3-4		
	Bd 1	Bd 2	Bd 3	Bd 1	Bd 2	Bd 3	Bd 1	Bd 2	Bd 3	Bd 1	Bd 2	Bd 3	Bd 1	Bd 2	Bd 3
weight	170	150	160	215	205	205	180	190	195	235	230	215	245	255	210
depth	12.0	10.5	10.0	15.5	14.0	15.5	15.0	14.0	15.0	19.5	20.0	19.0	25.0	25.0	23.0
density	76.1	76.7	85.9	74.5	78.6	71.0	64.4	72.9	69.8	64.7	61.8	60.8	52.6	54.8	49.0
SWE	9.1	8.1	8.6	11.5	11.0	11.0	9.7	10.2	10.5	12.6	12.4	11.5	13.2	13.7	11.3

December 1, 1994

	SITE T1-1			SITE T1-2			SITE T1-3			SITE T1-4			SITE T2-1			SITE T2-2		
	Bd 1	Bd 2	Bd 3	Bd 1	Bd 2	Bd 3	Bd 1	Bd 2	Bd 3	Bd 1	Bd 2	Bd 3	Bd 1	Bd 2	Bd 3	Bd 1	Bd 2	Bd 3
weight	555	545	525	635	640	640	680	680	665	695	695	675	500	515	525	690	595	685
depth	26.0	26.0	26.0	31.5	29.0	30.0	32.0	32.0	32.0	35.0	34.0	34.0	25.0	25.5	25.5	32.0	28.5	31.5
density	114.6	112.6	108.4	108.5	118.5	114.6	114.1	114.1	111.6	106.6	109.8	106.6	107.4	108.5	110.6	115.8	112.1	116.8
SWE	29.8	29.3	28.2	34.1	34.4	34.4	36.5	36.5	35.7	37.3	37.3	36.3	26.9	27.7	28.2	37.1	32.0	36.8

	SITE T2-3			SITE T3-1			SITE T3-2			SITE T3-3			SITE T3-4		
	Bd 1	Bd 2	Bd 3	Bd 1	Bd 2	Bd 3	Bd 1	Bd 2	Bd 3	Bd 1	Bd 2	Bd 3	Bd 1	Bd 2	Bd 3
weight	780	740	735	555	560	565	665	650	645	665	650	645	820	820	780
depth	38.5	36.0	34.0	29.5	30.0	28.5	36.0	34.5	35.5	37.0	35.0	37.0	41.0	44.0	42.0
density	108.8	110.4	116.1	101.0	100.3	106.5	99.2	101.2	97.6	96.5	99.7	93.6	107.4	100.4	99.7
SWE	41.9	39.7	39.5	29.8	30.1	30.3	35.7	34.9	34.6	35.7	34.9	34.6	44.0	44.0	41.9

weight (gm); depth (cm); density (kg/cm^3); SWE (mm)

Table B-2 (cont). Storm SWE measurements for each site and storm board.

December 9, 1994

	SITE T1-1			SITE T1-2			SITE T1-3			SITE T1-4			SITE T2-1			SITE T2-2		
	Bd 1	Bd 2	Bd 3	Bd 1	Bd 2	Bd 3	Bd 1	Bd 2	Bd 3	Bd 1	Bd 2	Bd 3	Bd 1	Bd 2	Bd 3	Bd 1	Bd 2	Bd 3
weight	240	240	250	250	245	225	255	275	250	295	280	280	250	245	245	205	215	200
depth	10.0	10.5	9.0	11.0	11.0	11.0	12.0	12.5	13.0	13.0	13.0	13.0	10.0	10.5	10.0	7.5	9.0	7.5
density	128.9	122.8	149.2	122.1	119.6	109.9	114.4	118.8	103.3	121.9	115.7	115.7	134.3	125.3	131.6	146.8	128.3	146.2
SWE	12.9	12.9	13.4	13.4	13.2	12.1	13.7	14.8	13.4	15.8	15.0	15.0	13.4	13.2	13.2	11.0	11.5	10.7

	SITE T2-3			SITE T3-1			SITE T3-2			SITE T3-3			SITE T3-4		
	Bd 1	Bd 2	Bd 3	Bd 1	Bd 2	Bd 3	Bd 1	Bd 2	Bd 3	Bd 1	Bd 2	Bd 3	Bd 1	Bd 2	Bd 3
weight	265	190	145	255	235	240	290	295	300	370	310	355	295	270	270
depth	9.5	7.5	5.5	11.5	10.0	8.5	13.5	14.0	14.0	15.0	14.0	15.0	13.0	12.0	13.0
density	149.8	136.1	141.6	119.1	126.2	151.6	115.4	113.2	115.1	136.0	118.9	127.1	121.9	120.8	111.5
SWE	14.2	10.2	7.8	13.7	12.6	12.9	15.6	15.8	16.1	20.4	16.6	19.1	15.8	14.5	14.5

December 16, 1994

	SITE T1-1			SITE T1-2			SITE T1-3			SITE T1-4			SITE T2-1			SITE T2-2		
	Bd 1	Bd 2	Bd 3	Bd 1	Bd 2	Bd 3	Bd 1	Bd 2	Bd 3	Bd 1	Bd 2	Bd 3	Bd 1	Bd 2	Bd 3	Bd 1	Bd 2	Bd 3
weight	130	120	115	125	130	125	130	135	140	135	130	140	180	180	175	180	185	205
depth	5.0	5.5	5.0	5.5	5.5	5.0	5.0	5.5	6.0	5.0	5.0	5.5	8.0	9.0	8.0	5.5	6.0	6.5
density	139.6	117.2	123.5	122.1	126.9	134.3	139.6	131.8	125.3	145.0	139.6	136.7	120.8	107.4	117.5	175.8	165.6	169.4
SWE	7.0	6.4	6.2	6.7	7.0	6.7	7.0	7.3	7.5	7.3	7.0	7.5	9.7	9.7	9.4	9.7	9.9	11.0

	SITE T2-3			SITE T3-1			SITE T3-2			SITE T3-3			SITE T3-4		
	Bd 1	Bd 2	Bd 3	Bd 1	Bd 2	Bd 3	Bd 1	Bd 2	Bd 3	Bd 1	Bd 2	Bd 3	Bd 1	Bd 2	Bd 3
weight	195	185	190	185	195	180	195	195	205	245	220	215	250	240	225
depth	7.0	6.5	7.0	7.5	8.0	7.0	7.5	8.0	8.0	9.5	8.0	8.0	10.0	10.5	9.0
density	149.6	152.9	145.8	132.5	130.9	138.1	139.6	130.9	137.6	138.5	147.7	144.3	134.3	122.8	134.3
SWE	10.5	9.9	10.2	9.9	10.5	9.7	10.5	10.5	11.0	13.2	11.8	11.5	13.4	12.9	12.1

weight (gm); depth (cm); density (kg/cm^3); SWE (mm)

Table B-2 (cont). Storm SWE measurements for each site and storm board.

December 18, 1994

	SITE T1-1			SITE T1-2			SITE T1-3			SITE T1-4			SITE T2-1			SITE T2-2		
	Bd 1	Bd 2	Bd 3	Bd 1	Bd 2	Bd 3	Bd 1	Bd 2	Bd 3	Bd 1	Bd 2	Bd 3	Bd 1	Bd 2	Bd 3	Bd 1	Bd 2	Bd 3
weight	135	155	160	235	240	220	235	230	225	235	230	250	155	155	155	100	100	120
depth	4.0	4.5	5.0	7.5	7.0	7.0	7.0	7.0	7.0	7.0	7.0	8.0	5.0	5.0	5.0	2.0	2.0	2.0
density	181.3	185.0	171.9	168.3	184.1	168.8	180.3	176.5	172.6	180.3	176.5	167.8	166.5	166.5	166.5	268.5	268.5	322.2
SWE	7.3	8.3	8.6	12.6	12.9	11.8	12.6	12.4	12.1	12.6	12.4	13.4	8.3	8.3	8.3	5.4	5.4	6.4

	SITE T2-3			SITE T3-1			SITE T3-2			SITE T3-3			SITE T3-4		
	Bd 1	Bd 2	Bd 3	Bd 1	Bd 2	Bd 3	Bd 1	Bd 2	Bd 3	Bd 1	Bd 2	Bd 3	Bd 1	Bd 2	Bd 3
weight	110	95	95	150	130	170	200	195	190	200	240	235	200	260	220
depth	2.0	2.0	2.0	4.5	4.0	4.5	6.0	5.0	5.5	5.0	6.0	6.0	5.0	7.0	4.0
density	295.4	255.1	255.1	179.0	174.5	202.9	179.0	209.5	185.5	214.8	214.8	210.3	214.8	199.5	196.9
SWE	5.9	5.1	5.1	8.1	7.0	9.1	10.7	10.5	10.2	10.7	12.9	12.6	10.7	14.0	11.8

December 29, 1994

	SITE T1-1			SITE T1-2			SITE T1-3			SITE T1-4			SITE T2-1			SITE T2-2		
	Bd 1	Bd 2	Bd 3	Bd 1	Bd 2	Bd 3	Bd 1	Bd 2	Bd 3	Bd 1	Bd 2	Bd 3	Bd 1	Bd 2	Bd 3	Bd 1	Bd 2	Bd 3
weight	60	65	60	130	125	90	100	100	105	145	130	145	60	65	60	55	55	70
depth	4.5	5.0	5.0	13.0	10.5	9.5	10.0	11.0	11.0	15.0	12.5	15.0	5.5	5.0	5.0	7.0	6.0	7.0
density	71.6	69.8	64.4	53.7	63.9	50.9	53.7	48.8	51.3	51.9	55.9	51.9	58.6	69.8	64.4	43.2	49.2	52.7
SWE	3.2	3.5	3.2	7.0	6.7	4.8	5.4	5.4	5.6	7.8	7.0	7.8	3.2	3.5	3.2	3.0	3.0	3.8

	SITE T2-3			SITE T3-1			SITE T3-2			SITE T3-3			SITE T3-4		
	Bd 1	Bd 2	Bd 3	Bd 1	Bd 2	Bd 3	Bd 1	Bd 2	Bd 3	Bd 1	Bd 2	Bd 3	Bd 1	Bd 2	Bd 3
weight	90	75	85	55	60	60	85	95	95	110	165	75	95	100	95
depth	9.5	9.5	8.0	6.0	5.5	5.5	9.5	9.0	8.0	10.0	13.0	9.5	13.0	13.0	13.0
density	50.9	42.4	57.1	49.2	58.6	58.6	48.1	56.7	63.8	59.1	68.2	42.4	39.2	41.3	39.2
SWE	4.8	4.0	4.6	3.0	3.2	3.2	4.6	5.1	5.1	5.9	8.9	4.0	5.1	5.4	5.1

weight (gm); depth (cm); density (kg/cm^3); SWE (mm)

Table B-2 (cont). Storm SWE measurements for each site and storm board.

January 7, 1995

	SITE T1-1			SITE T1-2			SITE T1-3			SITE T1-4			SITE T2-1			SITE T2-2		
	Bd 1	Bd 2	Bd 3	Bd 1	Bd 2	Bd 3	Bd 1	Bd 2	Bd 3	Bd 1	Bd 2	Bd 3	Bd 1	Bd 2	Bd 3	Bd 1	Bd 2	Bd 3
weight	145	130	130	135	130	120	125	130	135	135	140	135	145	145	145	125	115	120
depth	8.0	7.0	7.5	8.0	8.0	8.0	8.0	7.0	8.0	7.0	7.0	7.5	8.0	10.0	10.0	6.0	6.0	6.5
density	97.3	99.7	93.1	90.6	87.3	80.6	83.9	99.7	90.6	103.6	107.4	96.7	97.3	77.9	77.9	111.9	102.9	99.1
SWE	7.8	7.0	7.0	7.3	7.0	6.4	6.7	7.0	7.3	7.3	7.5	7.3	7.8	7.8	7.8	6.7	6.2	6.4

	SITE T2-3			SITE T3-1			SITE T3-2			SITE T3-3			SITE T3-4		
	Bd 1	Bd 2	Bd 3	Bd 1	Bd 2	Bd 3	Bd 1	Bd 2	Bd 3	Bd 1	Bd 2	Bd 3	Bd 1	Bd 2	Bd 3
weight	140	120	130	120	130	125	140	140	140	155	135	130	175	170	165
depth	7.0	7.0	6.5	8.0	7.5	7.5	9.0	9.5	9.0	8.0	8.0	8.0	10.0	10.0	8.0
density	107.4	92.1	107.4	80.6	93.1	89.5	83.5	79.1	83.5	104.1	90.6	87.3	94.0	91.3	110.8
SWE	7.5	6.4	7.0	6.4	7.0	6.7	7.5	7.5	7.5	8.3	7.3	7.0	9.4	9.1	8.9

January 11, 1995

	SITE T1-1			SITE T1-2			SITE T1-3			SITE T1-4			SITE T2-1			SITE T2-2		
	Bd 1	Bd 2	Bd 3	Bd 1	Bd 2	Bd 3	Bd 1	Bd 2	Bd 3	Bd 1	Bd 2	Bd 3	Bd 1	Bd 2	Bd 3	Bd 1	Bd 2	Bd 3
weight	240	235.0	230	300	300	305	305	300	300	335	325	330	230	240	245	300	290	300
depth	12.0	12.0	11.5	16.0	15.0	15.0	15.0	15.0	15.0	15.0	14.5	15.0	13.5	12.5	12.5	13.0	12.5	13.0
density	107.4	105.2	107.4	100.7	107.4	109.2	109.2	107.4	107.4	119.9	120.4	118.2	91.5	103.1	105.3	123.9	124.6	123.9
SWE	12.9	13	12.4	16.1	16.1	16.4	16.4	16.1	16.1	18.0	17.5	17.7	12.4	12.9	13.2	16.1	15.6	16.1

	SITE T1-1			SITE T3-1			SITE T3-2			SITE T3-3			SITE T3-4		
	Bd 1	Bd 2	Bd 3	Bd 1	Bd 2	Bd 3	Bd 1	Bd 2	Bd 3	Bd 1	Bd 2	Bd 3	Bd 1	Bd 2	Bd 3
weight	330	310	335	245	255	245	300	300	310	325	310	325	390	390	380
depth	13.0	13.0	13.5	13.0	13.5	13.0	14.5	15.0	14.0	15.0	13.5	15.0	17.0	17.0	16.0
density	136.3	128.1	133.3	101.2	101.4	101.2	111.1	107.4	118.9	116.4	123.3	116.4	123.2	123.2	127.6
SWE	17.7	16.6	18.0	13.2	13.7	13.2	16.1	16.1	16.6	17.5	16.6	17.5	20.9	20.9	20.4

weight (gm); depth (cm); density (kg/cm^3); SWE (mm)

Table B-2 (cont). Storm SWE measurements for each site and storm board.

January 12, 1995

	SITE T1-1			SITE T1-2			SITE T1-3			SITE T1-4			SITE T2-1			SITE T2-2		
	Bd 1	Bd 2	Bd 3	Bd 1	Bd 2	Bd 3	Bd 1	Bd 2	Bd 3	Bd 1	Bd 2	Bd 3	Bd 1	Bd 2	Bd 3	Bd 1	Bd 2	Bd 3
weight	65	60	60	80	85	75	80	85	80	85	95	90	60	60	60	75	65	80
depth	3.0	4.0	4.0	5.0	5.0	5.0	5.0	5.0	5.0	6.0	5.5	5.0	3.0	4.0	4.0	3.0	2.5	3.5
density	116.4	80.6	80.6	85.9	91.3	80.6	85.9	91.3	85.9	76.1	92.8	96.7	107.6	80.6	80.3	134.3	139.6	122.8
SWE	3.5	3.2	3.2	4.3	4.6	4.0	4.3	4.6	4.3	4.6	5.1	4.8	3.2	3.2	3.2	4.0	3.5	4.3

	SITE T2-3			SITE T3-1			SITE T3-2			SITE T3-3			SITE T3-4		
	Bd 1	Bd 2	Bd 3	Bd 1	Bd 2	Bd 3	Bd 1	Bd 2	Bd 3	Bd 1	Bd 2	Bd 3	Bd 1	Bd 2	Bd 3
weight	80	75	50	75	70	70	90	85	95	85	85	90	100	100	110
depth	4.0	3.5	3.0	4.0	4.0	4.0	6.0	5.5	6.0	5.0	4.5	4.5	7.0	7.0	7.0
density	107.4	115.1	89.5	100.7	94.0	94.0	80.6	83.0	85.0	91.3	101.4	107.4	76.7	76.7	84.4
SWE	4.3	4.0	2.7	4.0	3.8	3.8	4.8	4.6	5.1	4.6	4.6	4.8	5.4	5.4	5.9

January 14, 1995

	SITE T1-1			SITE T1-2			SITE T1-3			SITE T1-4			SITE T2-1			SITE T2-2		
	Bd 1	Bd 2	Bd 3	Bd 1	Bd 2	Bd 3	Bd 1	Bd 2	Bd 3	Bd 1	Bd 2	Bd 3	Bd 1	Bd 2	Bd 3	Bd 1	Bd 2	Bd 3
weight	230	235	215	260	255	255	280	285	275	310	305	315	225	240	240	330	330	335
depth	15.0	16.0	15.0	18.0	18.0	18.0	18.0	18.5	18.0	20.0	19.0	20.0	16.0	16.5	16.5	18.0	18.0	19.0
density	82.3	78.9	77.0	77.6	76.1	76.1	83.5	82.7	82.1	83.2	86.2	84.6	75.5	78.1	78.1	98.5	98.5	94.7
SWE	12.4	12.6	11.5	14.0	13.7	13.7	15.0	15.3	14.8	16.6	16.4	16.9	12.1	12.9	12.9	17.7	17.7	18.0

	SITE T2-3			SITE T3-1			SITE T3-2			SITE T3-3			SITE T3-4		
	Bd 1	Bd 2	Bd 3	Bd 1	Bd 2	Bd 3	Bd 1	Bd 2	Bd 3	Bd 1	Bd 2	Bd 3	Bd 1	Bd 2	Bd 3
weight	395	395	370	310	310	300	380	385	375	385	630	410	460	480	500
depth	22.0	21.0	19.5	19.0	19.0	19.0	23.5	23.0	22.5	22.0	23.0	24.0	25.0	25.0	26.0
density	96.4	101.0	101.9	87.6	87.6	84.8	86.8	89.9	89.5	94.0	100.4	91.7	98.8	103.1	103.3
SWE	21.2	21.2	19.9	16.6	16.6	16.1	20.4	20.7	20.1	20.7	23.1	22.0	24.7	25.8	26.9

weight (gm); depth (cm); density (kg/cm^3); SWE (mm)

Table B-2 (cont). Storm SWE measurements for each site and storm board.

January 26, 1995

	SITE T1-1			SITE T1-2			SITE T1-3			SITE T1-4			SITE T2-1			SITE T2-2		
	Bd 1	Bd 2	Bd 3	Bd 1	Bd 2	Bd 3	Bd 1	Bd 2	Bd 3	Bd 1	Bd 2	Bd 3	Bd 1	Bd 2	Bd 3	Bd 1	Bd 2	Bd 3
weight	230	235	215	355	335	335	390	395	395	495	500	525	210	215	220	225	235	265
depth	15.0	16.0	15.0	21.5	20.0	20.5	24.0	24.0	24.0	28.0	28.0	28.0	12.0	12.0	12.5	15.0	14.0	15.0
density	82.3	78.9	77.0	88.7	90.0	87.8	87.3	88.4	88.4	94.9	95.9	100.7	94.0	96.2	94.5	80.6	90.1	94.9
SWE	12.4	12.6	11.5	19.1	18.0	18.0	20.9	21.2	21.2	26.6	26.9	28.2	11.3	11.5	11.8	12.1	12.6	14.2

	SITE T2-3			SITE T3-1			SITE T3-2			SITE T3-3			SITE T3-4		
	Bd 1	Bd 2	Bd 3	Bd 1	Bd 2	Bd 3	Bd 1	Bd 2	Bd 3	Bd 1	Bd 2	Bd 3	Bd 1	Bd 2	Bd 3
weight	400	415	500	225	250	240	350	345	365	395	435	415	520	525	510
depth	22.5	22.5	23.5	13.0	12.5	12.5	19.5	21.0	20.0	21.0	23.5	23.0	26.5	26.5	26.0
density	95.5	99.1	114.3	93.0	107.4	103.1	96.4	88.2	98.0	101.0	99.4	96.9	105.4	106.4	105.3
SWE	21.5	22.3	26.9	12.1	13.4	12.9	18.8	18.5	19.6	21.2	23.4	22.3	27.9	28.2	27.4

Febuary 9, 1995

	SITE T1-1			SITE T1-2			SITE T1-3			SITE T1-4			SITE T2-1			SITE T2-2		
	Bd 1	Bd 2	Bd 3	Bd 1	Bd 2	Bd 3	Bd 1	Bd 2	Bd 3	Bd 1	Bd 2	Bd 3	Bd 1	Bd 2	Bd 3	Bd 1	Bd 2	Bd 3
weight	120	130	130	130	125	130	125	125	125	135	135	135	115	110	120	120	100	120
depth	7.0	7.0	7.0	7.0	7.0	6.0	7.0	7.0	7.0	7.0	7.0	7.0	6.0	5.0	5.0	6.0	5.0	6.0
density	92.1	99.7	99.7	99.7	95.9	116.4	95.9	95.9	95.9	103.6	103.6	103.6	102.9	118.2	128.9	107.4	107.4	107.4
SWE	6.4	7.0	7.0	7.0	6.7	7.0	6.7	6.7	6.7	7.3	7.3	7.3	6.2	5.9	6.4	6.4	5.4	6.4

	SITE T2-3			SITE T3-1			SITE T3-2			SITE T3-3			SITE T3-4		
	Bd 1	Bd 2	Bd 3	Bd 1	Bd 2	Bd 3	Bd 1	Bd 2	Bd 3	Bd 1	Bd 2	Bd 3	Bd 1	Bd 2	Bd 3
weight	------	155	120	100	110	110	125	135	135	130	135	135	185	180	165
depth	------	7.5	5.0	5.0	6.0	6.0	6.0	7.0	7.0	8.0	8.0	7.0	9.5	9.0	9.0
density	------	111.0	128.9	107.4	98.5	98.5	111.9	106.9	106.9	87.3	90.6	103.6	104.6	107.4	98.5
SWE	------	8.3	6.4	5.4	5.9	5.9	6.7	7.3	7.3	7.0	7.3	7.3	9.9	9.7	8.9

weight (gm); depth (cm); density (kg/cm^3); SWE (mm)

Table B-2 (cont). Storm SWE measurements for each site and storm board.

Febuary 26, 1995

	SITE T1-1			SITE T1-2			SITE T1-3			SITE T1-4			SITE T2-1			SITE T2-2		
	Bd 1	Bd 2	Bd 3	Bd 1	Bd 2	Bd 3	Bd 1	Bd 2	Bd 3	Bd 1	Bd 2	Bd 3	Bd 1	Bd 2	Bd 3	Bd 1	Bd 2	Bd 3
weight	85	80	80	105	95	95	90	100	105	110	100	110	85	75	75	130	120	------
depth	7.0	6.0	7.0	9.0	8.0	8.0	8.0	9.0	10.0	10.0	9.0	10.0	6.0	5.0	5.0	9.0	7.0	------
density	65.2	71.6	61.4	62.7	63.8	63.8	60.4	59.7	56.4	59.1	59.7	59.1	76.1	80.6	80.6	77.6	92.1	------
SWE	4.6	4.3	4.3	5.6	5.1	5.1	4.8	5.4	5.6	5.9	5.4	5.9	4.6	4.0	4.0	7.0	6.4	------

	SITE T2-3			SITE T3-1			SITE T3-2			SITE T3-3			SITE T3-4		
	Bd 1	Bd 2	Bd 3	Bd 1	Bd 2	Bd 3	Bd 1	Bd 2	Bd 3	Bd 1	Bd 2	Bd 3	Bd 1	Bd 2	Bd 3
weight	140	140	------	80	------	80	140	140	140	145	155	150	175	175	160
depth	8.5	8.5	------	5.0	------	5.0	9.0	10.0	9.0	7.5	10.0	8.0	11.0	11.0	10.0
density	88.5	88.5	------	85.9	------	85.9	83.5	75.2	83.5	103.8	83.2	100.7	85.4	85.4	85.9
SWE	7.5	7.5	------	4.3	------	4.3	7.5	7.5	7.5	7.8	8.3	8.1	9.4	9.4	8.6

March 3, 1995

	SITE T1-1			SITE T1-2			SITE T1-3			SITE T1-4			SITE T2-1			SITE T2-2		
	Bd 1	Bd 2	Bd 3	Bd 1	Bd 2	Bd 3	Bd 1	Bd 2	Bd 3	Bd 1	Bd 2	Bd 3	Bd 1	Bd 2	Bd 3	Bd 1	Bd 2	Bd 3
weight	345	340	345	385	380	390	385	405	405	385	395	395	300	310	315	325	320	375
depth	26.0	26.0	25.0	30.0	29.0	30.0	29.0	31.0	31.0	30.0	29.0	30.0	22.0	22.0	23.0	22.0	22.0	26.0
density	71.3	70.2	74.1	68.9	70.4	69.8	71.3	70.2	70.2	68.9	73.2	70.7	73.2	75.7	73.6	79.3	78.1	77.5
SWE	18.5	18.3	18.5	20.7	20.4	20.9	20.7	21.8	21.8	20.7	21.2	21.2	16.1	16.6	16.9	17.5	17.2	20.1

	SITE T2-3			SITE T3-1			SITE T3-2			SITE T3-3			SITE T3-4		
	Bd 1	Bd 2	Bd 3	Bd 1	Bd 2	Bd 3	Bd 1	Bd 2	Bd 3	Bd 1	Bd 2	Bd 3	Bd 1	Bd 2	Bd 3
weight	360	370	310	340	335	295	380	385	350	370	375	365	350	370	370
depth	25.0	27.0	24.0	24.5	24.0	20.0	28.5	28.0	25.5	27.0	27.0	26.0	27.0	28.0	28.0
density	77.3	73.6	69.4	74.5	75.0	79.2	71.6	70.9	73.7	73.6	74.6	75.4	69.6	71.0	71.0
SWE	19.3	19.9	16.6	18.3	18.0	15.8	20.4	20.1	18.8	19.9	20.1	19.6	18.8	19.9	19.9

weight (gm); depth (cm); density (kg/cm^3); SWE (mm)

Table B-2 (cont). Storm SWE measurements for each site and storm board.

March 15, 1995

	SITE T1-1			SITE T1-2			SITE T1-3			SITE T1-4			SITE T2-1			SITE T2-2		
	Bd 1	Bd 2	Bd 3	Bd 1	Bd 2	Bd 3	Bd 1	Bd 2	Bd 3	Bd 1	Bd 2	Bd 3	Bd 1	Bd 2	Bd 3	Bd 1	Bd 2	Bd 3
weight	90	85	95	195	165	175	210	210	205	250	245	260	75	80	80	155	155	190
depth	5.0	3.5	5.0	9.0	7.0	8.0	10.0	10.0	10.0	11.0	11.0	12.0	3.5	3.0	3.0	9.0	9.0	11.0
density	96.7	130.4	102.0	116.4	126.6	117.5	112.8	112.8	110.1	122.1	119.6	116.4	115.1	143.2	143.2	92.5	92.5	92.8
SWE	4.8	4.6	5.1	10.5	8.9	9.4	11.3	11.3	11.0	13.4	13.2	14.0	4.0	4.3	4.3	8.3	8.3	10.2

	SITE T2-3			SITE T3-1			SITE T3-2			SITE T3-3			SITE T3-4		
	Bd 1	Bd 2	Bd 3	Bd 1	Bd 2	Bd 3	Bd 1	Bd 2	Bd 3	Bd 1	Bd 2	Bd 3	Bd 1	Bd 2	Bd 3
weight	185	240	180	135	115	115	180	180	180	180	180	180	320	330	340
depth	14.0	13.0	12.5	6.0	5.0	5.0	10.0	10.0	10.0	12.0	12.0	11.5	17.0	17.0	17.0
density	71.0	99.1	77.3	120.8	123.5	123.5	96.7	96.7	96.7	80.6	80.6	84.1	101.1	104.3	107.4
SWE	9.9	12.9	9.7	7.3	6.2	6.2	9.7	9.7	9.7	9.7	9.7	9.7	17.2	17.7	18.3

March 24, 1995

	SITE T1-1			SITE T1-2			SITE T1-3			SITE T1-4			SITE T2-1			SITE T2-2		
	Bd 1	Bd 2	Bd 3	Bd 1	Bd 2	Bd 3	Bd 1	Bd 2	Bd 3	Bd 1	Bd 2	Bd 3	Bd 1	Bd 2	Bd 3	Bd 1	Bd 2	Bd 3
weight	865	825	910	1845	1810	1835	1945	2095	1885	2215	2300	2300	930	985	990	1245	1135	1450
depth	46.0	45.0	37.0	79.5	76.5	78.0	82.0	87.0	77.0	89.0	94.0	90.0	53.0	54.0	57.0	44.0	42.0	48.5
density	101.0	98.5	132.1	124.6	127.1	126.3	127.4	129.3	131.5	133.7	131.4	137.2	94.2	98.0	93.3	152.0	145.1	160.6
SWE	46.5	44.3	48.9	99.1	97.2	98.5	104.5	112.5	101.2	119.0	123.5	123.5	49.9	49.9	53.2	66.9	61.0	77.9

	SITE T2-3			SITE T3-1 *			SITE T3-2			SITE T3-3			SITE T3-4		
	Bd 1	Bd 2	Bd 3	Bd 1	Bd 2	Bd 3	Bd 1	Bd 2	Bd 3	Bd 1	Bd 2	Bd 3	Bd 1	Bd 2	Bd 3
weight	1535	1585	1755	------	------	------	1230	1370	1305	1730	2055	1850	2100	2155	2195
depth	50.0	50.0	55.0	42.0	45.0	41.0	* 49.0	49.5	46.5	60.0	69.0	71.0	69.0	76.0	74.0
density	164.9	170.2	171.4	154.0	154.0	154.0	134.8	148.6	150.7	154.9	159.9	139.9	163.5	152.3	159.3
SWE	82.4	85.1	94.3	64.7	69.3	63.1	66.1	73.6	70.1	92.9	110.4	99.4	112.8	115.7	117.9

* all measurement equipment removed (stolen) from site before event

* average density from sites T1-1-4 and T2-1 (n=15) applied to depths taken from board locations

weight (gm); depth (cm); density (kg/cm^3); SWE (mm)

APPENDIX C

STORM METEOROLOGICAL DATA

Table C-1. Bridger Bowl ridge storm data.

		12Z (0500 hrs)		0Z (1700 hrs)	
Storm number	Date Nov.	Temp. (deg C)	Vel. (m/s)	Temp. (deg C)	Vel. (m/s)
1	12			-4	8
	13	-10	5		
2	17	-10	6	-13	1
	18	-14	3		
3	26	-9	6	-11	6
	27	-13	4		
4	28			-11	4
	29	-10	7		
	Dec.				
5	1			-2	4
	2	-3	3	-6	3
	3	-7	5	-6	3
	4	-12	3		
6	16			-6	9
	17	-4	9		
	Jan				
7	7			-7	5
	8	-4	10		
8	11	-2	6	-4	4
9	12	-7	6	-5	4
	13	-6	6		

Table C-1 (cont.). Bridger Bowl ridge storm data.

		12Z (0500 hrs)		0Z (1700 hrs)	
Storm number	Date Jan.	Temp. (deg C)	Vel. (m/s)	Temp. (deg C)	Vel. (m/s)
10	14			-1	8
	15	-4	4	-7	5
	16	-8	5		
11	26			-1	4
	27	-3	4	-5	5
	28	-7	3		
	Feb.				
12	9			-8	5
	10	-13	4	-17	5
	11	-23	6		
13	26	-2	7	0	3
	27	-11	2	-10	4
	28	-16	3		
	Mar.				
14	3			-6	2
	4	-8	3	-9	5
	5	-9	4		
15	15			-0	8
	16	-6	0		
16	24	-3	5	-7	12
	25	-2	8	-10	4
	26	-14	5		

Table C-2. Great Falls 850 mb storm data.

		12 z (0500 hrs)					0 z (1700 hrs)				
Storm number	Date Nov.	Temp. (deg. C)	Rel. Hum. (%)	Azimuth (true)	Azimuth (0 = 135)	Vel. (m/s)	Temp. (deg. C)	Rel. Hum. (%)	Azimuth (true)	Azimuth (0 = 135)	Vel. (m/s)
1	12						4	56	262	127	2
	13	-1	41	248	113	13					
2	17	-8	91				-10	90			
	18	-13	74	250	115	4					
3	26	-6	92	284	149	5	-9	80	300	165	2
	27	-4	42	257	122	15					
4	28						-3	44	279	144	10
	29	-5	43	249	114	14					
	Dec.										
5	1						6	44	238	103	11
	2	4	43	239	104	9	3	34	248	113	15
	3	-20	86	356	221	1	-21	79			
	4	-19	65								
6	16						2	49	253	118	22
	17	3	51	228	93	12					
	Jan										
7	7						-11	59	144	9	2
	8	3	62	230	95	14					
8	11	7	47				5	52	243	108	13
9	12						4	41	242	107	9
	13	3	62	237	102	9					

Table C-2 (cont.). Great Falls 850 mb storm data.

		12 z (0500 hrs)					0 z (1700 hrs)				
Storm number	Date Nov.	Temp. (deg. C)	Rel. Hum. (%)	Azimuth (true)	Azimuth (0 = 135)	Vel. (m/s)	Temp. (deg. C)	Rel. Hum. (%)	Azimuth (true)	Azimuth (0 = 135)	Vel. (m/s)
10	14						6	49	234	99	13
	15	4	54	248	113	9	3	49			
	16	-4	96	308	173	3					
11	26						6	50			
	27	3	84	282	147	5	3	64	347	212	3
	28	0	64	263	128	6					
	Feb										
12	9						-4	93	350	215	13
	10	-12	96	319	184	7	-16	69	309	174	7
	11	-18	66	305	170	4					
13	26	-4	95	285	150	6	-9	80	19	244	3
	27	-18	95	52	277	6	-15	79	29	254	3
	28	-16	64	106	331	3					
	Mar.										
14	3						-9	95	51	276	5
	4	-12	92	351	216	2	-19	92			
	5	-22	88								
15	15						8	38	237	102	8
	16	2	46								
16	24	3	53	296	161	7	-1	92	286	151	13
	25	-4	92	321	186	21	-6	59	347	212	15
	26	-10	49	324	189	9					

Table C-3. Great Falls 700 mb storm data.

		12 z (0500 hrs)					0 z (1700 hrs)				
Storm number	Date Nov.	Temp. (deg. C)	Rel. Hum. (%)	Azimuth (true)	Azimuth (0 = 135)	Vel. (m/s)	Temp. (deg. C)	Rel. Hum. (%)	Azimuth (true)	Azimuth (0 = 135)	Vel. (m/s)
1	12						-8	83	316	181	9
	13	-12	40	283	148	8					
2	17	-13	89	347	212	6	-19	82	342	207	4
	18	-15	60	270	135	6					
3	26	-11	91	327	192	11	-13	90	334	199	15
	27	-15	39	316	181	15					
4	28						-16	75	303	168	11
	29	-15	33	303	168	13					
	Dec.										
5	1						-6	70	247	112	18
	2	-10	66	251	116	14	-12	63	261	126	16
	3	-13	84	240	105	16	-16	92	307	172	7
	4	-19	32	287	152	10					
6	16						-8	26	281	146	27
	17	-7	76	295	160	13					
	Jan										
7	7						-12	55	269	134	7
	8	-8	89	287	152	16					
8	11	-5	57	253	118	16	-8	71	277	142	13
9	12						-9	58	285	150	8
	13	-9	85	274	139	8					

Table C-3 (cont.). Great Falls 700 mb storm data.

		12 z (0500 hrs)					0 z (1700 hrs)				
Storm number	Date Jan.	Temp. (deg. C)	Rel. Hum. (%)	Azimuth (true)	Azimuth (0 = 135)	Vel. (m/s)	Temp. (deg. C)	Rel. Hum. (%)	Azimuth (true)	Azimuth (0 = 135)	Vel. (m/s)
10	14						-5	46	279	144	14
	15	-7	54	293	158	8	-10	79	294	159	3
	16	-12	74	298	163	5					
11	26						-5	78	220	85	4
	27	-7	91	334	199	4	-9	92	328	193	6
	28	-11	73	250	115	3					
	Feb										
12	9						-15	89	353	218	14
	10	-20	90	318	183	20	-25	40	356	221	17
	11	-24	29	339	204	9					
13	26	-10	87	276	141	10	-10	78	258	123	17
	27	-15	95	287	152	12	-20	85	295	160	11
	28	-21	39	313	178	5					
	Mar.										
14	3						-12	94	198	63	5
	4	-13	95	256	121	4	-14	77	287	152	9
	5	-14	95								
15	15						-6	90	277	142	11
	16	-10	46								
16	24	-5	50	116	341	6	-10	96	345	210	21
	25	-12	94	345	210	24	-14	77	343	208	15
	26	-18	22	353	218	14					

Table C-4. Great Falls 500 mb storm data.

		12 z (0500 hrs)					0 z (1700 hrs)				
Storm number	Date Nov.	Temp. (deg. C)	Rel. Hum. (%)	Azimuth (true)	Azimuth (0 = 135)	Vel. (m/s)	Temp. (deg. C)	Rel. Hum. (%)	Azimuth (true)	Azimuth (0 = 135)	Vel. (m/s)
1	12						-22	80	203	68	14
	13	-29	64	239	104	19					
2	17	-31	72	136	1	9	-32	50	80	305	6
	18	-32	22	304	169	2					
3	26	-30	67	205	70	10	-32	27	330	195	15
	27	-32	64	317	182	12					
4	28						-35	48	265	130	12
	29	-26	61	316	181	25					
	Dec.										
5	1						-22	28	257	122	30
	2	-28	32	245	110	25	-28	19	256	121	33
	3	-30	49	248	113	31	-30	73	247	112	32
	4	-28	18	261	126	26					
6	16						-31	60	297	162	24
	17	-18	26	308	173	31					
	Jan										
7	7						-24	93	294	159	25
	8	-25	52	290	155	17					
8	11	-22	35	254	119	15	-27	75	258	123	7
9	12						-28	45	286	151	15
	13	-27	73	284	149	14					

Table C-4 (cont.). Great Falls 500 mb storm data.

		12 z (0500 hrs)					0 z (1700 hrs)				
Storm number	Date Nov.	Temp. (deg. C)	Rel. Hum. (%)	Azimuth (true)	Azimuth (0 = 135)	Vel. (m/s)	Temp. (deg. C)	Rel. Hum. (%)	Azimuth (true)	Azimuth (0 = 135)	Vel. (m/s)
10	14						-24	45	236	101	27
	15	-26	29	252	117	10	-28	68	279	144	4
	16	-30	67	175	40	2					
11	26						-23	65	224	89	10
	27	-24	74	221	86	5	-26	78	247	112	6
	28	-28	65	276	141	5					
	Feb										
12	9						-31	76	310	175	26
	10	-33	73	308	173	43	-36	37	326	191	30
	11	-34	23	328	193	17					
13	26	-25	31	276	141	21	-26	17	271	136	32
	27	-31	30	285	150	24	-30	44	309	174	24
	28	-30	22	309	174	17					
	Mar.										
14	3						-26	65	273	138	22
	4	-27	75	254	119	14	-32	66	249	114	19
	5	-34	62	278	143	14					
15	15						-22	52	205	70	25
	16	-29	44	265	130	17					
16	24	-23	74	154	19	14	-23	78	70	295	9
	25	-26	75				-25	51	338	203	14
	26	-26	44	352	217	12					

APPENDIX D

SNOW DISTRIBUTIONS AND INTERPOLATED SURFACES

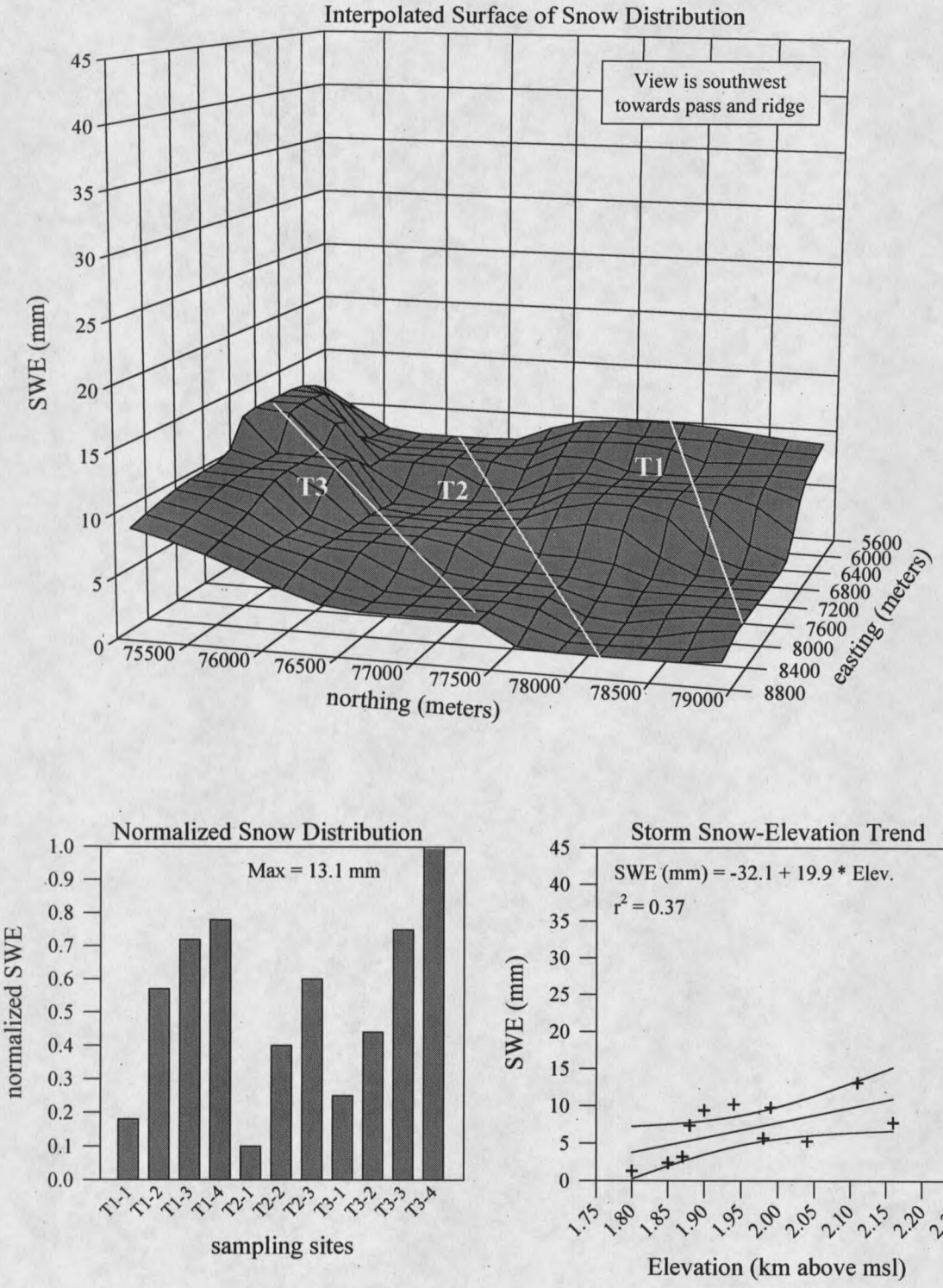

Figure D-1. Storm #1, November 12, 1994. Storm class 1.

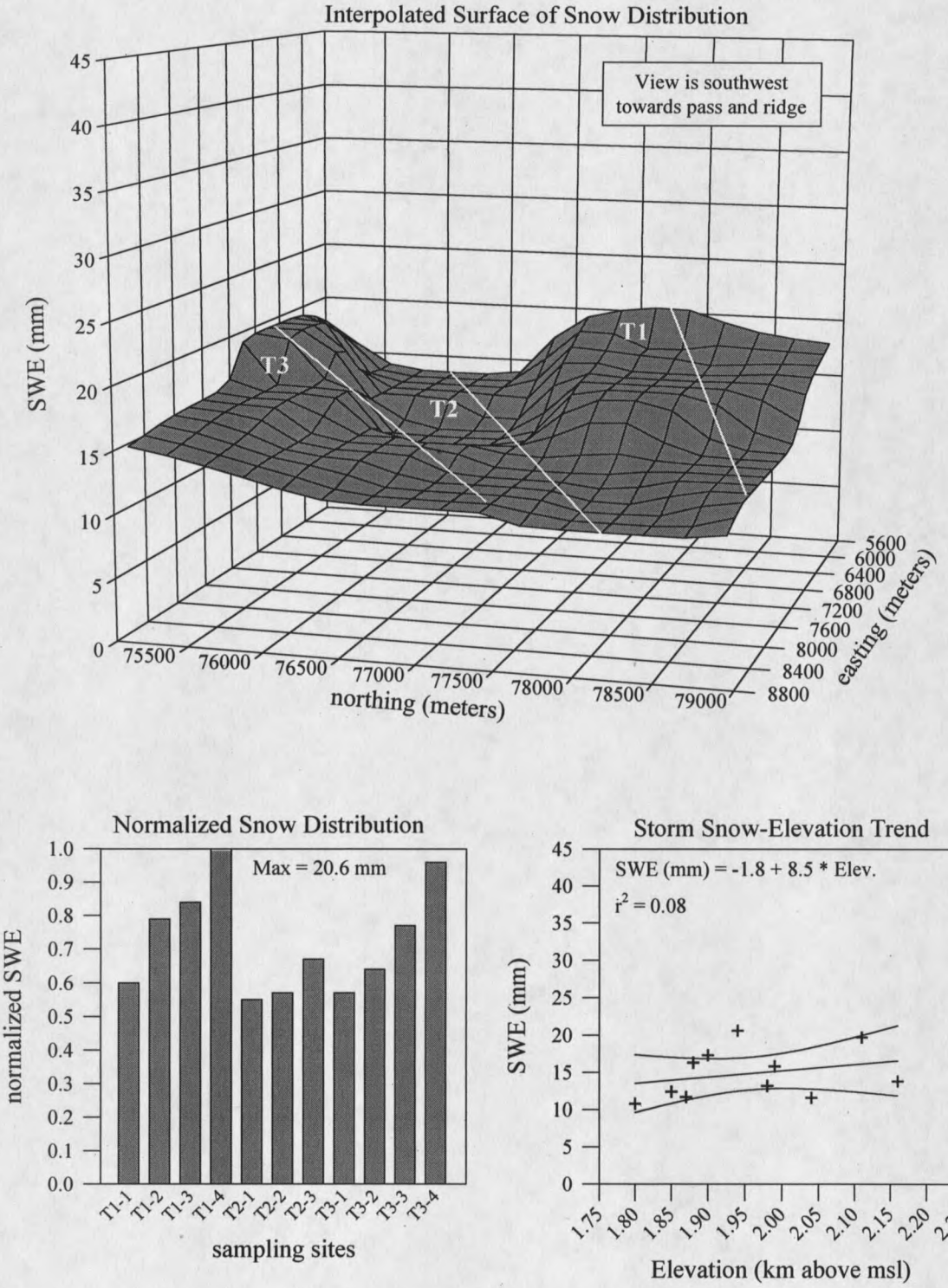

Figure D-2. Storm # 2, November 17, 1994. Storm class 1a.

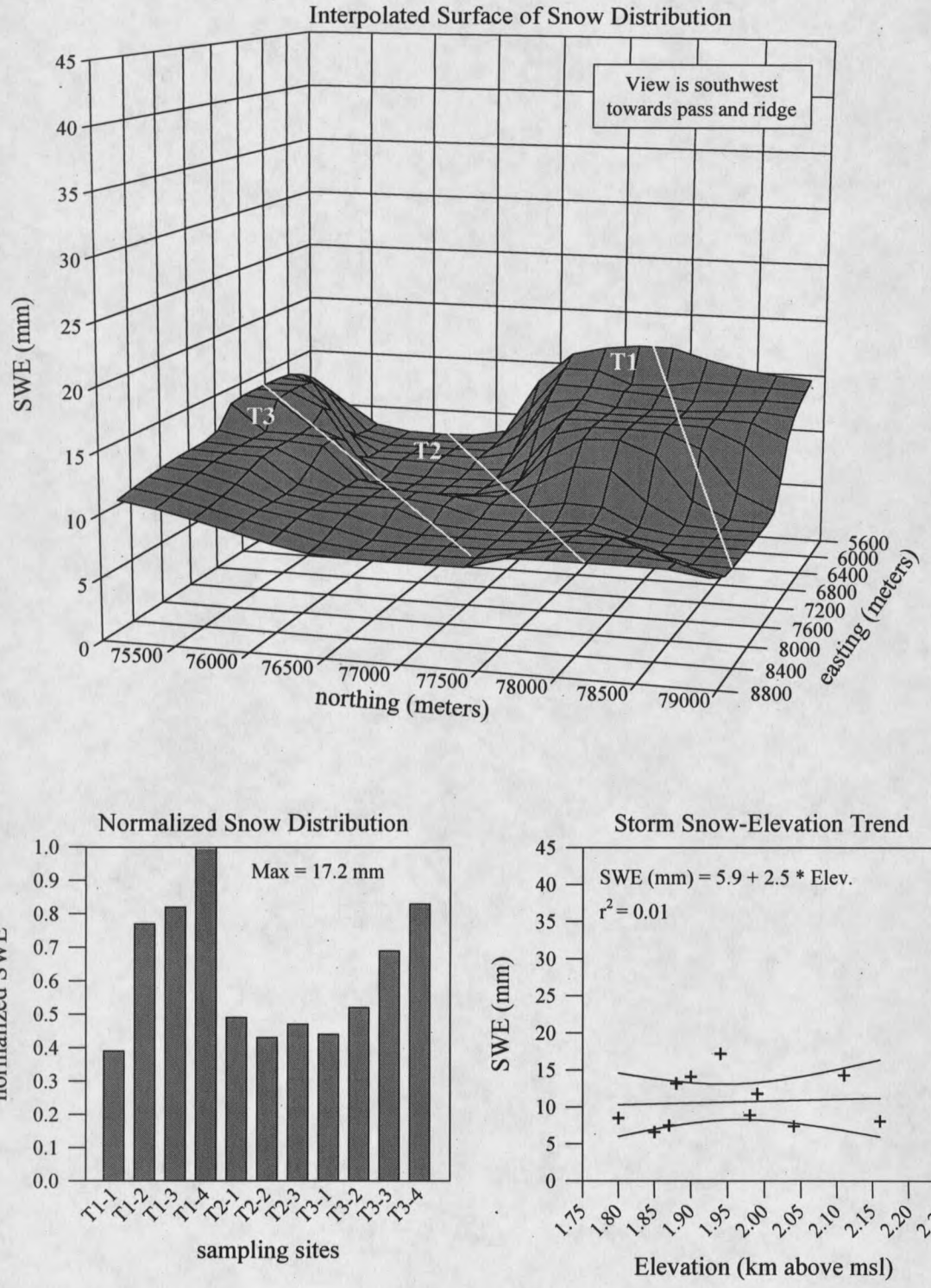

Figure D-3. Storm # 3, November 26, 1994. Storm classs 1a.

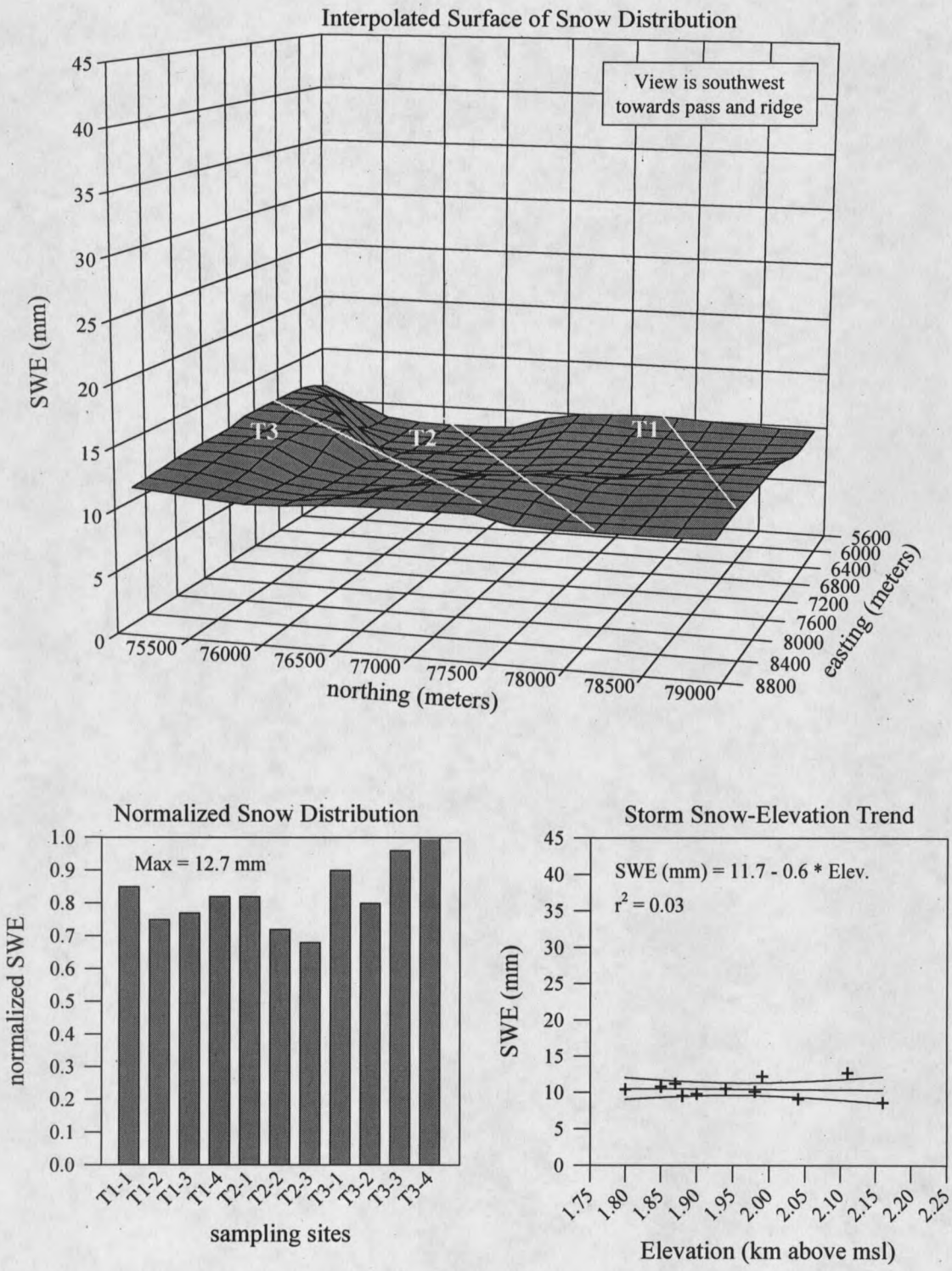

Figure D-4. Storm # 4, November 28, 1994. Storm class 4.

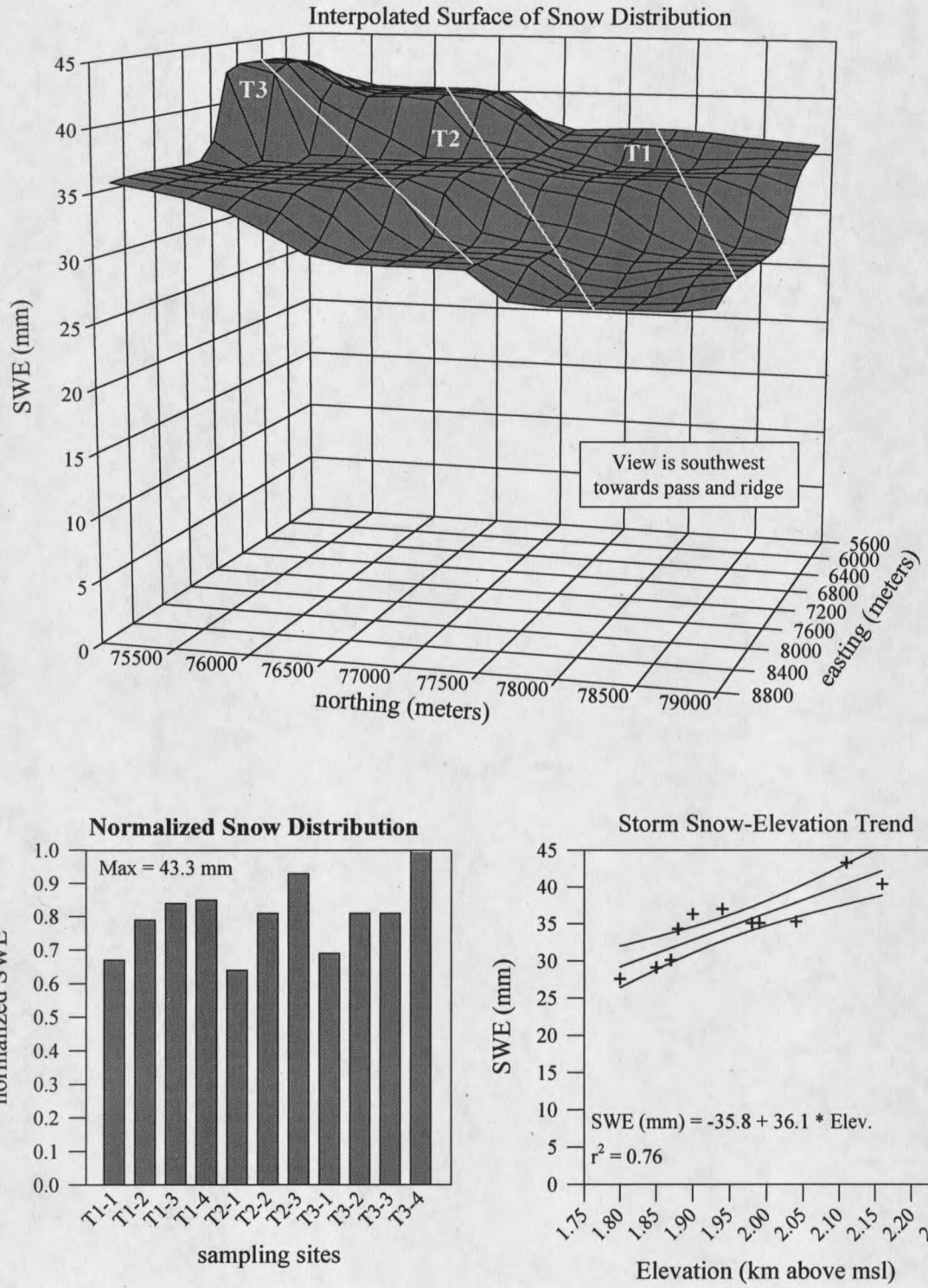

Figure D-5. Storm # 5, December 1, 1994. Storm class 2.

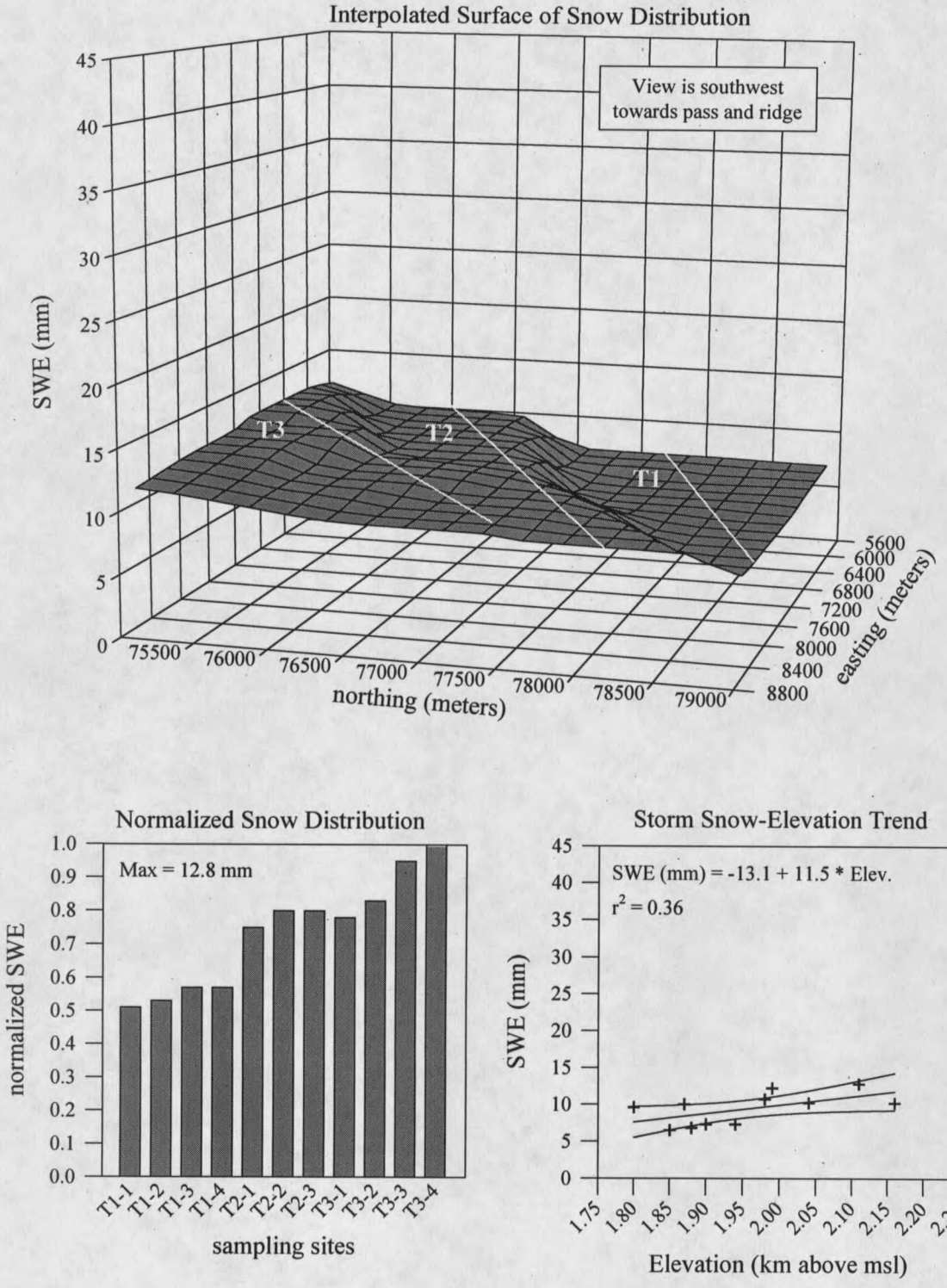

Figure D-6. Storm # 6, December 16, 1994. Storm class 2a.

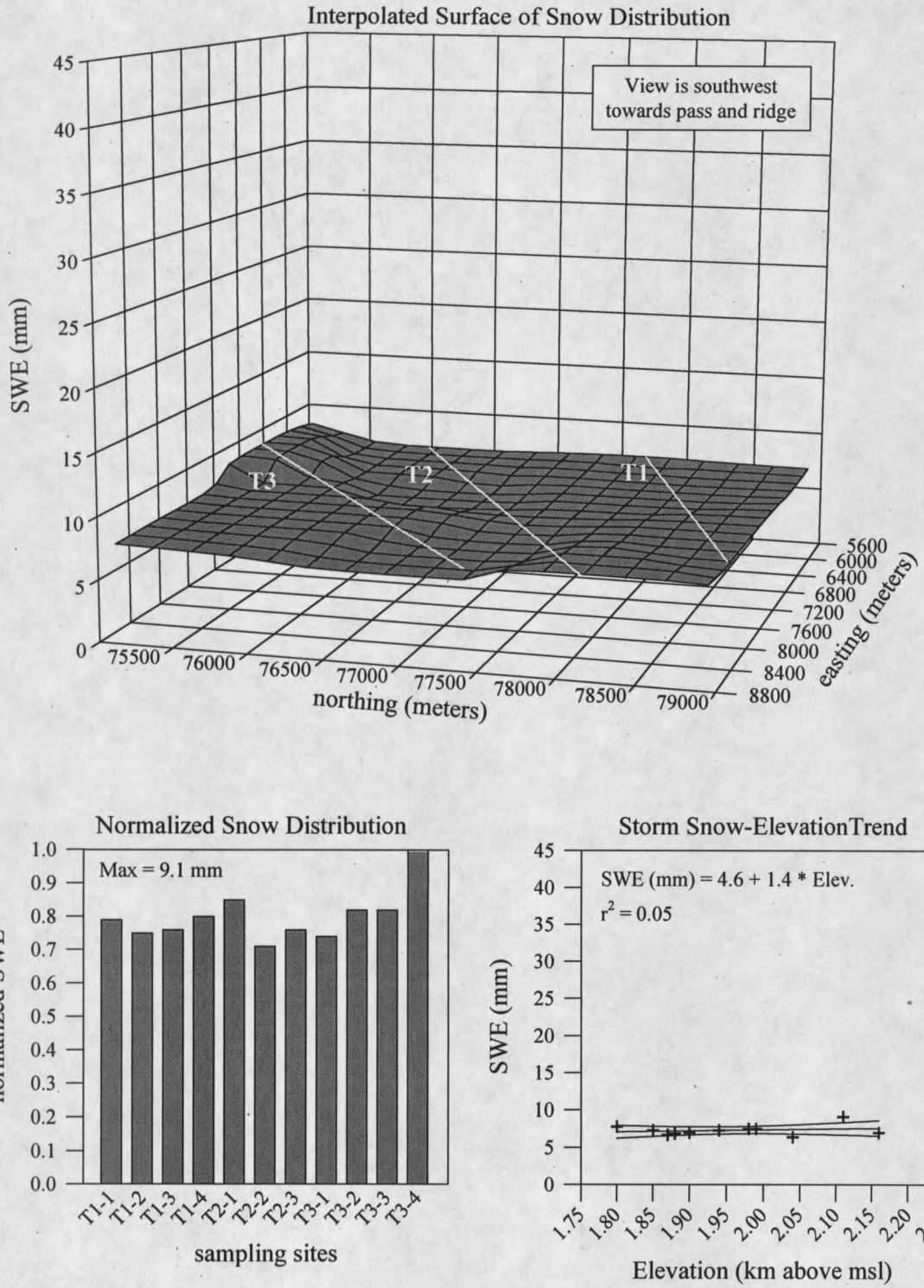

Figure D-7. Storm # 7, January 7, 1995. Storm class 4.

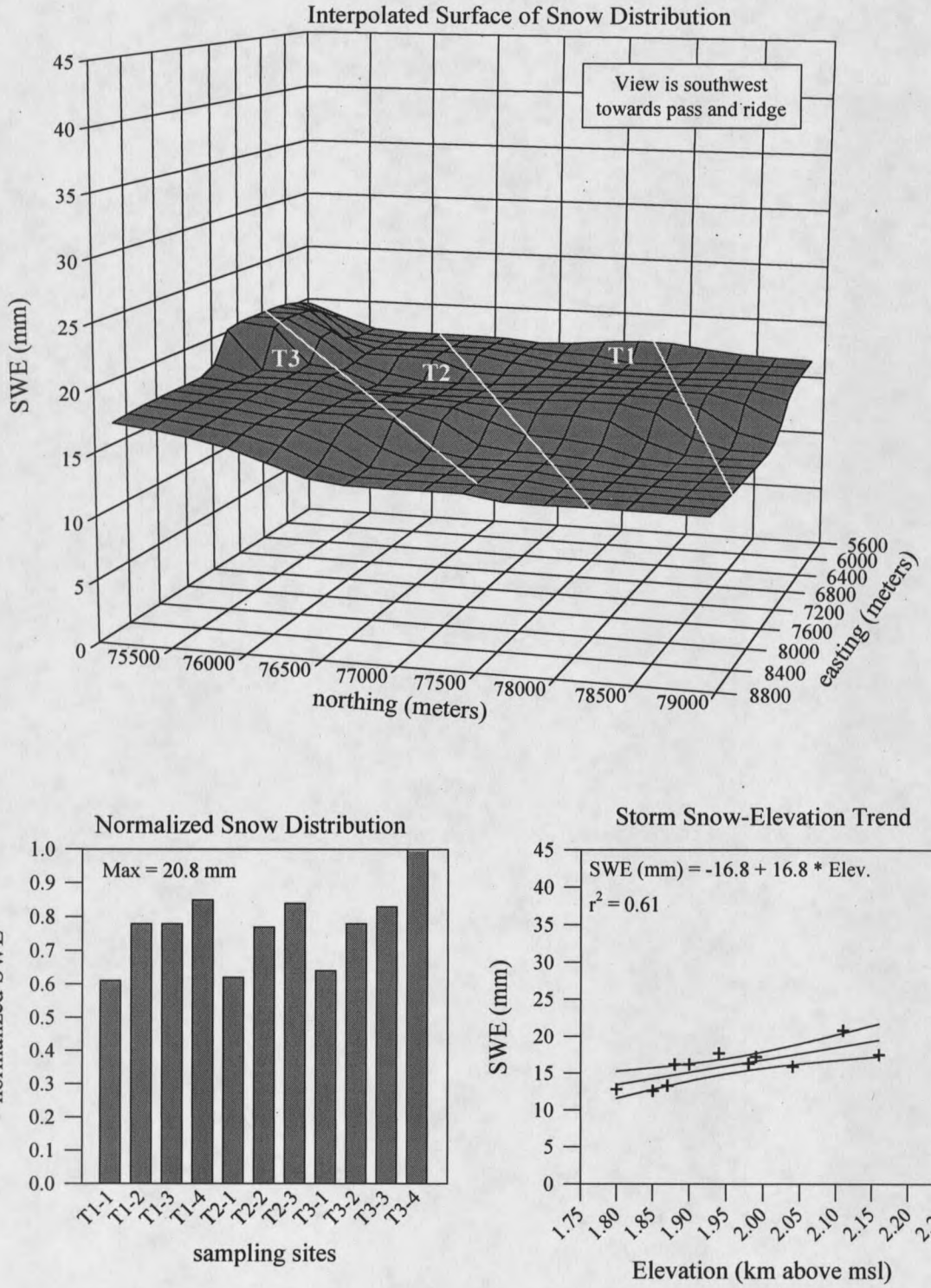

Figure D-8. Storm # 8, January 11, 1995. Storm class 2.

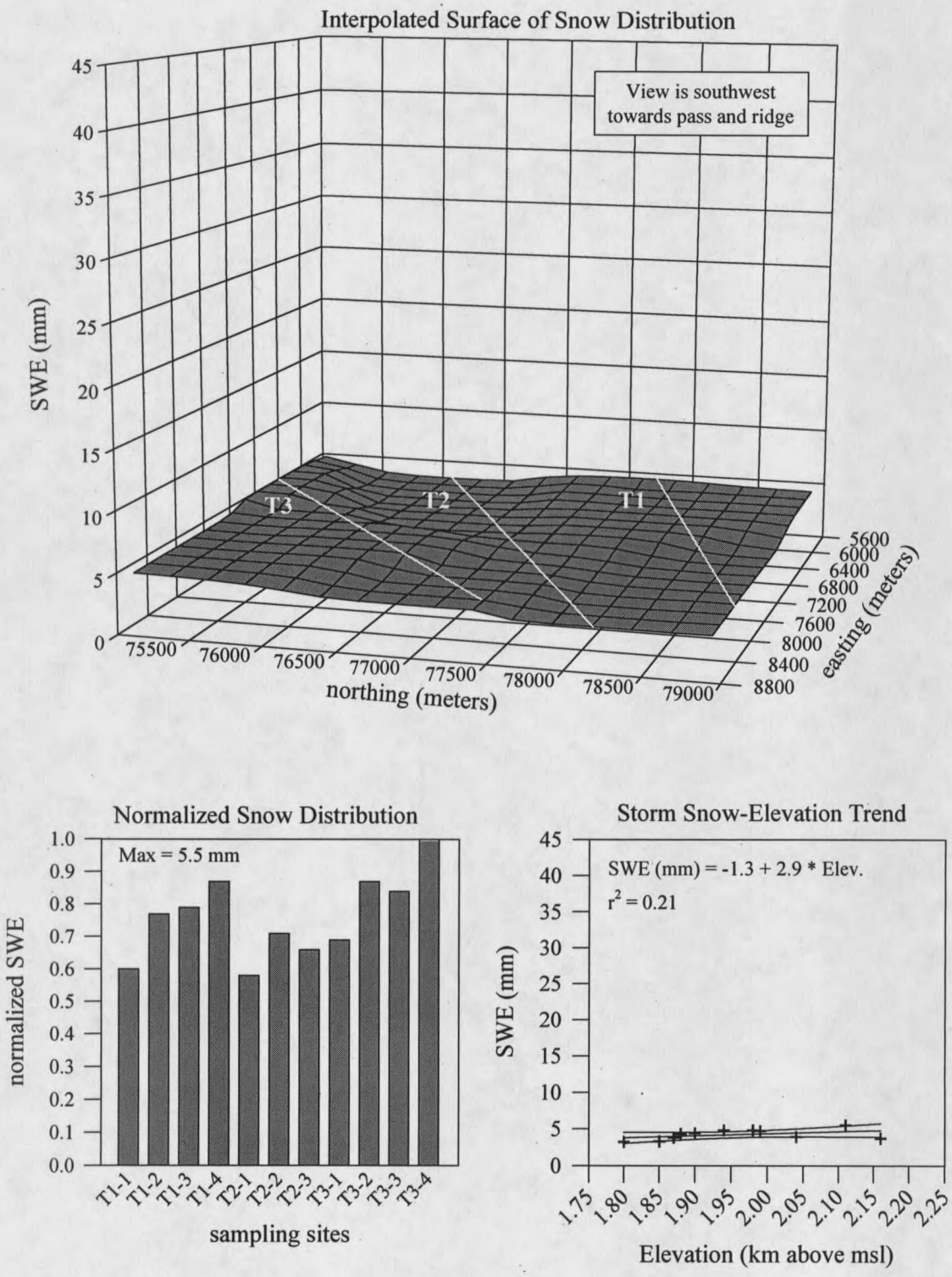

Figure D-9. Storm # 9, January 13, 1995. Storm class 3.

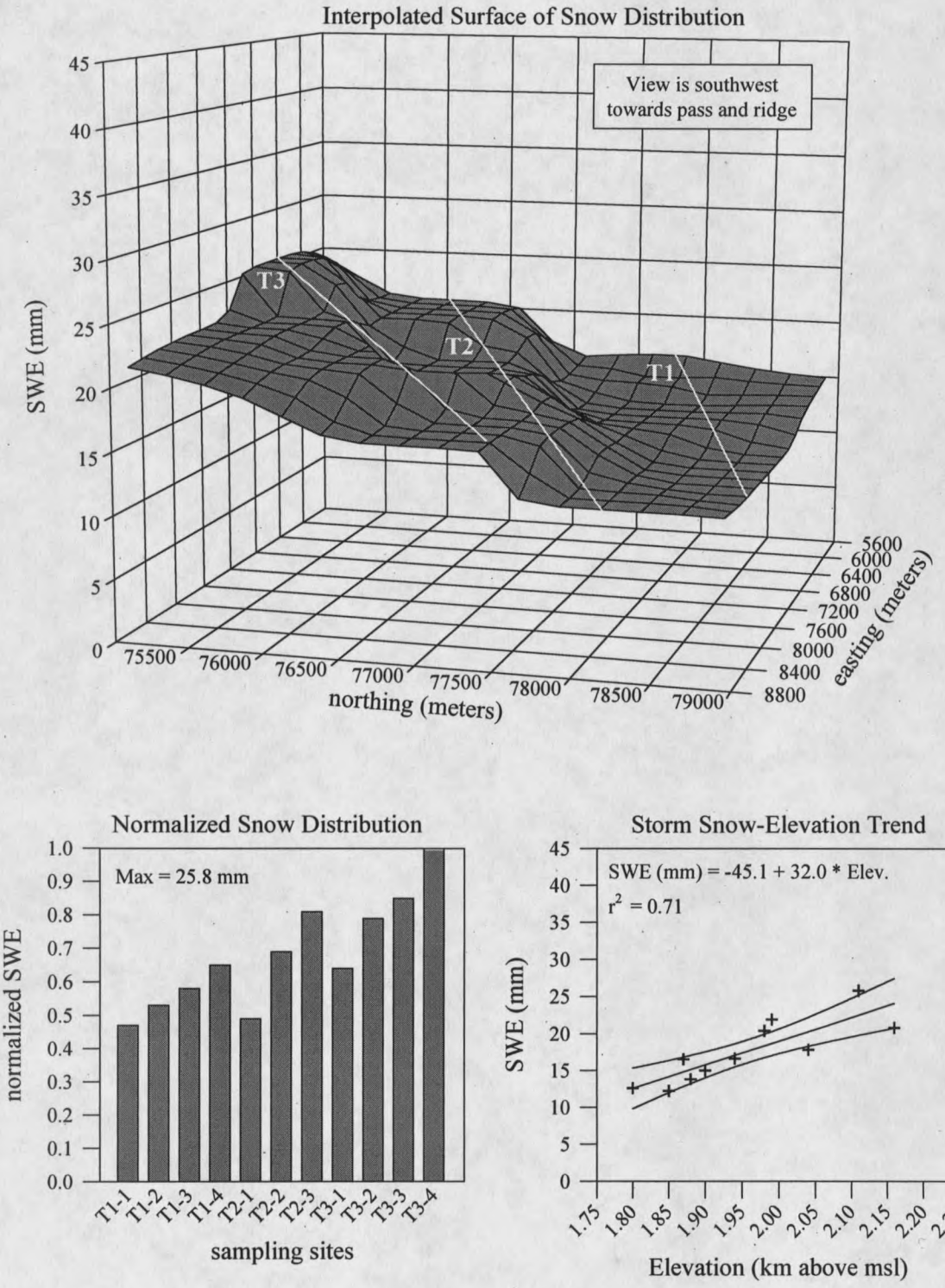

Figure D-10. Storm # 10, January 14, 1995. Storm class 2a.

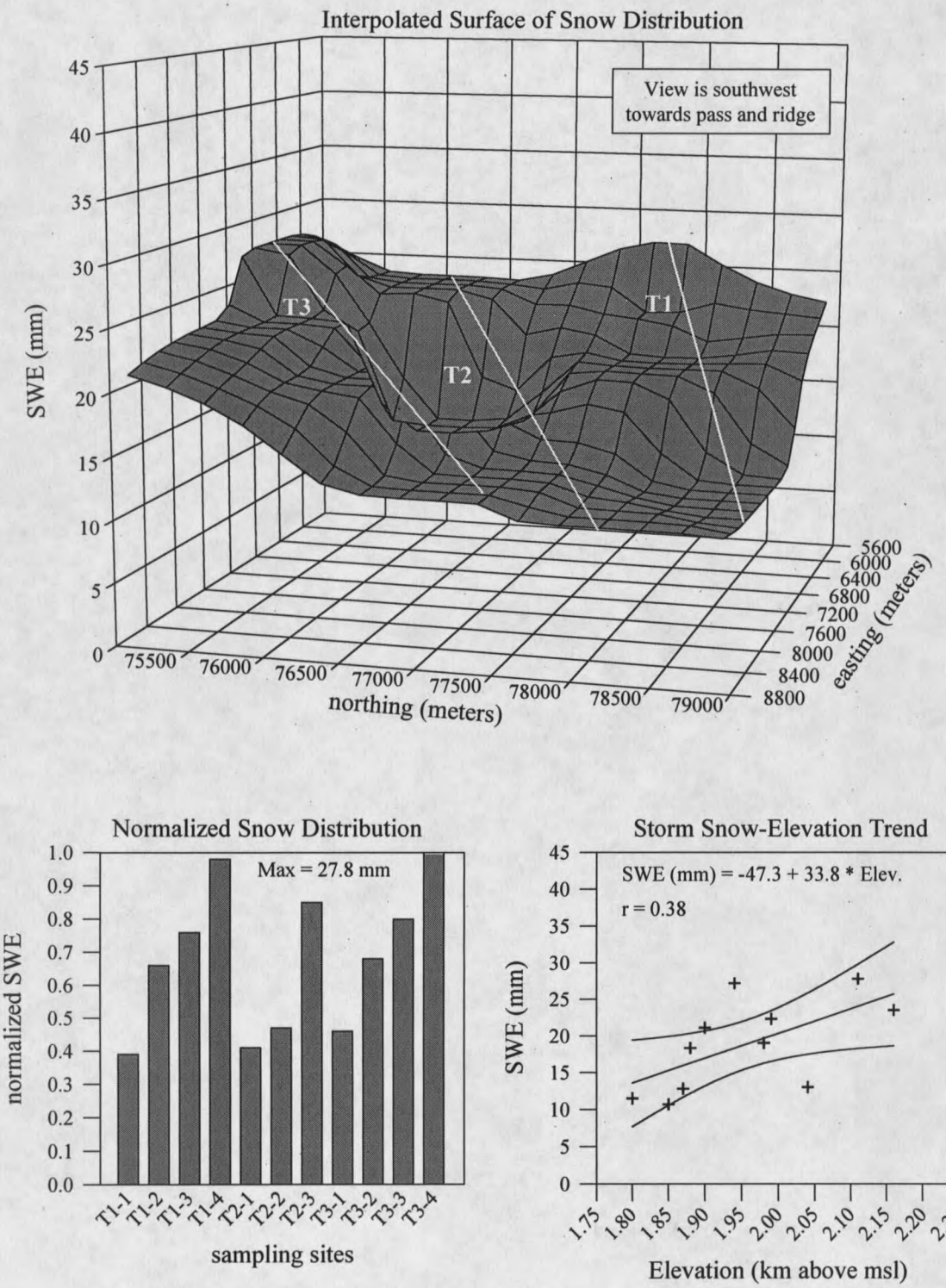

Figure D-11. Storm # 11, January 26, 1995. Storm class 1.

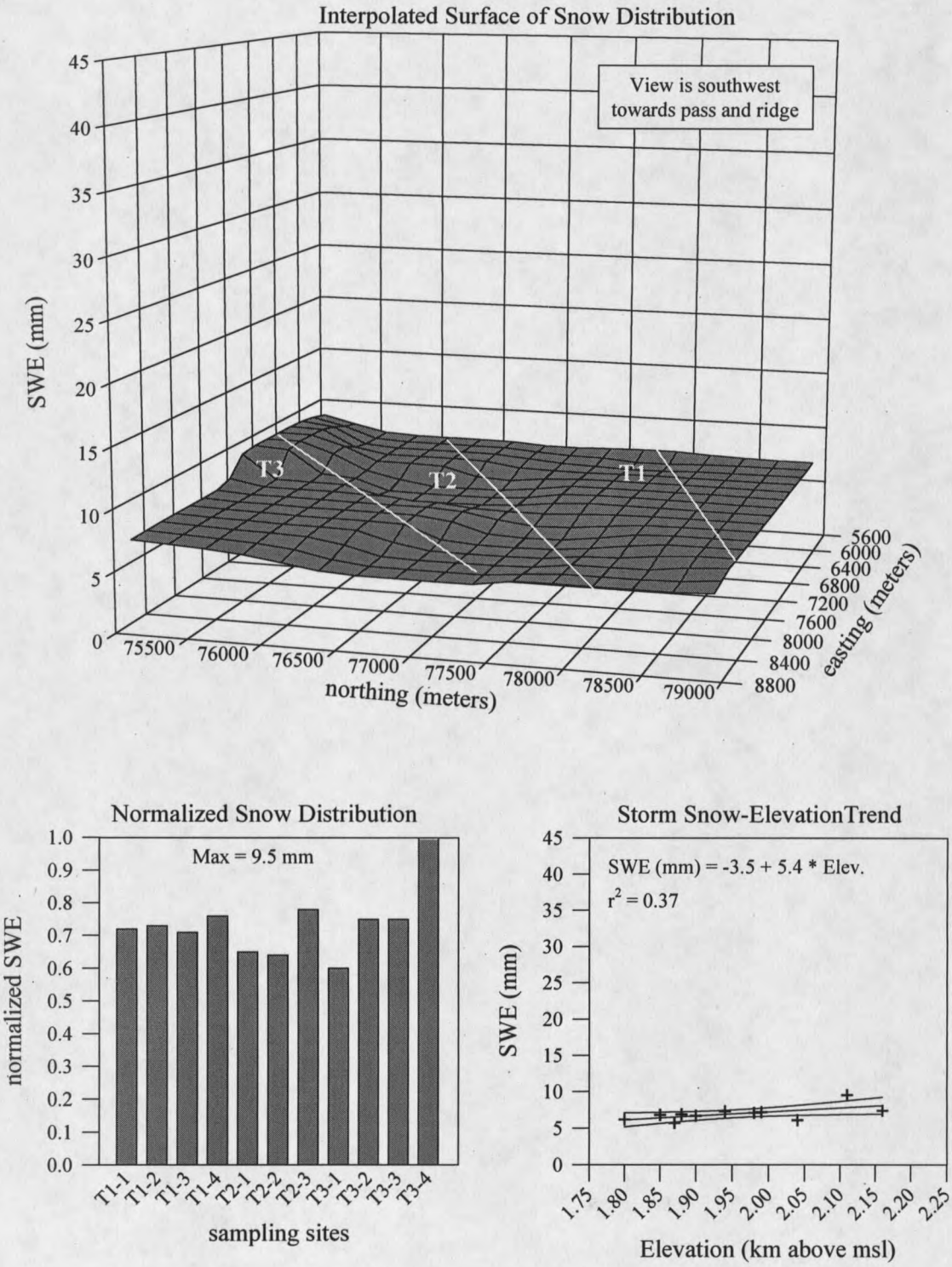

Figure D-12. Storm # 12, February 9, 1995. Storm class 2.

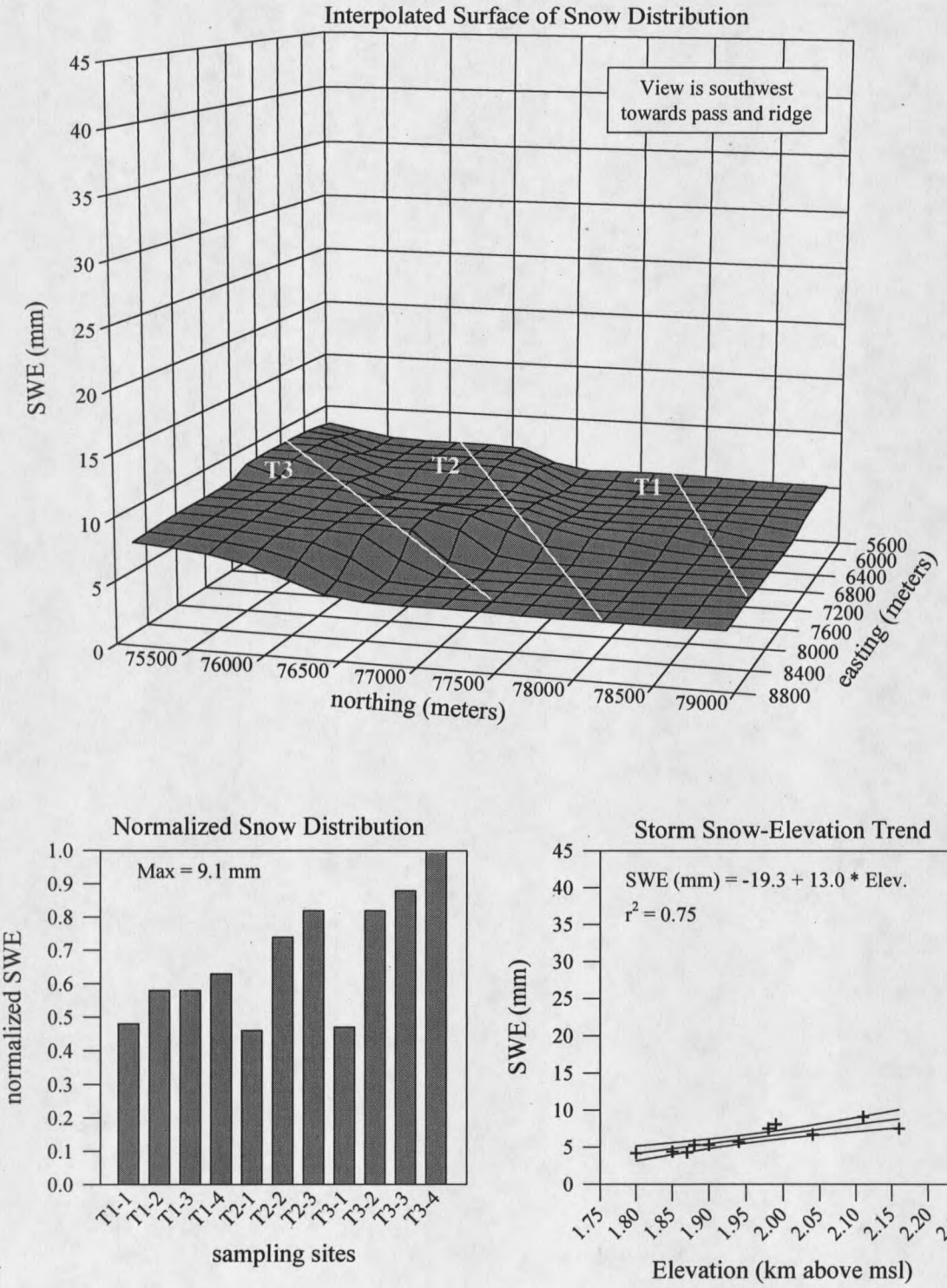

Figure D-13. Storm # 13, February 26, 1995. Storm class 2a.

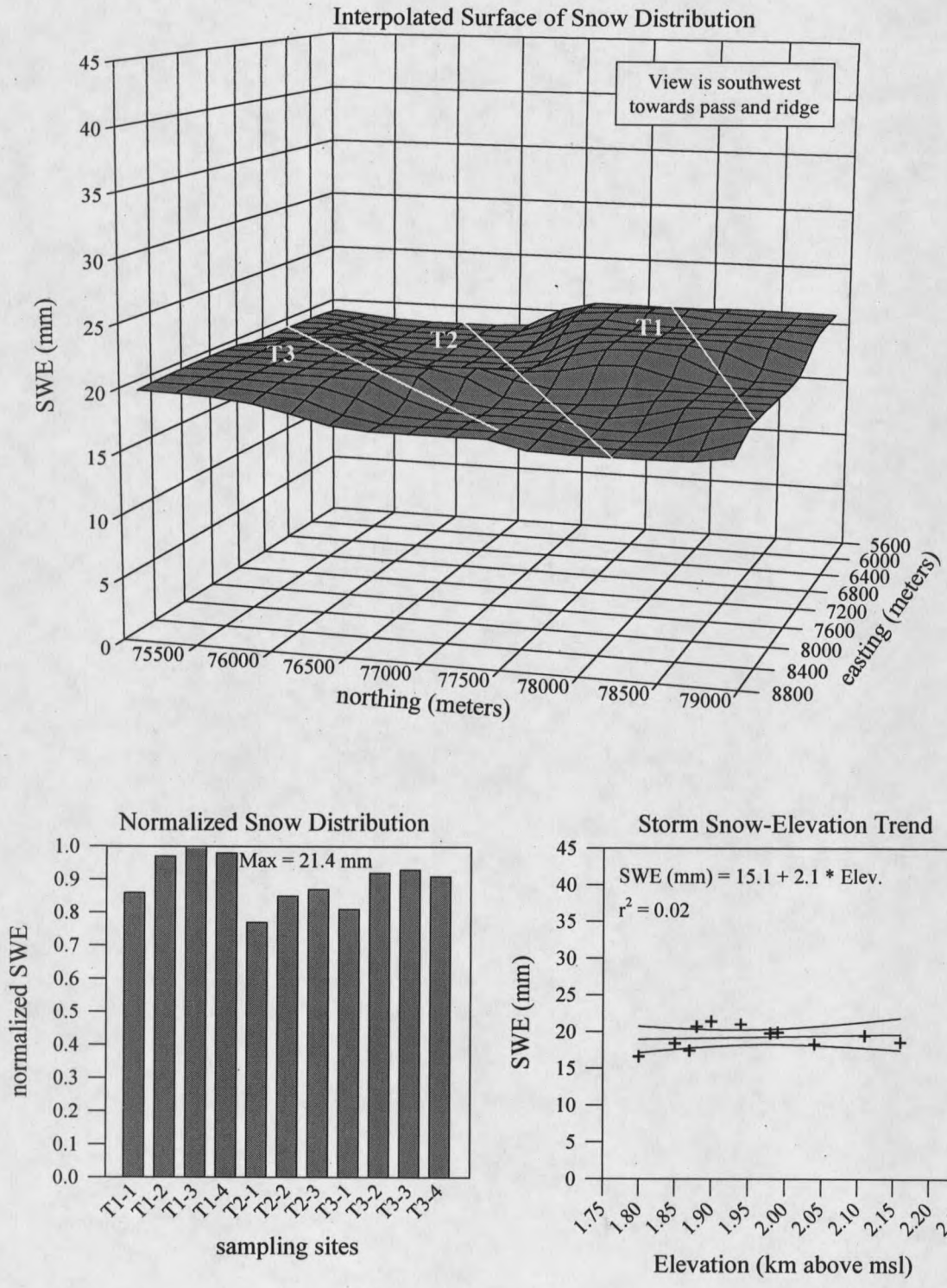

Figure D-14. Storm # 14, March 3, 1995. Storm class 3.

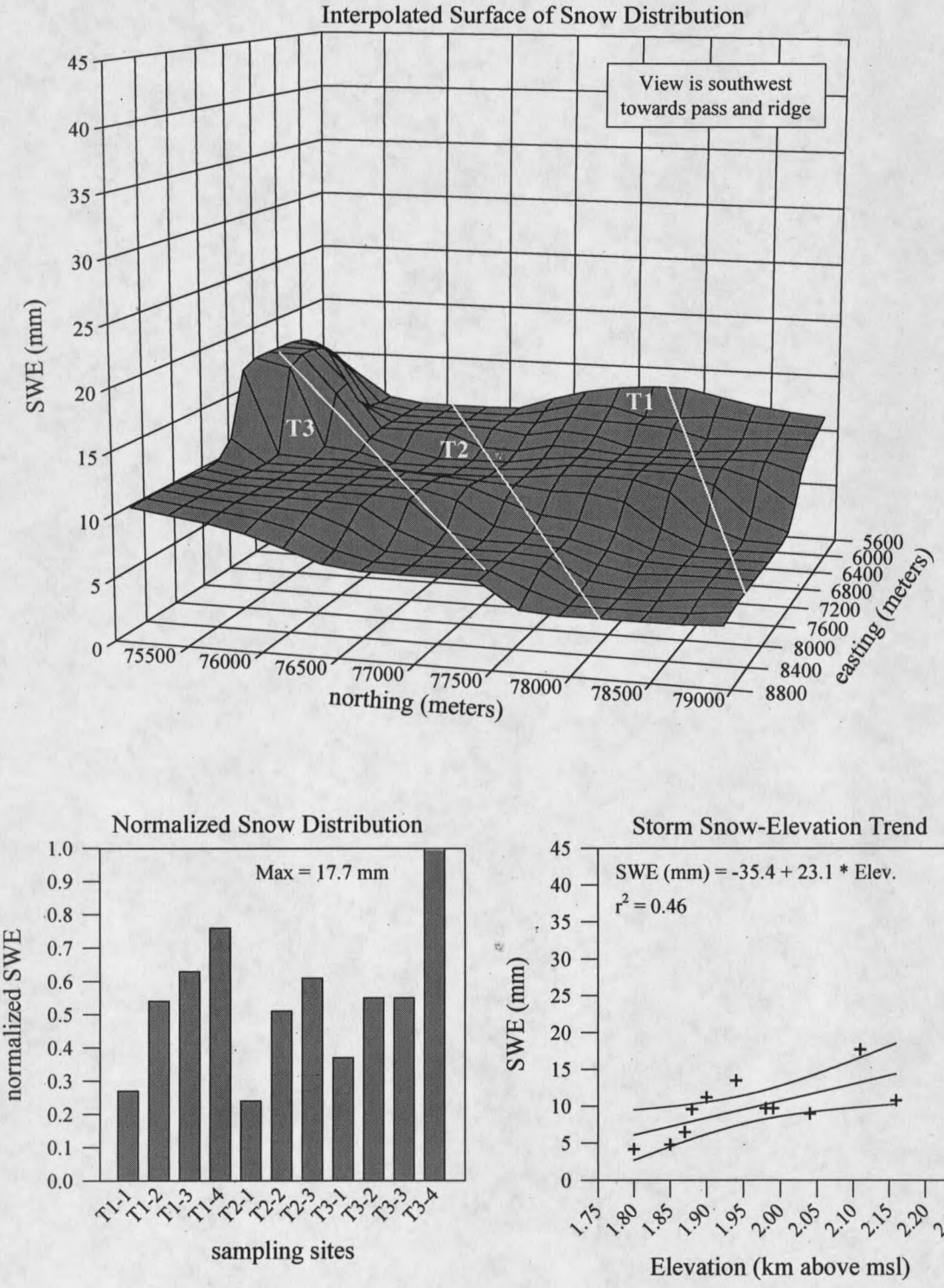

Figure D-15. Storm # 15, March 15, 1995. Storm class 1.

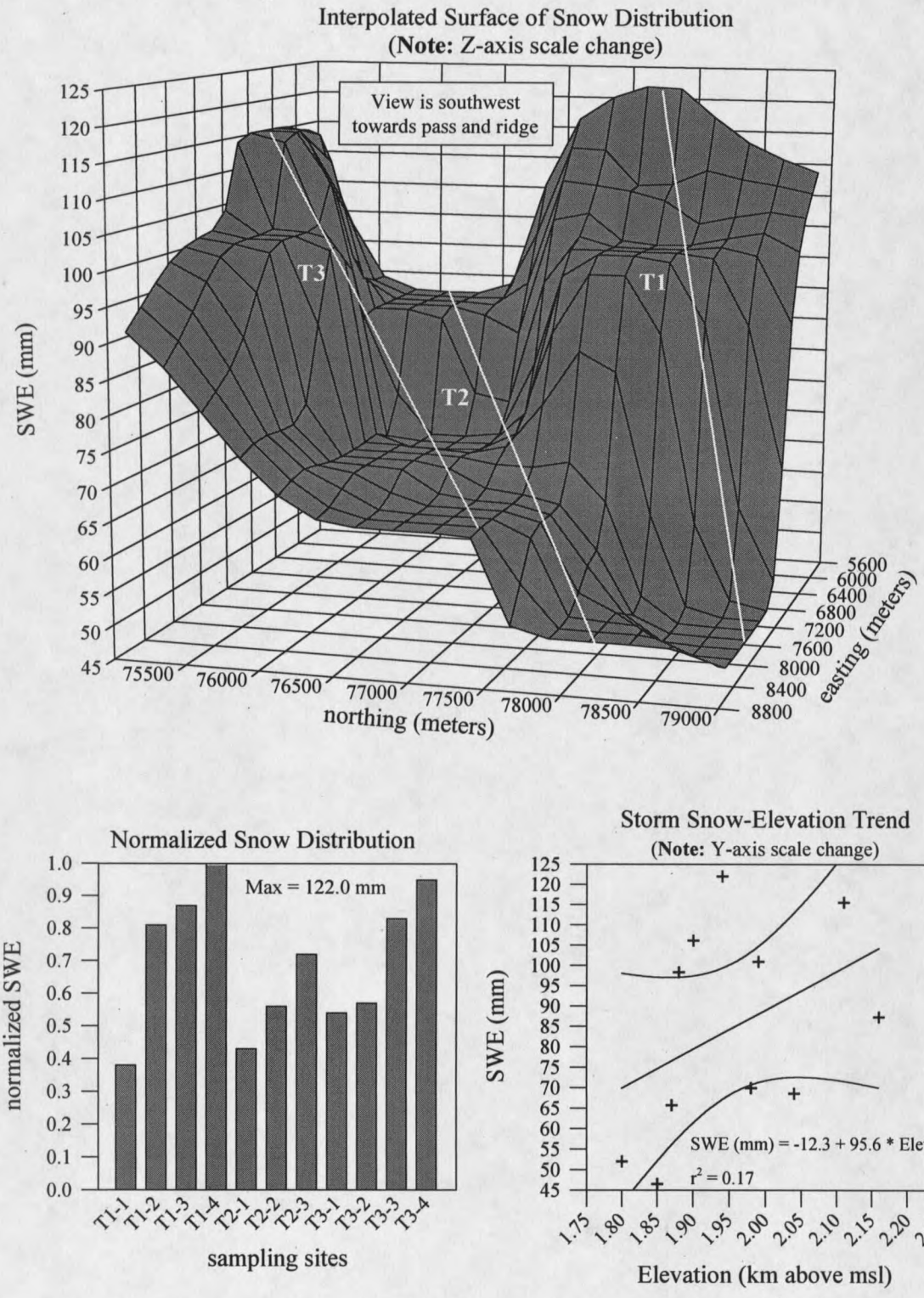

Figure D-16. Storm # 16, March 24, 1995. Storm class 1a.

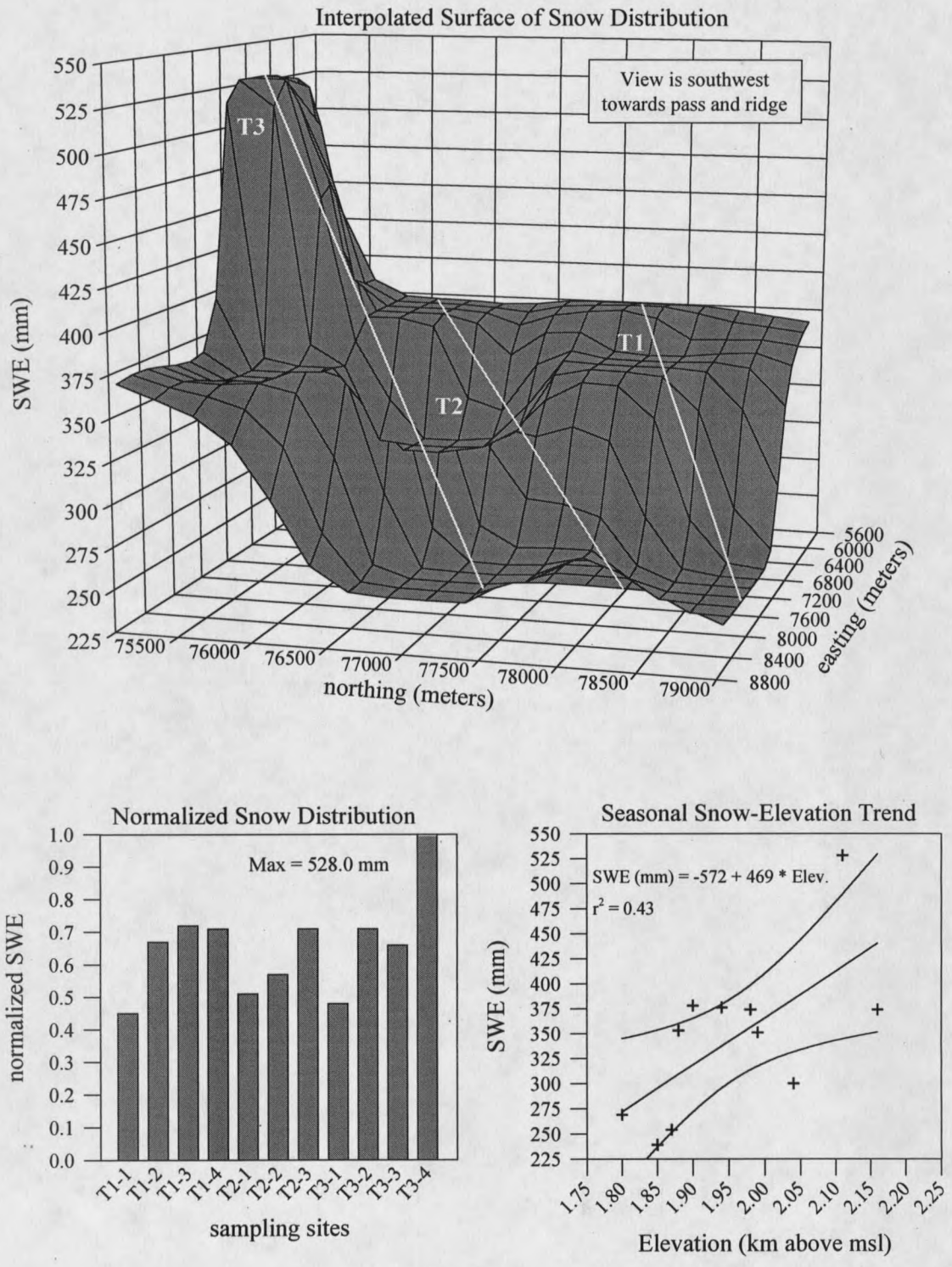

Figure D-17. April 1, 1995 seasonal snowpack - Ross Pass Study Area.